

K.N.M.I.
de Bilt

CENTRALE LANDBOUWCATALOGUS

0000 0086 5515

NN08201,893

H.A.R. de Bruin

The Energy Balance of the Earth's Surface
a practical approach

Proefschrift

*ter verkrijging van de graad van
doctor in de landbouwwetenschappen,
op gezag van de rector magnificus,
dr. C.C. Oosterlee,
hoogleraar in de veeteeltwetenschap,
in het openbaar te verdedigen
op vrijdag 7 mei 1982
des namiddags te vier uur in de aula
van de Landbouwhogeschool te Wageningen*

ISN-159394-03

Promotor : dr.ir. L. Wartena, hoogleraar in de
landbouweerkunde en omgevingsnatuurkunde

Co-promotor: dr.ir. H. Tennekes, hoogleraar in de meteo-
rologie aan de Vrije Universiteit te Amsterdam

NNOP201, 893

STELLINGEN

1. De temperatuurfluctuatiemethode voor het bepalen van de voelbare warmtestroom is geschikt voor operationele toepassingen.

Dit proefschrift.

2. Het gedrag van de Priestley-Taylor parameter α kan goed worden beschreven met een eenvoudig grenslaag/oppervlaktelaagmodel.

Dit proefschrift.

3. Een grenslaag/trajectoriënmodel heeft als voordeel dat de verticale gradiënten van de luchttemperatuur en vochtigheid goed kunnen worden beschreven. Dit is met name van belang voor verwachtingen op korte termijn van bewolking.

4. Het is zinvol op een meteorologisch station de standaarddeviatie van de horizontale windsnelheid te bepalen, daar deze een directe maat is voor de schuifspanning.

5. In de zomer kan de verdamping van een meer redelijk nauwkeurig worden geschat uit de 2e term van de Penmanformule.

H.A.R. de Bruin, J. Appl. Meteor., 17 (1978), 1132-1134.

6. Door in de formule van Ogura T (=luchttemperatuur) te vervangen door $T_e = T_n + \delta T$ (T_n = natte-bol-temperatuur, δT = correctieterm evenredig met de nettostraling) verkrijgt men een vollediger model voor ijsdiktegroei.

Y. Ogura, J. Met. Soc. Japan, 30 (1952), 231-239.

7. De Makkinkformule levert een goede schatting op van de potentiële verdamping van gras.

G.F. Makkink, J. Inst. of Wat. Eng., 11 (1957), 277-288.

H.A.R. de Bruin, CHR-TNO, Proc. Inf., 28 (1981), 25-37.

	Page
4. The temperature fluctuation method	II.51
4.1 Introduction	II.51
4.2 Theoretical background	II.51
4.3 Experimental	II.57
4.4 Results	II.57
4.5 Discussion and conclusion	II.62
Appendix	II.64
III. A simple parameterization of the surface fluxes of sensible and latent heat during daytime compared with the Penman-Monteith concept.	
1. Introduction	III.3
2. Experimental data	III.3
3. The models	III.4
3a. Introduction	III.4
3b. The Penman-Monteith model	III.4
3c. The modified Priestley-Taylor model	III.7
4. Model comparison	III.9
5. Results	III.11
6. Discussion	III.18
7. Conclusions	III.23
IV. A boundary layer model coupled to the Penman- Monteith equation.	
1. Introduction	IV.4
2. The model of Perrier	IV.5
3. Our model	IV.8
3.1 The boundary layer sub-model	IV.8
3.1.1 Parameterization of the entrainment of dry and warm air at $z = h$	IV.10
3.1.2 The evolution of θ_m and h	IV.13
3.2 The surface fluxes	IV.14
3.2.2 Net radiation and soil heat flux	IV.16
3.3 Relaxation equation for δq	IV.17
4. Comparison with the model of Perrier	IV.18

	Page
5. Results from model calculations	IV.19
6. Discussion and conclusions	IV.26
Appendix	IV.28
V. The Priestley-Taylor evaporation model applied to a large, shallow lake in the Netherlands.	
1. Introduction	V.3
2. Experimental	V.5
3. Results	V.8
3a. Daily values	V.8
3b. The diurnal variation of α	V.11
3c. The seasonal variation of α	V.12
4. Discussion	V.17
VI. Temperature and energy balance of a water reservoir determined from standard weather data of a land station.	
1. Introduction	VI.3
2. Experimental data	VI.3
3. The model	VI.5
4. Important features of the model	VI.8
5. Net radiation and wind function	VI.13
6. Verification of the model	VI.15
7. Conclusions	VI.19
VII. References	

Voorwoord

Geen proefschrift komt tot stand zonder steun van anderen. Ik wil daarom iedereen bedanken voor de hulp die zij mij verleenden.

Allereerst ben ik het KNMI zeer erkentelijk voor de vele faciliteiten die het mij heeft geboden. Zonder deze steun was dit proefschrift nooit tot stand gekomen.

Ik ben zeer dankbaar voor de begeleiding die mijn promotor, Bert Wartena, mij heeft gegeven. Bert, naast je wetenschappelijke steun, zijn je geduld, je doortastendheid op de juiste momenten en vooral je vriendschap van zeer veel waarde geweest.

Mijn co-promotor, Henk Tennekes, ben ik zeer erkentelijk voor de tijd en aandacht die hij aan mijn proefschrift heeft besteed. Ik het bijzonder bedank ik je voor je radactionele opmerkingen en adviezen. Deze zijn voor mij van zeer veel waarde geweest. Ook stel ik je stimulerende rol op prijs, die je als directeur Wetenschappelijk Onderzoek hebt gespeeld bij het tot stand komen van dit proefschrift.

Han Keijman en Bert Holtslag, mede auteurs van publicaties behorend bij dit proefschrift, bedank ik voor hun bijdrage en voor de prettige samenwerking.

Verder ben ik zeer erkentelijk voor de steun die ik van veel van mijn collega's heb gekregen en/of voor gegevens die zij mij beschikbaar hebben gesteld. Met name bedank ik Han Keijman, Wim Kohsiek, Wouter Slob, Anton Beljaars, Herman Wessels, Aad van Ulden, Frans Nieuwstadt en Ad Driedonks.

Een deel van dit onderzoek betreft metingen, die zijn verricht te Cabauw. Mijn dank gaat uit naar allen die hierbij betrokken zijn geweest. In dit verband is de steun die ik heb gekregen van de Instrumentele Afdeling onmisbaar geweest. Ik dank met name Arie Unlandt en de medewerkers van de Buitendienst. Verder ben ik erkentelijk voor de hulp van de medewerkers van de sectie Fysische Meteorologie, met name de inzet en steun van Rob Slikker en Gijs van Vliet heb ik zeer op prijs gesteld. Dit geldt ook voor de bijdragen van Erik Cornelissen en Paul Schotanus.

Ik bedank verder Drs. J.C. van der Vlucht van het R.I.D. en Ir. H.F. Kaltenbrunner van de Brabantse Biesbosch N.V. voor het beschikbaar stellen van watertemperatuurgegevens.

Een deel van dit onderzoek werd verricht op het Institut National de Recherche Agronomique te Versailles, waar ik eind 1981 twee maanden werk-

zaam ben geweest. De discussies die ik in die tijd met Alain Perrier en Bernard Itier heb gevoerd zijn voor mij van grote betekenis geweest.

Tot slot kom ik bij de vormgeving van dit proefschrift. Anja de Bree ben ik zeer veel dank verschuldigd voor de perfecte, en niet te vergeten, snelle wijze waarop zij het tikwerk heeft verzorgd. Verder dank ik de medewerkers van de tekenkamer en de drukkerij voor hun vakkundige bijdragen.

Samenvatting

Deze studie handelt over de verschillende componenten van de energiebalans van het aardoppervlak, waarbij het accent op praktische toepassingen ligt.

Het meest eenvoudige beeld van de energiehuishouding van het aardoppervlak is het volgende. Per seconde en per vierkante meter ontvangt het oppervlak een netto hoeveelheid stralingsenergie. Deze wordt voor een gedeelte door de zon geleverd; een ander deel is afkomstig van de atmosfeer (= infrarode straling afkomstig van wolken, waterdamp en CO_2). Deze "winstposten" moeten worden verminderd met de volgende "verliezen": (a) de door het oppervlak teruggekaatste straling en (b) de infrarode straling, die door het oppervlak zelf wordt uitgezonden. Uiteindelijk houden we een netto hoeveelheid stralingsenergie over, die aan het aardoppervlak ten goede komt. Deze wordt kortweg *nettostraling* genoemd. Aan het aardoppervlak wordt de nettostraling verdeeld in drie porties. Een portie wordt gebruikt om de bodem op te warmen (= de *bodemwarmtestroom*). Een tweede gedeelte wordt gebruikt om water te verdampen, dat meestal aanwezig is aan het oppervlak (= de *verdamping*). Tenslotte wordt een gedeelte van de nettostraling gebruikt om de atmosfeer van onderen af op te warmen (= *voelbare warmtestroom*).

In dit eenvoudige beeld zijn kleine termen verwaarloosd, zoals bijvoorbeeld de energie die de planten gebruiken voor fotosynthese.

Omdat water een hoge verdampingswarmte heeft is de verdamping vaak een belangrijke post op de energiebalans. Via de verdamping is de energiebalans gekoppeld aan de waterbalans van zowel de atmosfeer als het oppervlak.

Vanuit verschillende vakgebieden is men geïnteresseerd in de energiebalans van het aardoppervlak. Voorbeelden zijn de landbouw, de hydrologie en de meteorologie.

In de hydrologie heeft men belangstelling voor de gemiddelde verdamping op regionale schaal gemiddeld per dag of langer. Dit betreft in de meeste gevallen landoppervlakken, maar men is ook geïnteresseerd in de verdamping van meren en spaarbekkens. In dit verband kan de problematiek ten aanzien van thermische verontreiniging van oppervlaktewater worden genoemd. De industrie en energiecentrales gebruiken oppervlaktewater voor koeling. Hier-

door wordt het water kunstmatig opgewarmd. Een te hoge temperatuur is schadelijk voor de kwaliteit van het water. Om de temperatuursverhoging ten gevolge van kunstmatige opwarming te kunnen bepalen moet men de zogenaamde *natuurlijke watertemperatuur* berekenen. Dit is de temperatuur, die het water zou hebben bij afwezigheid van de kunstmatige opwarming. Het blijkt dat de natuurlijke watertemperatuur nauw samenhangt met de energiebalans aan het oppervlak. In hoofdstuk VI wordt een model behandeld, waarmee de energiebalans en de (natuurlijke) temperatuur van wateroppervlakken kunnen worden bepaald uit standaard weergegevens.

Ook in de landbouw is men geïnteresseerd in de verdamping. Zo wil men weten hoelang het duurt voordat een van buiten nat gewas opdroogt.

Verder bestaat er voor veel landbouwgewassen een verband tussen het waterverbruik van het gewas en de opbrengst. De opbrengst is maximaal, wanneer de verdamping potentieel is (= maximaal verder de gegeven weersomstandigheden). Verdamt het gewas niet potentieel, omdat de bodem te droog is, dan kan men de opbrengst vergroten door kunstmatige beregening toe te passen.

Voor dit soort van vraagstukken zijn eenvoudige meettechnieken nodig om de verdamping te kunnen meten. In hoofdstuk II wordt hier aandacht aan besteed.

Ontwikkelingen in de meteorologie van de laatste tien jaar hebben de belangstelling voor de energiebalans van het aardoppervlak vanuit dit vakgebied doen toenemen. Het blijkt dat in weersverwachtingsmodellen voor zowel korte (12-24 uur) als voor middellange (3-10 dagen) termijn de energieuitwisselingsprocessen aan de grond moeten worden beschreven. Dit betekent dat voor dit soort van toepassingen de energiebalans moet worden uitgedrukt in voorspelbare weergrootheden. Een dergelijk model (voor overdag) wordt in hoofdstuk III behandeld.

In de (micro)meteorologie bestaat belangstelling voor de atmosferische grenslaag. Dit is de onderste laag van de atmosfeer die direct door het aardoppervlak wordt beïnvloedt.

De dikte van deze laag varieert in de tijd. Na zonsopgang neemt deze dikte toe. De snelheid, waarmee dit gebeurt, hangt nauw samen met de hoe-

veelheid warmte die aan de grond in de atmosfeer wordt gebracht en dus met de energiebalans aan de grond. In hoofdstuk IV wordt deze samenhang beschreven, alsmede hoe de temperatuur en vochttoestand van de grenslaag afhangen van de energiebalans. Dit laatste is bijvoorbeeld van belang voor korte termijnverwachtingen van temperatuur en vocht.

De grenslaag is ongeveer de laag waarover luchtverontreiniging wordt verspreid. Is de grenslaag dik dan is de concentratie aan de grond van luchtverontreiniging relatief laag; is de grenslaag dun dan is daarentegen de grondconcentratie, en dus de overlast, hoog. Omdat de grenslaaghoogte samenhangt met de voelbare warmtestroom, speelt ook in luchtverontreinigingsvraagstukken de energiebalans van het aardoppervlak een rol.

In het algemeen kan men slechts beschikken over gegevens die op een standaard weerstation operationeel worden verzameld. Daarom komen veel praktische vragen neer op: "Hoe kan de energiebalans van het aardoppervlak worden bepaald uit standaard weergegevens?". In de hoofdstukken III en VI worden hier voor mogelijke oplossingen gegeven.

We zullen nu de verschillende hoofdstukken apart beschouwen.

Hoofdstuk II handelt over eenvoudige meetmethoden voor het bepalen van de verdamping en van de voelbare warmtestroom op routine basis. Deze worden vergeleken met een ingewikkelder techniek (de Bowen-verhouding methode), die algemeen als betrouwbaar wordt beschouwd.

Als eerste wordt de flux-profiel methode behandeld. Het blijkt dat deze voldoende nauwkeurige resultaten oplevert. Vereist worden metingen van de temperatuur op twee hoogten en van de windsnelheid op tenminste één niveau. Voor de verdamping is verder nog een meting (of schatting) van de nettostraling nodig.

Verder blijkt uit het onderzoek, dat in niet te droge gevallen, de bekende Penman formule ook goede schattingen van de etmaalgemiddelde verdamping oplevert. Een voorstel wordt gedaan om de profiel methode te combineren met de Penman formule.

Een nadeel van de profiel methode is dat nogal veel rekenwerk moet worden verricht, waarvoor een computer nodig is. Dit is een beperking als het om routine metingen gaat. Daarom hebben wij gezocht naar vereenvoudigde

berekeningswijzen. Deze worden in hoofdstuk II.3 behandeld. Met deze eenvoudige berekeningswijzen is het mogelijk de verdamping en de voelbare warmtestroom ter plaatse te bepalen uit de meetgegevens, bijvoorbeeld met een microprocessor.

Als tweede wordt in hoofdstuk II de temperatuurfluctuatiemethode behandeld. Deze is gebaseerd op het verband dat er bestaat tussen de intensiteit van de temperatuurfluctuaties en de voelbare warmtestroom (overdag). Dus uit de eerste kan men de tweede bepalen. Het gaat hier om snelle temperatuursveranderingen (binnen een seconde kan de luchttemperatuur op een bepaalde plaats enkele graden veranderen). De methode vereist daarom een kleine, snel reagerende thermometer. De methode levert zeer bemoedigende resultaten op. Het grote voordeel van de methode is dat slechts op één hoogte hoeft te worden gemeten.

Zowel de profiel- als de fluctuatiemethode zijn geschikt om te worden toegepast op een standaard weerstation, waarbij de laatste methode wellicht de voorkeur verdient. Op zo'n station zou dan in de toekomst de voelbare warmtestroom en de verdamping kunnen worden gemeten op operationele basis.

In hoofdstuk III worden twee modellen voor de verdamping en de voelbare warmtestroom met elkaar vergeleken. Beide hebben standaard weergegevens als invoer en een indicatie van de vochttoestand in de bodem. Het ene model bevat meer fysica, maar eist meer invoergegevens, terwijl het andere weinig fysica bevat, maar minder invoergegevens behoeft. Het blijkt dat beide modellen vergelijkbare resultaten opleveren. Voor sommige praktische toepassingen verdient daarom het eenvoudige model de voorkeur. Voor dit vergelijkend onderzoek werden micrometeorologische gegevens, verzameld te Cabauw, geanalyseerd.

Hoofdstuk IV is een beetje een buitenbeentje, omdat het een meer theoretisch karakter heeft. Hierin wordt een, door ons ontwikkeld, model gepresenteerd, waarmee onder andere de resultaten van hoofdstuk III kunnen worden verklaard. Het gaat om een gekoppeld grenslaag-energiebalans model. Het beschrijft het verloop overdag van de hoogte, de temperatuur en de vochtigheid van de grenslaag, alsmede de termen van de energiebalans, als de beginprofielen van temperatuur en specifieke vochtigheid bekend zijn

tezamen met de zonnestraling en de vochttoestand aan het aardoppervlak. Modeluitkomsten komen redelijk overeen met metingen.

De hoofdstukken V en VI handelen over wateroppervlakken. In hoofdstuk V wordt een empirisch verdampingsmodel (dat ook in hoofdstuk III wordt toegepast voor land) getoetst met hydrologische en meteorologische waarnemingen verricht boven het voormalige Flevomeer. Het model blijkt in de zomer goed te voldoen voor dagsommen. Echter, afwijkingen worden gevonden in het voor- en najaar en ook als het gaat om tijdsintervallen van 3 uur.

In hoofdstuk VI tenslotte wordt een model behandeld, waarmee de gemiddelde temperatuur en energiebalans van een meer kunnen worden berekend uit standaardweergegevens. De berekende en gemeten watertemperatuur van twee, vlak bij elkaar gelegen, waterreservoirs worden met elkaar vergeleken. Deze waterbekkens zijn ongeveer even groot, maar ze verschillen aanzienlijk in diepte (5 en 15 m). Dit is van belang, want de waterdiepte bepaalt mede de watertemperatuur.

De resultaten van de vergelijkingen, die enkele jaren betreffen, zijn bevredigend.

I. Introduction

1. Purpose and background.

This study is devoted to the energy balance of the earth's surface with a special emphasis on practical applications. A simple picture of the energy exchange processes that take place at the ground is the following. Per unit time and area an amount of radiant energy is supplied to the surface. This radiation originates partly from the sun, but another fraction is coming from the atmosphere (= infra-red radiation emitted by clouds, water vapour and CO_2). From these gain terms the following losses must be subtracted: (a) the reflected solar radiation and (b) the infra-red radiation emitted by the surface itself. The final result is that a net amount of radiant energy is received by the surface, simply denoted as net radiation. At the ground net radiation is used to heat the ground (soil heat flux), to evaporate liquid water (evaporation), and to heat the atmosphere (sensible heat flux). In this simple picture we have neglected minor terms such as the energy used by the plants for their photosynthesis.

Due to the high value of the latent heat of vaporization, the energy needed for evaporation is often an important term in the energy balance. In addition the energy balance of the earth's surface is linked with the water budget of both the atmosphere and the earth's surface, through the evaporation at the ground.

Several practical questions in agriculture, hydrology and meteorology require information on the energy balance of the surface. It is the purpose of this study to find solutions for some of these problems.

In hydrology one is mainly concerned in evaporation averaged over 1 day or more on a regional scale. Generally, this refers to land surfaces, but the evaporation of inland lakes or reservoirs is also of interest. In this context we also mention the problem of thermal pollution of open water bodies by industry or power plants. For this the so-called *natural* water temperature must be known, which is the temperature of the water in the hypothetical case that there is no artificial heating. It appears that this temperature depends mainly on the energy balance at the surface. In Chapter VI a model dealing with this problem is discussed.

I.2

In agriculture one is interested also in evaporation. Now time intervals ranging from half an hour to several days are of interest.

The relation between evaporation on the one side and plant diseases and pest control on the other can be mentioned.

Furthermore, the yield of several agricultural crops is the greatest when the evapotranspiration is potential (= a maximum under the given weather conditions). When the crop transpires less than the potential rate, because the soil is too dry, the yield can be augmented by artificial precipitation. For applications such as these cheap and simple techniques are required for measuring the actual and potential evaporation. This applies also to agricultural research projects, e.g. to determine yield-water use relationships.

In Chapter II simple measurement techniques are considered.

Recent developments in meteorology have led to an increase of the interest in the energy balance of the earth's surface, especially in the input of heat and humidity at ground level into the atmosphere. Examples are models for the atmospheric boundary layer and related models for short range weather forecasts (12-18 h ahead). These models require simple parameterizations of the surface fluxes. This applies also to weather forecast models on a medium time range (3-10 days ahead).

Since the height of the boundary layer is related to the heat input at the ground information on the surface energy balance is needed also for air pollution problems.

In Chapter III a simple parameterization for evaporation and sensible heat flux is described that can be used for these type of problems.

Usually, the only available data are standard weather observations. For that reason, many of the practical questions, mentioned above, can be formulated as: "How can the surface energy balance be estimated from standard weather data only?" In Chapters III and VI possible answers to that question are discussed.

Chapter II is devoted to simple measuring techniques that, in principle, can be used on an operational base. These methods will be compared with the so-called energy-balance method, using Bowen's ratio.

In Chapter III two models for evaporation and sensible heat flux during daytime are compared. Both require standard weather data as input and an indication of the surface wetness. The first model needs more data, but contains more physics. The second is less complete, but requires less input data.

Chapter IV has a mainly theoretical character. A model is presented that couples the evolution of the atmospheric boundary layer to the surface energy balance. It describes the course of the height, temperature and humidity of the boundary layer, together with the surface fluxes, when the initial profiles of temperature and humidity the radiative forcing and the surface wetness are known. It is restricted to convective conditions. Model output will be compared with observations.

In Chapter V an empirical evaporation model for open water is considered. Comparisons with observations of evaporation of the former Lake Flevo will be made; the annual and the diurnal cycle will be considered.

In Chapter VI a model for the (natural) temperature and energy balance of inland lakes and water reservoirs is discussed that requires standard weather data only. A comparison between the calculated and measured water temperature will be given. This concerns two adjacent water reservoirs, which have about the same size, but which differ in depth (5 and 15 m). This is of importance, since the water temperature also depends on water depth.

At some places we made new modifications, but most of the theoretical concepts applied in this study are adopted from literature. This is inherent in our practical approach. Some of the theories used have been available for many years. But, e.g. because no suitable instruments were available, they were not usefull for practical applications. Recent developments in the field of instrumentation and data handling have changed the situation to our advantage. A good example is the temperature fluctuation method for measuring the sensible heat flux

(discussed in II.4). The theoretical basis for this approach was given by Prandtl already in 1932. But for an experimental verification we had to wait until the sixties and early seventies. In that period instruments were developed to measure turbulent surface fluxes and fast temperature fluctuations, while also the data handling techniques were improved significantly. Finally, the method wouldn't be operationally until quite recently.

For the verification of the parameterizations, measuring techniques and models treated in this study, we used data collected at the 200 m mast at Cabauw, and at the nearby micrometeorological field, of the Royal Netherlands Meteorological Institute.

2. Editorial comments.

Except Chapters I and II this dissertation consists of parts that are published or submitted as individual journal papers. Unfortunately, it was not possible to keep the notation uniform. For that reason a list of symbols is added to each chapter. Each chapter also has its individual numbering of pages, figures and equations. The reader is cautioned that in some chapters the water vapor pressure e is used as moisture variable, while in others the specific humidity q is taken. This has consequences for the value and definition of related quantities, such as the psychrometric constant γ and the parameters describing saturated air.

II. Simple methods for the measurements of the surface fluxes of sensible heat and water vapor.

Abstract

The aim of this study is to investigate methods for the determination of the sensible heat flux density H and the evaporation E , which are applicable for routine, operational use. The first part is devoted to the standard flux profile method, with which H can be evaluated from observations of temperature (at 2 levels) and wind speed (at 1 or 2 levels). A comparison is made with the energy-balance method, using Bowen's ratio. The agreement appears to be acceptable, especially during daytime. Reliable estimates of daily evaporation are obtained from H , determined with the flux profile method, and additional observations of net radiation. A procedure is proposed to combine this approach with the Penman equation. The use of the latter must be preferred in rainy periods. In the second part simplifications of the standard flux profile method are presented. With these the data handling becomes so simple that the fluxes can be evaluated on the site with a microprocessor. Finally, the temperature fluctuation method is considered. This method is based on the fact that during daytime H is determined by the standard deviation of the temperature. It is concluded that this approach is very attractive for operational use.

II.2

List of symbols

$a_x = \frac{z_{x1}}{z_{x2}}$, $x = m$ or h	(-)
c_p specific heat of air at constant pressure	(J.kg ⁻¹ .K ⁻¹)
g acceleration of gravity	(m.s ⁻²)
h^* dimensionless heat flux	(-)
h_o^* value of h^* in free convection regime	(-)
h_o^* free convection constant	(-)
k von Karman constant	
n length of daytime	(h)
p_x empirical parameter (Fig. 10); $x = m$ or h	(-)
q specific humidity	(kg.kg ⁻¹)
q_* humidity scale	(kg.kg ⁻¹)
s slope of saturation spec. hum. - temp. curve	(K ⁻¹)
u horizontal wind speed	(m.s ⁻¹)
u_* friction velocity	(m.s ⁻¹)
w vertical wind speed	(m.s ⁻¹)
$x = (1 - 16 z/L)^{1/4}$	(-)
z height	(m)
z_o roughness length	(m)
z_x level at which wind ($x = m$ or u) or temperature ($x = h$) is observed	(m)
$z_x^* = \frac{z_{x1} - z_{x2}}{\ln(a_x)}$	(m)
B the Bowen ratio	(-)
C_1, C_2, C_3 constants	(-)
F_x defined by eq. (39); $x = m$ or h	(-)
G soil heat flux density	(W.m ⁻²)
H sensible heat flux density	(W.m ⁻²)
H_f value of H in the free convection regime	(W.m ⁻²)
H_o value of H when $\psi_m = \psi_h$ are taken zero (eq. 37)	(W.m ⁻²)
L Obukhov length	(m)
L_o defined by eq. (38)	

II.3

Q^*	net radiation	($W.m^{-2}$)
Ri	Richardson number	(-)
T	absolute air temperature	(K)
T_w	wet-bulb temperature	(K)
$\gamma = c_p/\lambda$		(K^{-1})
δe	saturation deficit	(mb)
θ	potential temperature	(K)
θ_*	temperature scale	(K)
λ	latent heat of vaporization	($J.kg^{-1}$)
ρ	air density	($kg.m^{-3}$)
σ_T	standard deviation of the temperature	(K)
τ	shearing stress	($N.m^{-2}$)
ϕ_x	stability function for heat ($x=h$), water vapor ($x=e$) or momentum ($x=m$)	(-)
ψ_x	idem, but in integrated flux - profile relations	(-)
$\left. \begin{array}{l} \Delta\theta, \\ \Delta u, \\ \Delta T, \\ \Delta T_w \end{array} \right\}$	vertical difference of θ , u , T and T_w	

1. Introduction

Many practical problems in meteorology, agriculture and hydrology require simple techniques to measure the sensible heat flux and evaporation from cropped surfaces. In meteorology one is mainly interested in the diurnal variation of these fluxes and therefore in this branch (half-) hourly values are required. On the other hand in hydrology the emphasis lays mainly on evapo(transpi)ration averaged over one day or longer. For agricultural purposes both half-hourly and daily values are of interest. In all application fields routine measurements are needed.

The requirements for the methods are:

- (i) the instruments must be robust so that they can withstand most weather situations and do not need complicated servicing.
- (ii) the datahandling must be so simple that the surface fluxes can be calculated from the observations on the spot, e.g. with a pocket calculator or a microprocessor.

In this study two methods will be considered that satisfy these requirements in principle, namely:

- (a) a simplified flux-profile method,
- (b) the temperature-fluctuation method.

Both techniques are based on the similarity theory of Monin and Obukhov (1954). Generally the governing equations of the methods have no analytic solution; they can only be solved with an iterative computation scheme for which a computer is indispensable. This does not satisfy the second requirement mentioned above. A large part of this study is devoted to approximative techniques that generate solutions that are accurate enough for practical calculations.

The reliability of the methods will be investigated by making comparisons with fluxes measured at Cabauw with the energy-balance method, using Bowen's ratio.

In section 2 the standard flux-profile method will be considered and a comparison with the energy-balance technique will be made.

In section 3 it will be shown how the flux-profile method can be simplified.

Finally in section 4 the temperature fluctuation method is treated.

2. The standard flux-profile method

2.1 Introduction

In the atmospheric surface layer, which extends from the ground to about one tenth of the atmospheric boundary layer, the vertical fluxes of momentum, sensible heat and water vapour are semiempirically related to the vertical gradients of temperature, horizontal wind speed and specific humidity. This is known already a long time. Many authors have developed methods for determining the fluxes according to profile measurements. A comprehensive review of the subject, both theoretical and experimental, have been given by Monin and Yaglom (1971, ch. 4). However, there are only a few publications which report on routine, operational applications of the approach. Examples are the recent papers of Stricker and Brutsaert (1978), Saugier and Ripley (1978), Grant (1975) and Itier (1981).

In this section we will follow the main lines of the work of Stricker and Brutsaert (1978) who used the flux-profile theory to determine the sensible heat flux, after which evaporation was evaluated from the simplified energy-balance equation. In this way they obtained the evaporation during a period of 90 days in the summer of 1976 from a catchment area in the Netherlands. However, they did not test their approach. In the present study the method of Stricker and Brutsaert will be investigated and a verification will be given for about 90 days in the summer of 1977. For this verification energy-balance measurements of the fluxes observed at Cabauw in the centre of the Netherlands will be used.

2.2 Theoretical background

On the basis of dimensional analysis Obukhov (1946, 1971) has shown that over horizontal uniform surfaces under stationary conditions the vertical fluxes of momentum, sensible heat and water vapour are related to the profiles of temperature, wind speed and humidity by

II.6

$$\frac{\partial \bar{\theta}}{\partial z} = \frac{\theta_*}{kz} \phi_h \left(\frac{z}{L} \right), \quad (1)$$

$$\frac{\partial \bar{q}}{\partial z} = \frac{q_*}{kz} \phi_e \left(\frac{z}{L} \right), \quad (2)$$

$$\frac{\partial \bar{u}}{\partial z} = \frac{u_*}{kz} \phi_m \left(\frac{z}{L} \right), \quad (3)$$

where the Obukhov length is defined by

$$L = \frac{T}{kg} \frac{u_*^2}{\theta_*} \quad (4)$$

and the friction velocity u_* by

$$u_* = \sqrt{\frac{\tau}{\rho}}. \quad (5)$$

Also the temperature (difference) and humidity scales θ_* and q_* follow from

$$H = -\rho c_p \theta_* u_* \quad (6)$$

$$E = -\rho u_* q_* \quad (7)$$

In eqs. (1)-(7) a bar denotes a mean value, θ is the potential temperature, q the specific humidity, ρ the density of air, c_p the specific heat at constant pressure of air, T the mean absolute temperature of the surface layer, g the acceleration of gravity, k the von Karman constant, u the horizontal wind speed, z the height, H the vertical flux density of sensible heat, τ the shearing stress and E the vertical flux density of water vapor (= evaporation). Finally ϕ_h , ϕ_e and ϕ_m are universal functions of the stability parameter $\frac{z}{L}$.

Monin and Obukhov (1954) were the first who presented experimental evidence for these relations. This is the reason that the literature refers to eqs. (1)-(3) as the Monin-Obukhov similarity theory. Since it is based on dimensional arguments, the theory does not predict the mathematical form of the ϕ -functions. Therefore this form has to be determined experimentally. In the last two decades many papers have been published on the structure of the ϕ 's. It is not useful to mention here the entire list of relevant references. Reviews on the subject are given in the standard textbooks by Lumley and Panofsky (1964) and Monin and Yaglom (1971) and in the papers by Dyer (1974) and Yaglom (1977). Unfortunately the mathematical form of the ϕ -functions is still uncertain, because it is difficult to measure the fluxes and profiles with sufficient accuracy.

Probably the best data set is that collected in Kansas in 1968, which is the basis for the flux-profile relations of Businger et al. (1971). However, their results deviate significantly from those obtained earlier by others, such as Dyer and Hicks (1970). The main discrepancies are the value of k (the Kansas measurements give $k = 0.35$, while most experiments yield $k \approx 0.4$) and the ratio ϕ_h/ϕ_m at $\frac{z}{L} = 0$ (≈ 1.35 found in Kansas, compared to 1 obtained by many others). Recently Wieringa (1980) gave a plausible explanation for these disagreements. He shows that obstacles in the Kansas mast have influenced the stress measurements. From his analysis it follows that u probably was underestimated 20-30%. When for this corrections are made k is found to be 0.41 while ϕ_h/ϕ_m at $\frac{z}{L} = 0$ becomes 1. After this revision the Kansas ϕ 's does not differ significantly from those obtained elsewhere.

In this study we will use the flux-profile relations proposed by Dyer (1974), which are also used by Stricker and Brutsaert (1978). They read as

$$k = 0.41 \quad (8)$$

$$\phi_m = \phi_h^{\frac{1}{2}} = \left(1 - 16 \frac{z}{L}\right)^{-\frac{1}{4}} \quad \text{for } \frac{z}{L} < 0, \quad (9)$$

(unstable case)

$$\phi_h = \phi_m = 1 + 5 \frac{z}{L} \quad \text{for } \frac{z}{L} > 0 \quad (10)$$

(stable case),

while

$$\phi_e = \phi_h \text{ for all } \frac{z}{L} \quad (11)$$

The Richardson number Ri is defined by

$$Ri = \frac{g}{T} \frac{\frac{\partial \bar{\theta}}{\partial z}}{\left(\frac{\partial \bar{u}}{\partial z}\right)^2} \quad (12)$$

From (9) it follows that in unstable conditions the Richardson number equals the stability parameter $\frac{z}{L}$:

$$Ri = \frac{z}{L} \quad (13)$$

In the surface layer the relative variation of the fluxes with height are negligibly small. Then the above flux-profile relations can be integrated. It is common to write the integrated form of the flux-profile relations in the form:

$$H = \frac{-\rho c_p k^2 \Delta \theta \Delta u}{\left[\ln\left(\frac{z_{h1}}{z_{h2}}\right) - \psi_h\left(\frac{z_{h1}}{L}\right) + \psi_h\left(\frac{z_{h2}}{L}\right) \right] \left[\ln\left(\frac{z_{m1}}{z_{m2}}\right) - \psi_m\left(\frac{z_{m1}}{L}\right) + \psi_m\left(\frac{z_{m2}}{L}\right) \right]} \quad (14)$$

and

$$u_* = \frac{k \Delta u}{\ln\left(\frac{z_{m1}}{z_{m2}}\right) - \psi_m\left(\frac{z_{m1}}{L}\right) + \psi_m\left(\frac{z_{m2}}{L}\right)} \quad (15)$$

Here $\Delta\theta = \bar{\theta}_1 - \bar{\theta}_2$ and $\Delta u = \bar{u}_1 - \bar{u}_2$, while z_{h1} and z_{h2} are the levels at which θ_1 and θ_2 are observed and z_{m1} and z_{m2} the heights of the wind measurements.

The functions ψ_m and ψ_h are defined by

$$\psi_m = \int_0^z \frac{1 - \phi_m\left(\frac{z'}{L}\right)}{z'} dz' \quad (16)$$

and

$$\psi_h = \int_0^z \frac{1 - \phi_h\left(\frac{z'}{L}\right)}{z'} dz' \quad (17)$$

From the set of equations (14)-(17) and the definition expressions (4) and (6) H and u_* can be solved iteratively when Δu and $\Delta\theta$ are known. It should be noted that in a complete formulation the buoyancy effects of water vapour have to be taken into account. This can be done by replacing θ_* by $\theta_*(1+0.07/B)$ in (4). Here $B(\equiv H/\lambda E)$ is the Bowen ratio (λ is the latent heat of vaporization). Over land surfaces the influence of E on H is generally less than 10% (see later). In the interests of simplicity we will ignore this effect.

We will apply the flux-profile method in its most simple form, namely in the case that the wind is observed at one and temperature at 2 levels. This is only possible for surfaces whose surface roughness length z_0 is known. Then our governing equations are:

$$H = \frac{-\rho c_p k^2 \Delta\theta u}{\left[\ln\left(\frac{z_1}{z_2}\right) - \psi_h\left(\frac{z_1}{L}\right) + \psi_h\left(\frac{z_2}{L}\right) \right] \left[\ln\left(\frac{z_u}{z_0}\right) - \psi_m\left(\frac{z_u}{L}\right) \right]}, \quad (18)$$

$$u_* = \frac{k u}{\left[\ln\left(\frac{z_u}{z_0}\right) - \psi_m\left(\frac{z_u}{L}\right) \right]}, \quad (19)$$

$$L = \frac{T}{gk} \frac{u_*^2}{\theta_*} \quad (20)$$

and

$$H = -\rho c_p u_* \theta_* \quad (21)$$

where θ is measured at z_1 and z_2 and u at z_u .[†]
(Eqs. (20) and (21) are the same as (4) and (6)).

From (9) and (10) and the definitions of the ψ 's it follows (Paulson, 1970) that for stable conditions ($\frac{z}{L} > 0$):

$$\psi_m = \psi_h = -5 \frac{z}{L}, \quad (22)$$

while for unstable conditions ($\frac{z}{L} < 0$):

$$\psi_h = 2 \ln \left[\frac{(1+x^2)}{2} \right], \quad (23)$$

$$\psi_m = 2 \ln \left[\frac{1+x}{2} \right] + \ln \left[\frac{1+x^2}{2} \right] - 2 \arctan(x) + \frac{\pi}{2} \quad (24)$$

where $x = (1 - 16 \frac{z}{L})^{\frac{1}{4}}$.

Generally this set of equations has no direct analytic solution and a time-consuming iterative procedure has to be followed [see e.g. Stricker and Brutsaert (1978) and Itier (1980)].

[†] In (18) and (19) we neglected $\psi_m\left(\frac{z_0}{L}\right)$.

2.2.1. Determination of E

After having determined H from (18)-(24) we can obtain E from the energy-balance equation:

$$Q^* - G = H + \lambda E, \quad (25)$$

in which Q^* is the net radiation and G the soil heat flux density. When the crop covers the ground completely G is generally small compared to Q^* in summertime. Then it is safe to neglect G when daily averages are considered, while G can be taken as

$$G = 0.1 Q^* \quad (26)$$

during daytime. The skill of (26) is rather good (De Bruin and Holtslag, 1982); it leads to a random scatter of about 5% in $Q^* - G$.

Adopting these approximations for G we arrive at the following estimates of E

$$\overset{-24}{\lambda E} = \overset{-24}{Q^*} - \overset{-24}{H_{pr}} \quad (27)$$

$\overset{-24}{X}$ means a 24-hourly average)

or

$$\lambda E = 0.9 Q^* - H_{pr} \quad (\text{daytime}) \quad (28)$$

valid during daytime. H_{pr} is H obtained with the profile method.

During nighttime, E is usually small, at least in summer. Then (28) can also be used to obtain a daily mean value of E:

$$\overset{-24}{\lambda E} = \left(0.9 \overset{-24}{Q^*} - \overset{-d}{H_{pr}} \right) \frac{n}{24} \quad (29)$$

where n is the duration of daytime (expressed in h).

In hydrological practice often the Penman equation is used to estimate the so-called potential evapo(transpi)ration.* For comparison purposes we will use this in the form

$$\frac{\lambda E_p}{24} = \frac{s(Q^* - G) + \gamma \cdot 7.4(0.5 + 0.54 u_2) \delta e}{s + \gamma}, \quad (30)$$

where s is the slope of the saturation specific humidity temperature curve, $\gamma = c_p/\lambda$, u the wind speed at 2 m and δe the saturation deficit. All variables in the right hand side of (30) are averaged over 24 h. For a background of this equation the reader is referred to Thom and Oliver (1977), De Bruin and Kohsiek (1979), Monteith (1981) and De Bruin (1982).

2.3 The energy-balance method, using Bowen's ratio

For comparison purposes in this study the fluxes determined with the well-known energy-balance method, using the Bowen ratio are used. This method is based (a) on the energy-balance equation (25):

$$Q^* - G = H + \lambda E, \quad (31)$$

and (b) on the fact that

$$\phi_h = \phi_e \quad \text{for all } \frac{z}{L} \quad (32)$$

(see eq. 11).

* This is the evapotranspiration of a certain crop when there is no shortage of water in the root zone.

Then it follows from (1), (2), (6) and (7) that the Bowen ratio $B \equiv H/\lambda E$ equals

$$B = \frac{c_p}{\lambda} \frac{\partial \bar{\theta} / \partial z}{\partial \bar{q} / \partial z} \quad (33)$$

Hence B can be determined from θ and q observed at 2 levels. When Q^* and G are measured also H and E then follows from

$$H = \frac{B}{1+B} (Q^* - G) \quad (34)$$

and

$$\lambda E = \frac{Q^* - G}{1+B} \quad (35)$$

The method breaks down when $Q^* - G = 0$, which is the case when $B = -1$. This can occur during the transition hours around sunset and sunrise.

Usually q is determined indirectly, e.g. with a psychrometer. This was the case in the Cabauw measurements discussed in the next section. Then B follows from

$$B = \left[\frac{\gamma + s}{\gamma} \frac{\Delta T_w}{\Delta T} - 1 \right]^{-1}, \quad (36)$$

where ΔT and ΔT_w are the vertical differences of the dry- and wet-bulb temperature respectively, s is the slope of the saturation specific humidity - temperature curve at T_w and $\gamma = \frac{c_p}{\lambda}$.

2.4 Experimental

In this study we will compare the fluxes evaluated with the standard flux-profile method with those determined with the energy-balance technique. For this we analysed a set of micrometeorological data

collected at Cabauw in the summer of 1977. The main features of this data set are:

- (a) The measurements were carried out at a field of 100 x 100 m covered with short grass of about 8 cm high. The surrounding fields are pastures.
- (b) The Bowen ratio was evaluated from the measurements of the dry- and wet-bulb temperature at 1.1 and 0.45 m. The thermometers used are ventilated and shielded. (Slob, 1978).
- (c) Net radiation was observed with a Funk-type pyrrometer.
- (d) The soil heat flux was determined with a method proposed by Slob (see De Bruin and Holtslag, 1982).
- (e) The wind speed was observed at 2 m with a cupanemometer.

The temperature and wind observations were used also to determine H with the profile approach.

The construction of daily means of the "energy-balance" fluxes was hindered by the fact that during the transition hours around sunset and sunrise the Bowen ratio often is near -1. Then H and E cannot be evaluated accurately with the energy-balance method. For these hours the lacking values of H and E were completed with those obtained with the flux-profile technique. In this way an artificial correlation between the two methods to be compared is introduced. However, because during these hours the fluxes are small this is a small effect.

2.5 The standard flux-profile method compared with the energy-balance approach

In this section the results of the flux-profile method are presented. It is applied as follows.

From the observed temperature at 0.45 and 1.1 m and the wind at 2 m H is evaluated every half hour by solving the set of equation (18)-(24)

iteratively. Then daily and daytime mean values, denoted as \overline{H}^{-24} and \overline{H}^{-d} respectively, were computed, where "daytime" is defined to be the period in which $Q^* > 0$. Finally the daily mean values of λE , denoted as $\overline{\lambda E}^{24}$, are evaluated with (27) and (29) respectively.

The roughness length is taken at $z_0 = 1$ cm, which is a representative value for grass of 8 cm high (Stricker and Brutsaert, 1978).

The influence of E on the Obukhov-length is not taken into account. From Fig. 1, where \overline{H}^d calculated with and without this effect is depicted, it is seen that this is permitted. It leads to an underestimation of \overline{H}^d of only a few percent.

We did not use a displacement height d as done by Stricker and Brutsaert (1978). This is perhaps questionable because our lowest observation level is 0.45 m which is not very large compared with the crop height. On the other hand we believe that the physical meaning of d , especially for sensible heat, is so unclear that it must be preferred to work as long as possible with only one parameter characterizing the surface, namely z_0 . We believe that in our case this has to be done. It is noted that the introduction of $d = 5$ cm, which is a representative value for a crop height of 8 cm (Brutsaert and Stricker, 1978), has the same effect as the lowering of z_0 from 1 to 0.6 cm.

In Fig. 2 the flux-profile measurements of \overline{H}^{-24} are compared with the corresponding energy-balance observations. This figure refers to about 90 days in May through August 1977. The agreement is rather good, but there is a tendency that the profile-measurements are greater than the energy-balance observations.

In Fig. 3 the results for the daily means of H are depicted. Again there is a good agreement, but now the profile method underestimates \overline{H}^d slightly with about 10% (when it is believed that the energy-balance observations are the "true" values). On these features we will comment later.

The results of eqs. (27) and (29) concerning the daily means of λE are presented in Figs. 4 and 5. Both show good agreement, even better than

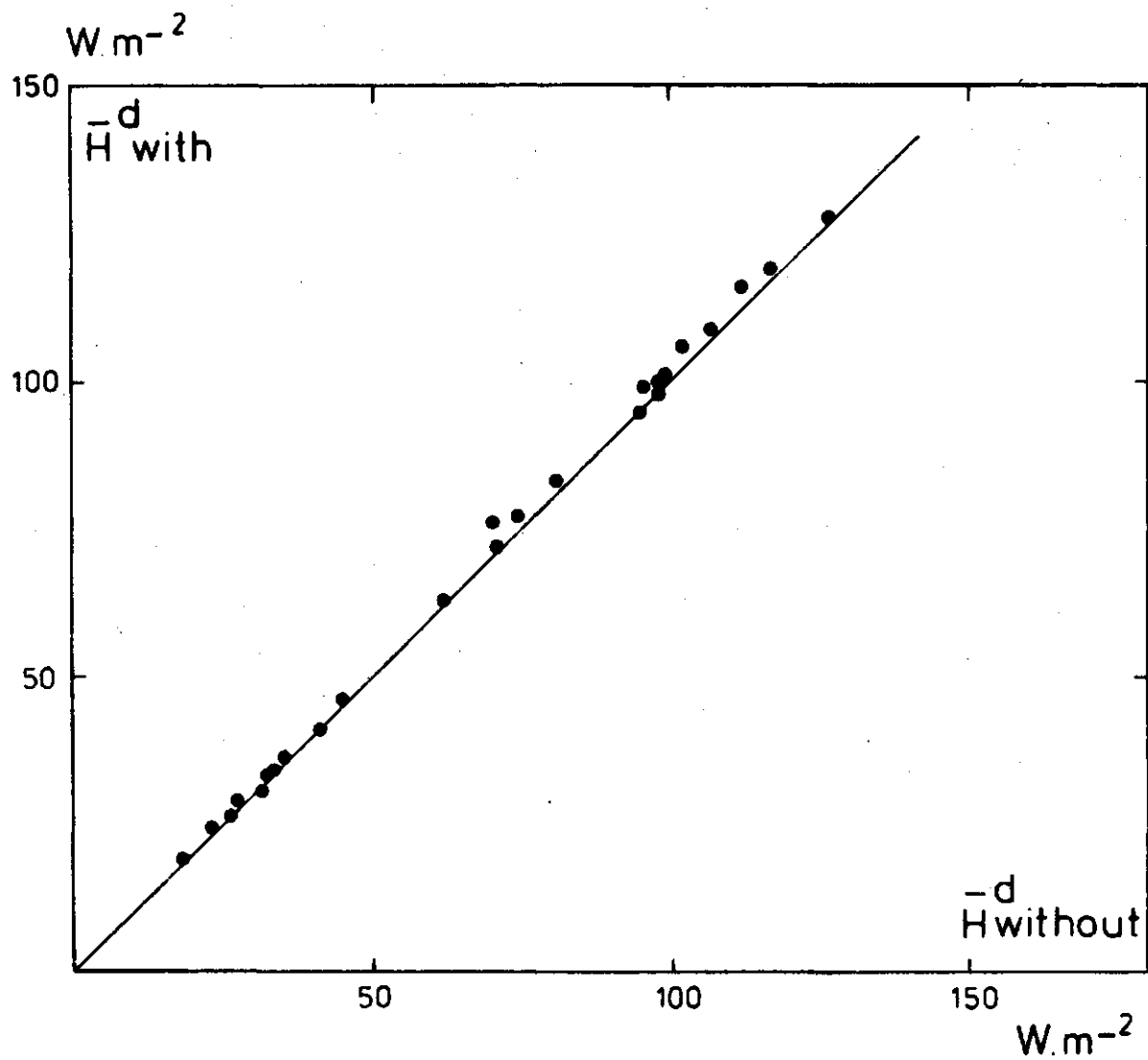


Fig. 1. Comparison between \bar{H}^d computed with and without the water vapor correction in L.

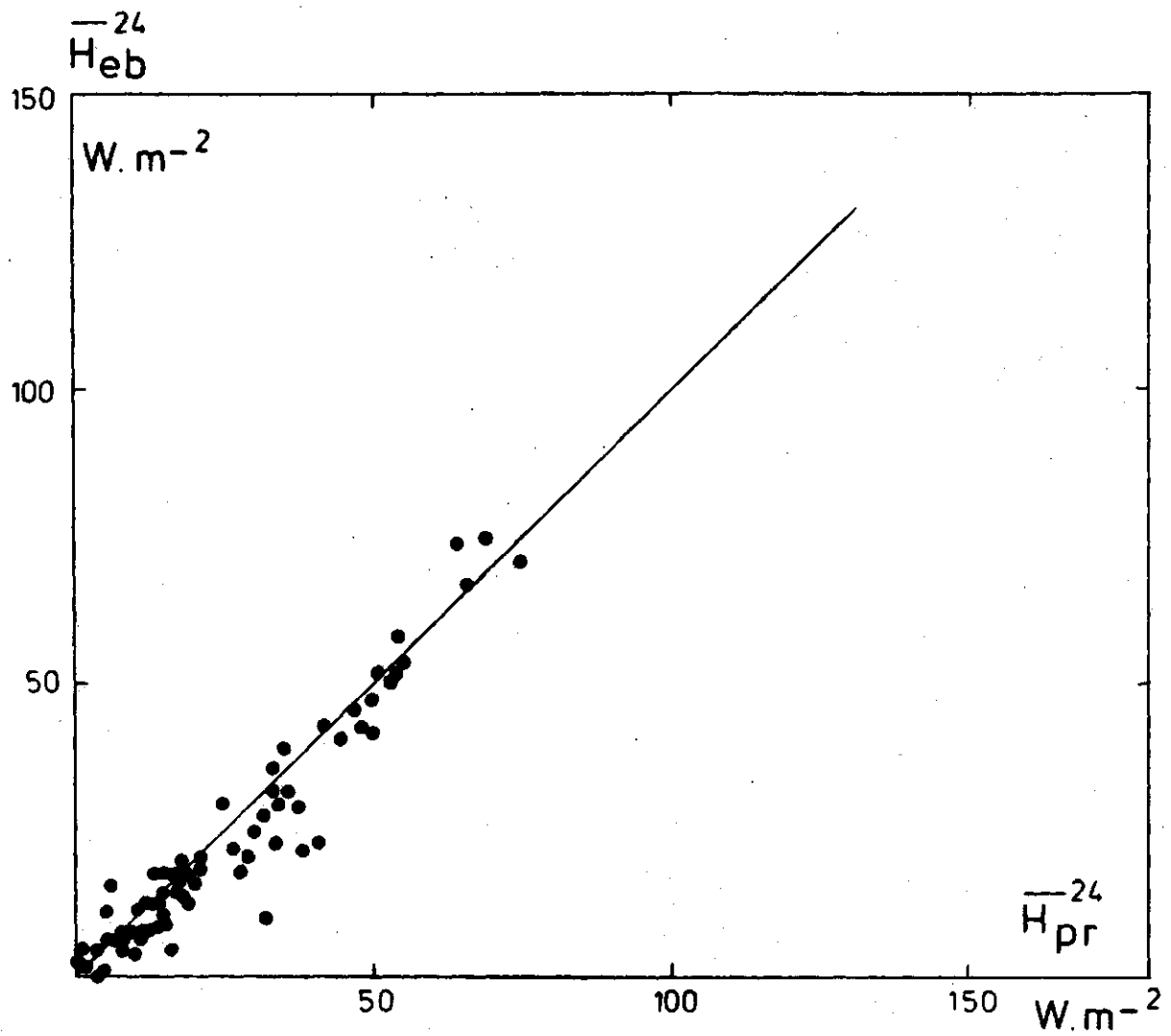


Fig. 2. Daily mean of H (\overline{H}^{24}) computed with the flux profile method vs the energy-balance observations of \overline{H}^{24} .
Cabauw, May through September 1977.

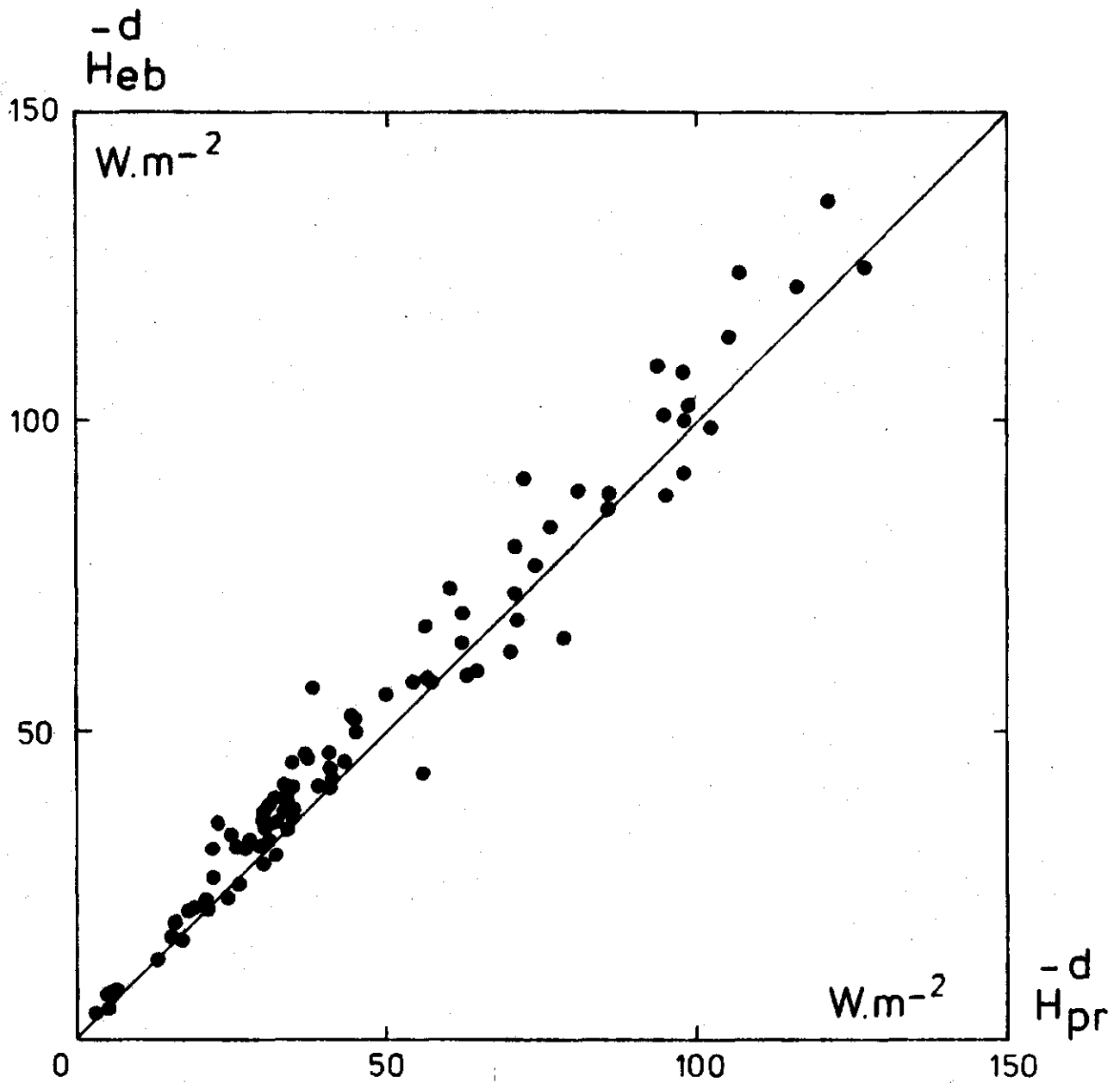


Fig. 3. As Fig. 2, but for \overline{H}^d (daytime mean of H ; $Q^* > 0$).

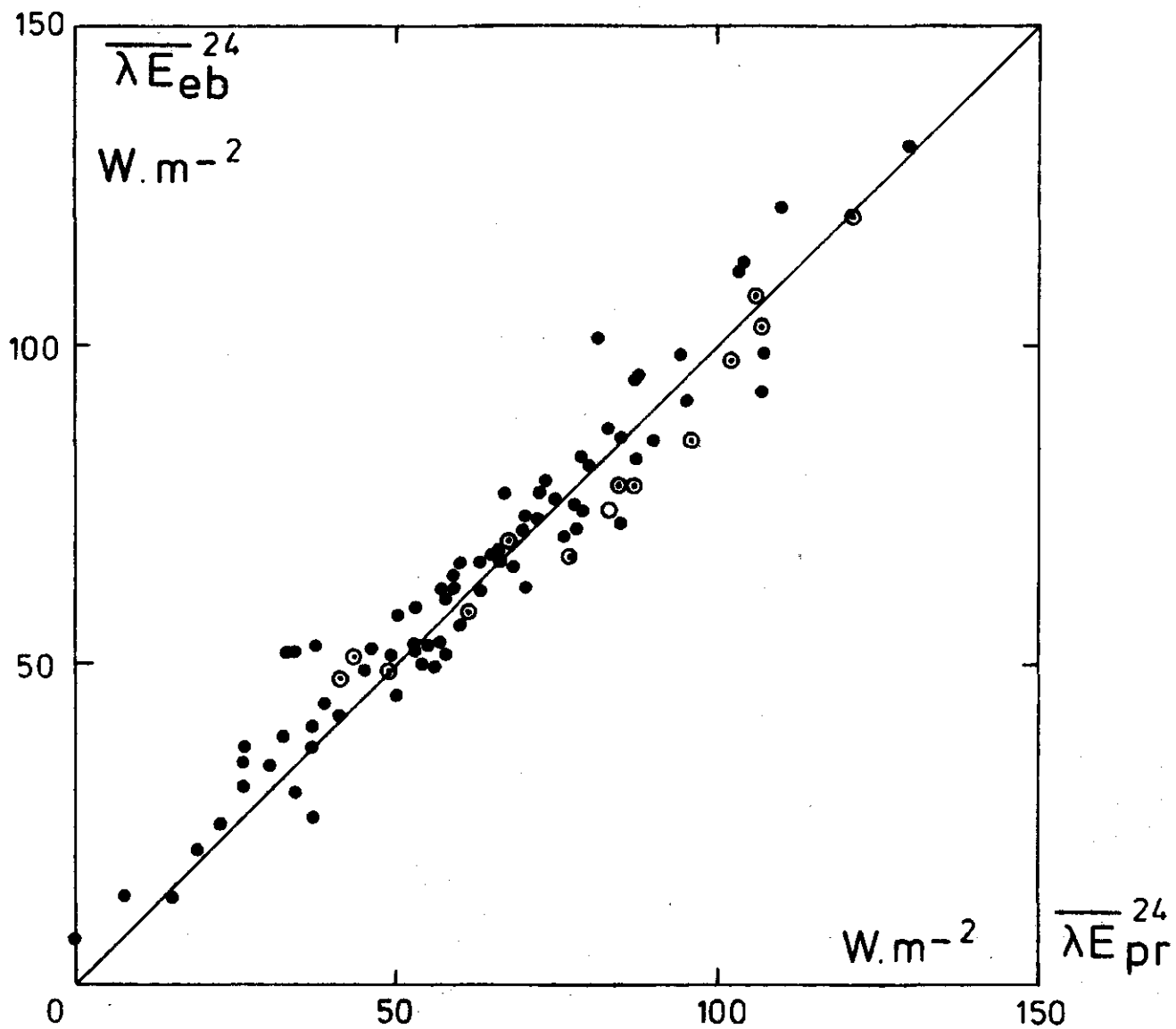


Fig. 4. $\overline{\lambda E}^{24}$ evaluated with (eq.27) vs the energy-balance observations.
The data from the dry period 3-17 July 1977 are encircled.

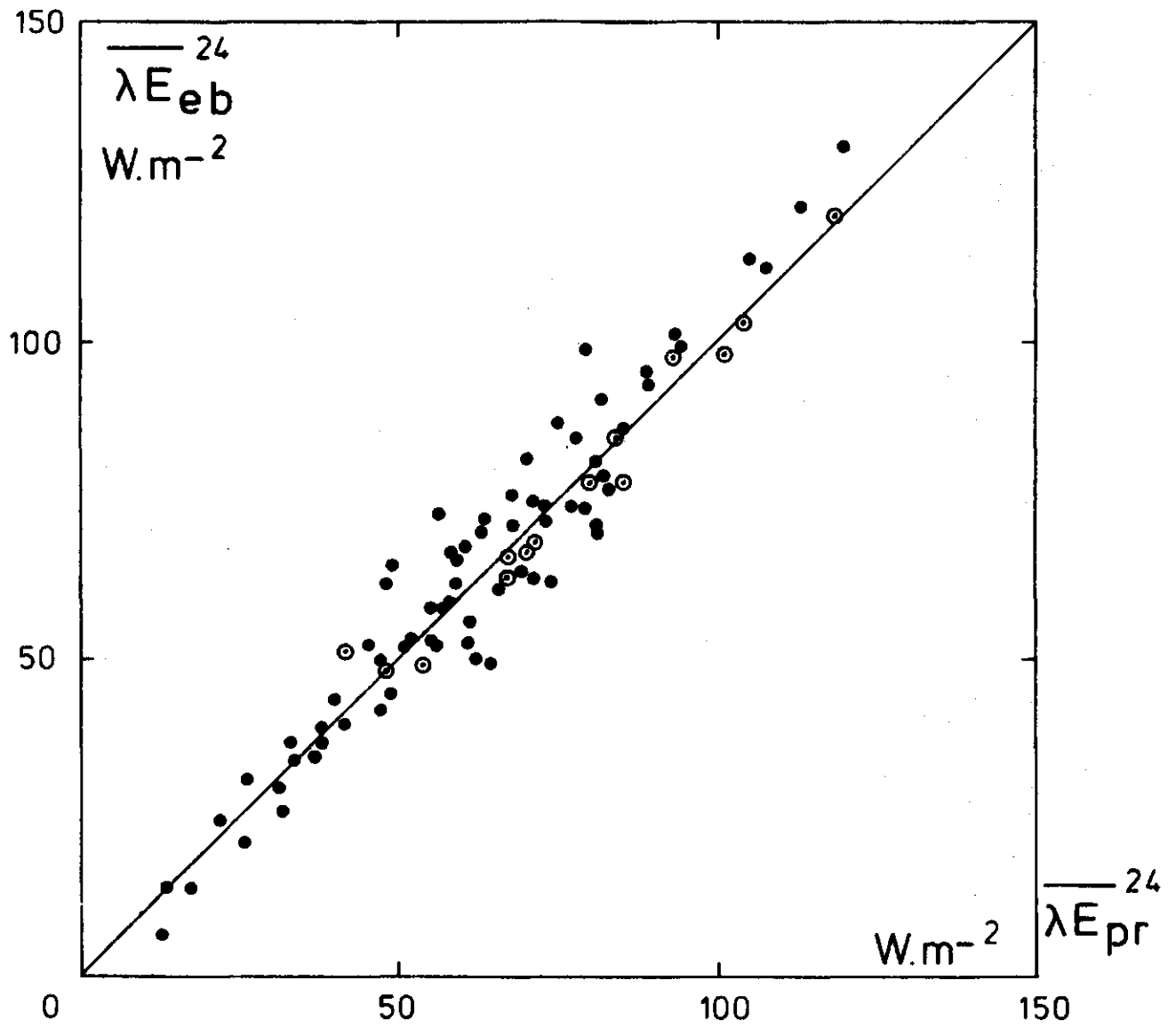


Fig. 5. As Fig. 4, but now $\overline{\lambda E}^{24}$ evaluated with eq. (29).

that obtained for H . A plausible explanation for this is the fact that usually $\lambda E > H$, so that an error in H causes a much smaller deviation in λE . But it must also be noted that the λE 's compared in Figs. 4 and 5 have the measured net radiation in common.

—24

In Fig. 6 the energy-balance observations of λE are compared with the corresponding values evaluated with Penman's equation (30). It is seen that, except for about twenty days, the agreement is good. Most of the days for which (30) gives too great values fall in the period 3-17 July during which there was a clear shortage of water in the soil (see also De Bruin and Holtslag, 1982). The data of these period are encircled in Figs. 4-6.

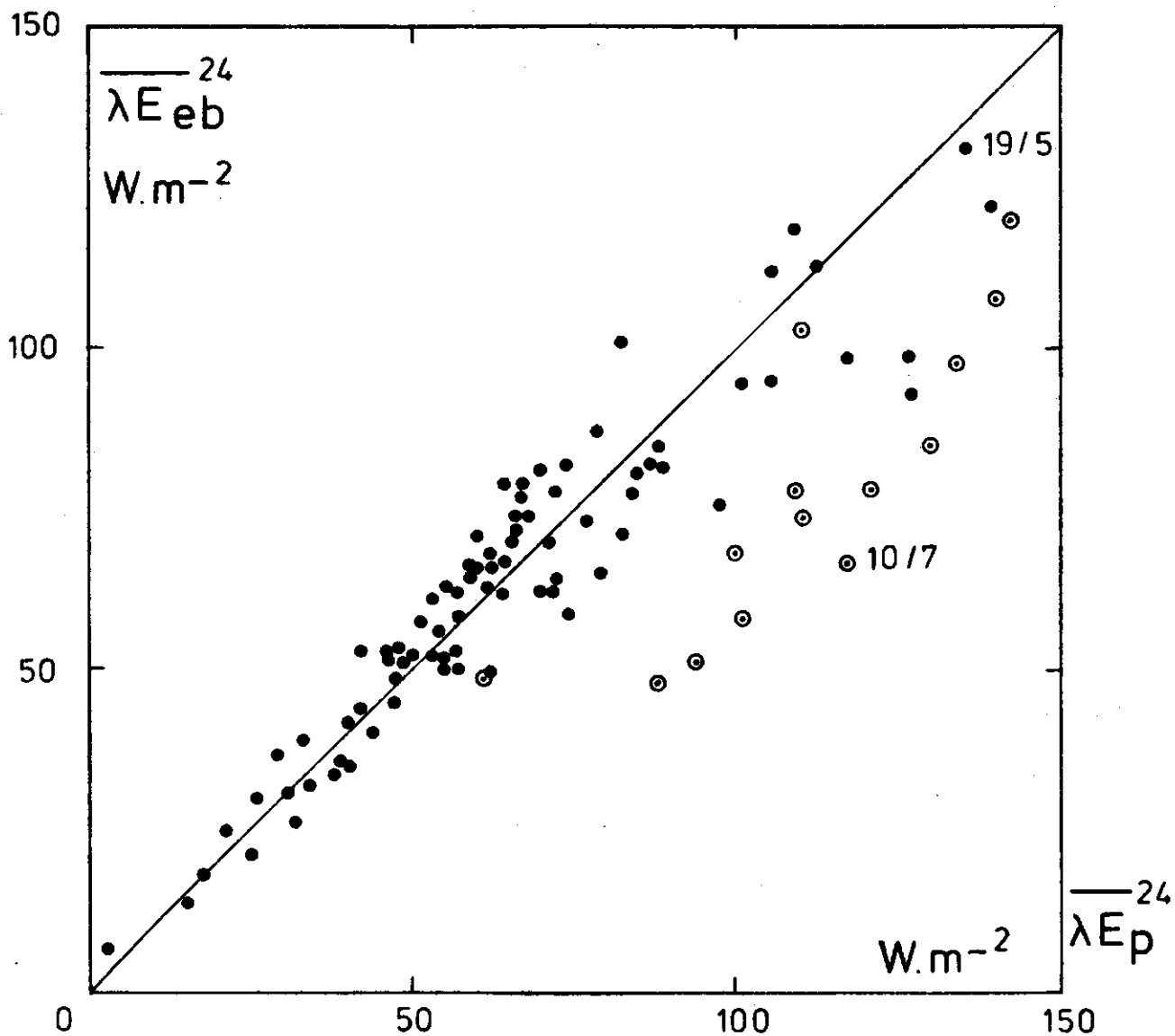


Fig. 6. Energy-balance measurements of $\overline{\lambda E}_{eb}^{24}$ vs $\overline{\lambda E}_p^{24}$ computed with Penman's equation (30). Data from the dry period 3-17 July are encircled.

2.6 Discussion

From the above it follows that the daytime means of H , evaluated with the flux-profile method, agree rather well with the energy-balance observations, while the 24-hourly values show more deviations. This implies that during nighttime the two methods do not yield similar fluxes. An explanation for this is the fact that under stable conditions it is very difficult to carry out reliable measurements. For instance, because all fluxes then are small, systematic errors in Q^* and G , which easily can be of the order of 10 W.m^{-2} , cause large percentual errors in the derived values of H and E . Moreover, the thermometers are often wetted by fog which is rather likely during the night and early morning. This reflects directly on both the results of the profile and the energy-balance method.

From this it must be concluded that it is very difficult to measure the surface fluxes under stable conditions on a routine basis. For this study it means that our results for the nighttime are inconclusive.

The uncertainties of the nighttime observations, of course, also reflect on the daily means of the measured fluxes. On nice summer days the daytime fluxes highly exceed those at night, so that on these days this effect on \overline{H}^{24} and \overline{AE}^{24} is small. However, on rainy overcast days this is no longer true. Moreover, then also during daytime the observations can easily be disturbed, e.g. due to wetting of the thermometers by rain. Although we exclude the days with pertinently erroneous data, there are certainly days which are not rejected but which contain hours with less reliable observations. We could not reject all these data because then it is impossible to construct daily and daytime mean values.

These feature can explain the relatively large scatter shown in Fig. 2 and 3 for \overline{H}^{24} or \overline{H}^d less than 40 W.m^{-2} , because those data refer mostly to rainy overcast days which were rather numerous especially in August 1977.

The experimental difficulties mentioned above are inherent in micrometeorological observations carried out on a routine basis in the Dutch climate. As far as we know there exist no techniques for measuring the surface

fluxes continuously which do not give problems during e.g. fog and rain.

If we take this into account and when we consider the results obtained for the days with \overline{H}^{24} or \overline{H}^d greater than 40 W.m^{-2} , which are of great importance for e.g. evaporation (see later), we may conclude that the flux-profile method yields acceptable results.

Let us now pay our attention to the daily evaporation. We note that the results shown in Figs. 4 and 5 are accurate enough for most practical applications. This is in agreement with the findings of Grant (1975). Also the Penman equation (30) yields good results, except in the dry July period (encircled points in Fig. 6).

Because the input data for Penman's equation are less sensitive to influences of unfavourable weather conditions a logical consequence of this is to combine the profile-method with the Penman approach for the determination of \overline{E}^{24} .

We propose the following procedure:

- (a) On days with rain or preceded by a rainy period the evaporation will not deviate much from its potential value and \overline{E}^{24} can be evaluated with the Penman formula (30).
- (b) On dry days E can be about E_p , but it is also possible that $E < E_p$. It appears that in the latter case the Bowen ratio is greater than 0.4 at the midday. With $G = 0.1 Q^*$ this implies that then $H \geq 0.25 Q^*$. Thus when E is considerably smaller than E_p H will be larger than $0.25 Q^*$. Adopting this criterium we arrive at the following:
When around noon H evaluated with the profile method exceeds $0.25 Q^*$ \overline{E}^{24} is determined with (29). Otherwise \overline{E}^{24} is computed with Penman's formula (Eq. 30).

The advantage of this approach is that the profile method now is applied only on dry days, i.e. under favourable weather conditions.

We found that a visual inspection of the diurnal course of $\Delta\theta$ can be of help to distinguish days for which $E \approx E_p$ from days where $E < E_p$. To make this clear the course of $\Delta\theta$ and Q^* is shown in Fig. 7 for two clear days. The first, 19 May 1977, is preceded by a rainy period of several days and consequently $\overline{E}^{24} \approx E_p$ (see Fig. 6). The second, 10 July 1977, falls in the dry July period described above.

It is seen that the net radiation of these days is almost the same, but the $\Delta\theta$ curves differ significantly. On 19 May $\Delta\theta$ does not exceed 0.65 K, while at 10 July $\Delta\theta > 0.8$ K during several hours. Furthermore it is striking that on 19 May $\Delta\theta$ becomes zero at the end of the day earlier than Q^* , whereas on 10 July $\Delta\theta$ and Q^* pass about simultaneously the zero-line.

These features, which are rather typical, can be used to distinguish visually days for which $E \approx E_p$ from those where $E < E_p$.

The above results refer to a short vegetation. Above a tall crop (heights ≥ 1 m) growing in small fields the method will be less applicable, because one must require that the observations are done in the internal boundary layer. Therefore we must demand: (a) the observation levels are larger than z_0 ($\frac{z}{z_0} \geq 50$) and (b) these are small with respect to the length (or width) of the field l ($\frac{l}{z} \geq 100$). These requirements are difficult to fulfill for tall crops growing in relatively small fields.

Furthermore, in the case of a tall vegetation it is no longer permitted to ignore the displacement height d . However, this is a very uncertain quantity (Reitsma, 1978). When the field of interest is small the lowest observation level can not be chosen much greater than d . This implies that then the uncertainty of d can cause considerable errors in the computed fluxes.

These features are serious restrictions of the profile method.

In section 4 a method is discussed, which is more attractive above tall vegetations.

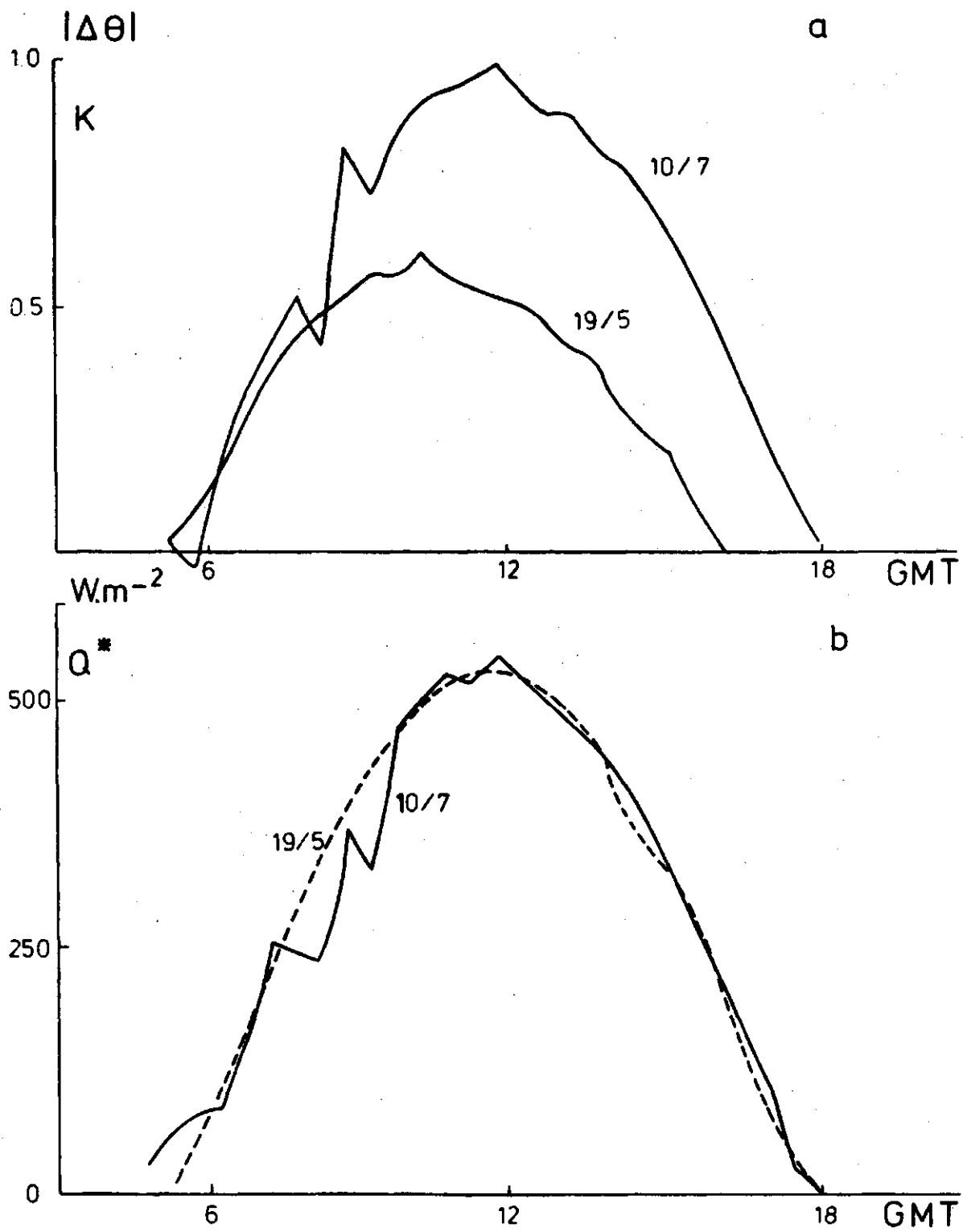


Fig. 7. Course of $\Delta\theta$ and Q^* for 19 May 1977 ($E \approx E_p$) and 10 July 1977 ($E < E_p$).

2.7 Conclusions

The main conclusions concerning the profile method are:

- (a) Above short vegetations (crop heights smaller than 0.5 m) the fluxes of sensible heat and water vapour can be measured accurately enough for most practical applications with the profile method.
This conclusion refers to daytime values of H and E and daily means of E.
- (b) The results referring to nighttime are inconclusive, because then the energy-balance method does not yield reliable results. At the moment there are no methods known to measure H and E on a routine base during nighttime.
- (c) For the determination of daily evaporation it is recommended to combine the profile-method (Eq. 29) with the Penman approach (Eq. 30): On "potential" days ($E \approx E_p$) the latter and on "non-potential" days ($E < E_p$) the first must be used. A visual inspection of the diurnal course of the vertical temperature difference $\Delta\theta$ can be of help to distinguish "potential" and "non-potential" days.
- (d) These results refer to short vegetations. For tall crops (heights ≥ 1 m) it is to be expected that the profile method meets difficulties because the observed profiles then are likely to be non-representative for the field of interest. This concerns especially small fields (less than 1 ha). Also the uncertainty of the displacement height is then a serious restriction of the profile method.

3. Simplifications of the standard flux profile method

3.1 Introduction

In section 2 it was shown how the sensible heat flux and evaporation can be obtained from the profiles of temperature and wind. It was seen that especially during daytime this approach yields good results. For a number of practical applications the complicated iteration scheme to be used to solve the governing equations is very inconvenient. For instance it is much too time-consuming in atmospheric modelling (Louis, 1979). Also the scheme is not useful when the fluxes must be evaluated on the site with a microprocessor or a pocket calculator.

In this study methods will be developed which enable us to simplify the calculation scheme significantly, so that this is applicable for practical purpose.

We will restrict ourselves to the unstable case, because then the profile method yields the best results.

3.2 Mathematical background

In this section we will rewrite the equations for H and L in such a way that approximative analytic solutions can be obtained. We assume that the Dyer relations for ϕ_m and ϕ_h are the best (and consequently the corresponding ψ 's given by (23) and (24)).

Let θ be observed at z_{h1} and z_{h2} and u at z_{m1} and z_{m2} and let us introduce $a_m \equiv z_{m1}/z_{m2}$ and $a_h \equiv z_{h1}/z_{h2}$. We will choose $z_{x1} > z_{x2}$, so that $a_x > 1$ ($x = m$ or h).

Also we define the quantities H_o and L_o by

$$H_o = \frac{k^2 \rho c_p |\Delta\theta| \Delta u}{\ln(a_h) \ln(a_m)} \quad (37)$$

and

$$L_o = \frac{T}{g} \frac{(\Delta u)^2}{\Delta\theta} \frac{\ln(a_h)}{\ln^2(a_m)}, \quad (38)$$

where $\Delta\theta = \theta_1 - \theta_2$ and $\Delta u = u_1 - u_2$.

H_0 and L_0 are the sensible heat flux density H and the Obukhov-length L respectively when the stability corrections are neglected, i.e. when the ψ 's in (18) and (19) are taken zero.

Furthermore we define

$$F_x = 1 - \frac{\psi_x\left(\frac{z_{x1}}{L}\right) - \psi_x\left(\frac{z_{x2}}{L}\right)}{\ln(z_{x1}) - \ln(z_{x2})} \quad (x = m \text{ or } h) \quad (39)$$

Then H and L can be written as (see eqs. 4, 14 and 15)

$$H = \frac{H_0}{F_h F_m} \quad (40)$$

and

$$L = L_0 \frac{F_h}{F_m} \quad (41)$$

Now we apply Cauchy's theorem for the mean value^{*}. This gives with

$$\left(\frac{\partial \psi_x}{\partial z}\right)_{z'} = (1 - \phi_x\left(\frac{z'}{L}\right))/z':$$

$$F_x = \phi_x\left(\frac{z_{x'}}{L}\right), \quad (x = m \text{ or } h), \quad (42)$$

where $z_{x'}$ is a level between z_{x1} and z_{x2} .

^{*} If $f(x)$ and $g(x)$ are regular in the interval a, b there is at least one value of x' with $a < x' < b$ for which $\frac{f(b) - f(a)}{g(b) - g(a)} = \frac{f'(x')}{g'(x')}$ ($g'(x') \neq 0$ inside a, b).

Consequently

$$H = \frac{H_0}{\phi_m\left(\frac{z'_m}{L}\right) \phi_h\left(\frac{z'_h}{L}\right)} \quad (43)$$

and

$$L = L_0 \frac{\phi_h\left(\frac{z'_h}{L}\right)}{\phi_m^2\left(\frac{z'_m}{L}\right)} \quad (44)$$

Under unstable conditions $\phi_h = \phi_m^2$ (eq. 9), so that then

$$L = L_0 \frac{\phi_h\left(\frac{z'_h}{L}\right)}{\phi_h\left(\frac{z'_m}{L}\right)} \quad (L < 0) \quad (45)$$

From (45) we obtain our first important results namely when $z'_h \approx z'_m$

$$L \approx L_0, \quad (z'_h \approx z'_m) \quad (46)$$

and consequently

$$H = \frac{H_0}{\phi_m\left(\frac{z'}{L_0}\right) \phi_h\left(\frac{z'}{L_0}\right)} = H_0 (1 - 16 \frac{z'}{L_0})^{3/4}, \quad (47)$$

where $z' = z'_h = z'_m$ and use has been made of (9).

The levels z'_h and z'_m will be about equal when θ and u are observed at the same levels. Thus we conclude that when temperature and wind are measured at the same height L can be estimated directly from the observations with (38) and (45). It is noted that z' in (47) is still unknown.

Several authors found (46) experimentally (Soer, 1977; Riou, 1982).

Generally z_h' and z_m' depend on L and a_h or a_m . From (42) and the Dyer relations (9) for the ϕ 's we find that

$$z_x' = \frac{|L|}{16} (F_x^{-n} - 1), \quad (x = m \text{ or } h) \quad (48)$$

where $n = 2$ when $x = h$ and $n = 4$ when $x = m$.

For $-L \rightarrow \infty$ $\psi_h \rightarrow 8 \frac{z}{-L}$ and $\psi_m \rightarrow 4 \frac{z}{-L}$, so that

$$\lim_{-L \rightarrow \infty} z_x' = \frac{z_{x1} - z_{x2}}{\ln(a_x)} \equiv z_x^*. \quad (x = m \text{ or } h) \quad (49)$$

This result is not surprising because when $-L$ is large the profiles becomes logarithmic.

From (48) and (49) it follows that z_x'/z_x^* is a function of z_x^*/L and a_x only.

In Figs. 8a and b z_h' and z_m' scaled with z_x^* are depicted as a function of $-z_x^*/L$ for different values of a_x . It is seen that when $a_h = a_m$ $z_h' < z_m'$, but the differences are small.

If $a_x \leq 6$ the variation of z_h' and z_m' with z^*/L is relatively small, so that for many practical applications it is safe to take these levels constant in that case.

Some authors, e.g. Itier (1980) and Riou (1982) use in this type of problems (see also Paulson, 1970)

$$z_x' = \sqrt{z_{x1} \cdot z_{x2}}. \quad (x = m \text{ or } h) \quad (50)$$

In Fig. 8a this estimate of z_h' (scaled with z_h^*) is indicated (with the symbol Δ). It is seen that it is situated in the centre of the interval over which the actual value of z_h' is varying for all $a_h \leq 100$. Consequently (50) is a proper choice for the case that $a \leq 6$.

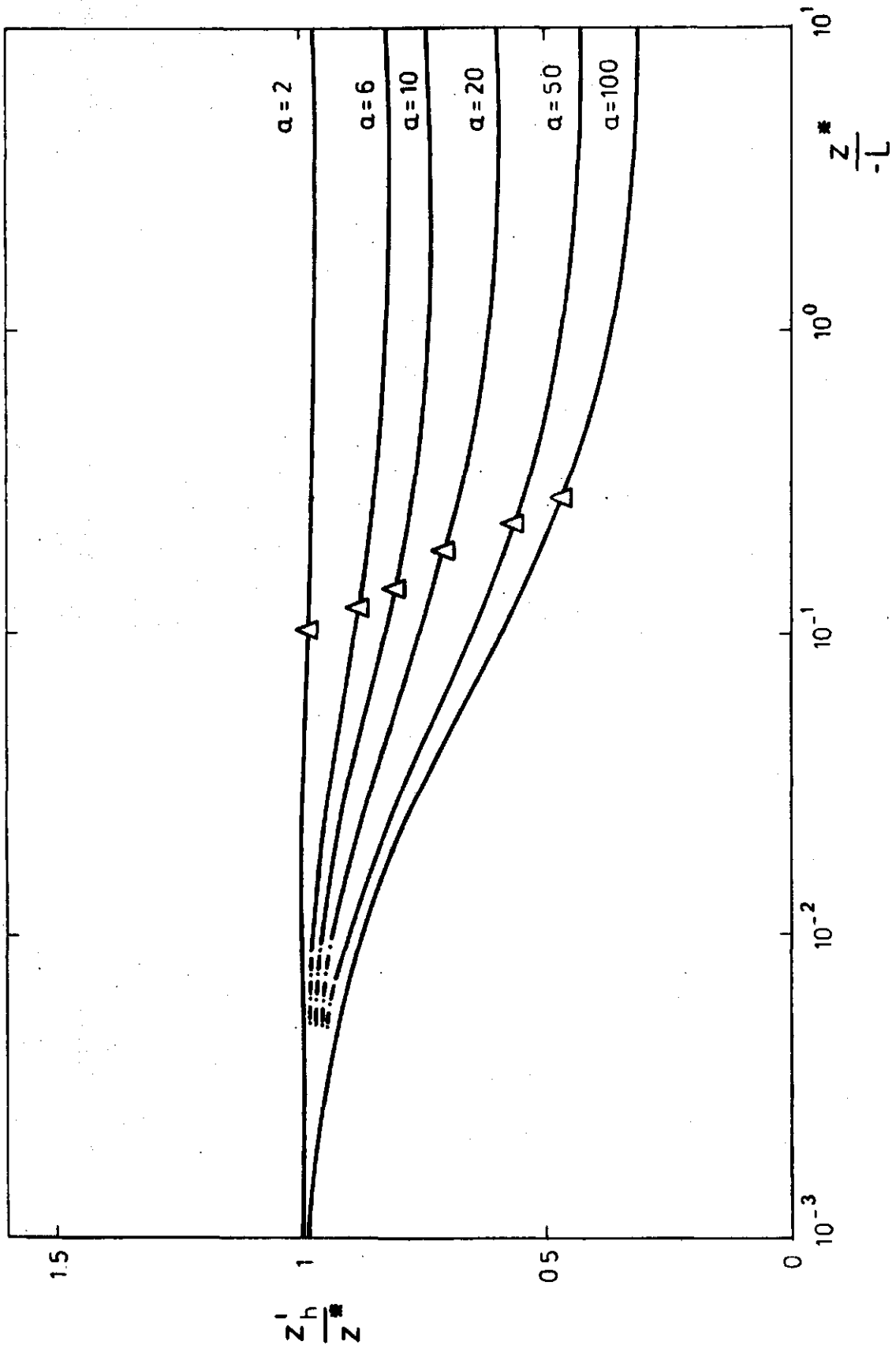


Fig. 8a. z_h^i/z_h^* as a function of z^*/L ($L < 0$) for different values of α .

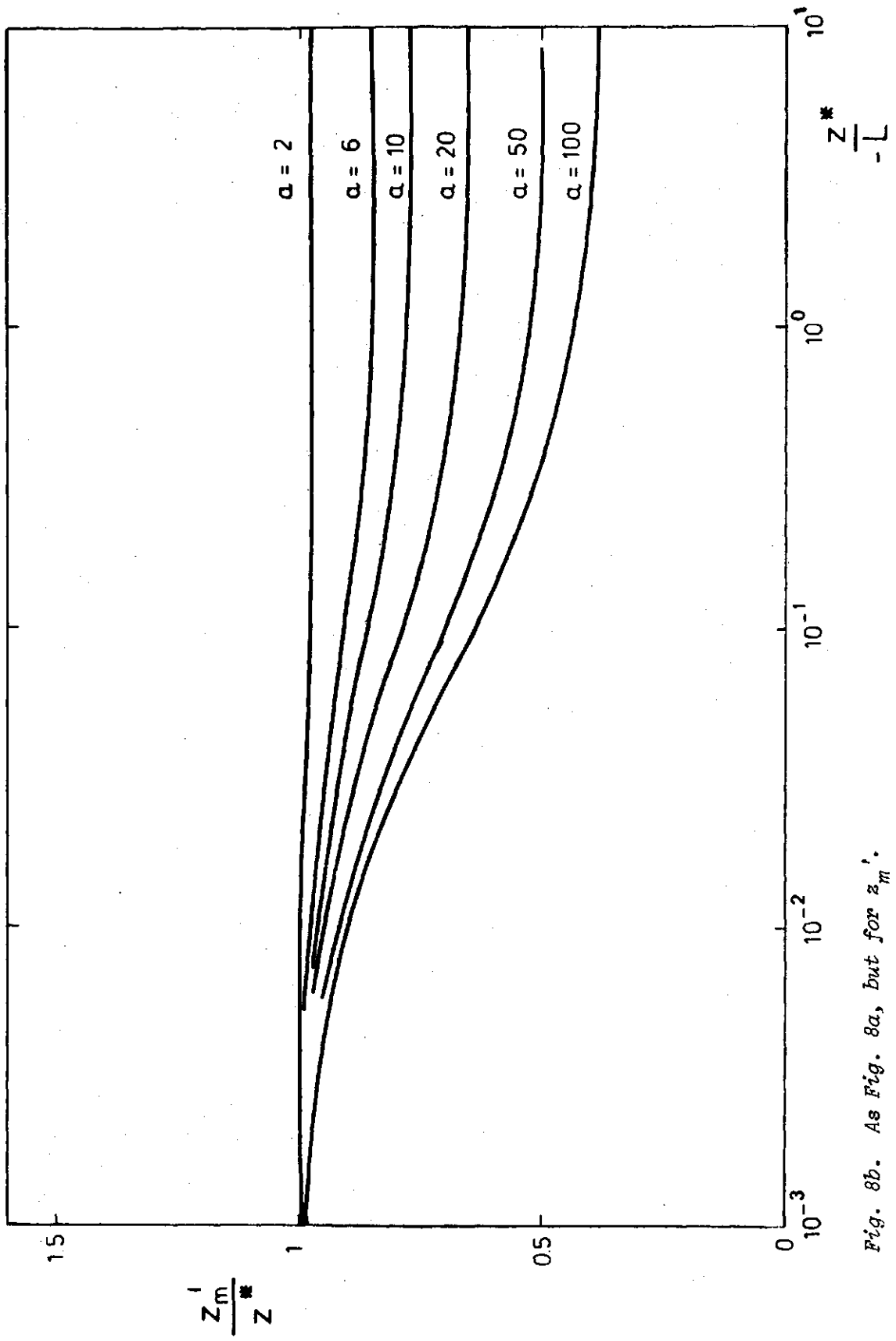


Fig. 8b. As Fig. 8a, but for z_m^1 .

3.3.1. Case a. $z_{m1}=z_{h1}$ and $z_{m2}=z_{h2}$

Here we will consider the case in which wind and temperature are measured at the same levels, thus when $z_{m1}=z_{h1}(\equiv z_1)$ and $z_{m2}=z_{h2}(\equiv z_2)$. From the foregoing it follows that then z_h' does not differ much from z_m' . As a result Eq. (46) will be a good approximation for L over a wide range of $z^*/-L$ and $a(\equiv \frac{z_1}{z_2})$. This is illustrated in Fig. 9 where $(\frac{L}{L_0} - 1)$ is depicted (at the bottom). We conclude that (46) is a very good approximation indeed. Even for $a = 100$ and $z^*/-L = 10$ the deviation is only 10%. We have seen also that when $a \leq 6$, z_m' and z_h' can be taken constant at $\sqrt{z_1 z_2}$, thus for that case we obtain

$$H = H_0 \left[1 - 16 \frac{\sqrt{z_1 z_2}}{L_0} \right]^{3/4} \quad (a \leq 6) \quad (51)$$

This expression is found earlier by Ricou (1982).

When $a > 6$ the assumption that z_h' and z_m' are independent of $z^*/-L$ is no longer valid and (51) can then not be applied.

We found that the curves shown in Figs. 8a and b can be approximated by the following empirical expression:

$$\frac{z_x'}{z_x^*} = \frac{1 - p_x \frac{z_x^*}{L}}{1 - 20 \frac{z_x^*}{L}} \quad (52)$$

where p_x is a constant which depends solely on a_x . From Fig. 10 the value of p_m and p_h can be read.

In this way we arrive at

$$H = H_0 \left[1 - 16 \frac{z_h'}{L_0} \right]^{3/4} \left[1 - 16 \frac{z_m'}{L_0} \right]^{1/4}, \quad (53)$$

where z_h' and z_m' are given by (52). For simplicity z_m' can be taken equal to z_h' , so that then we get

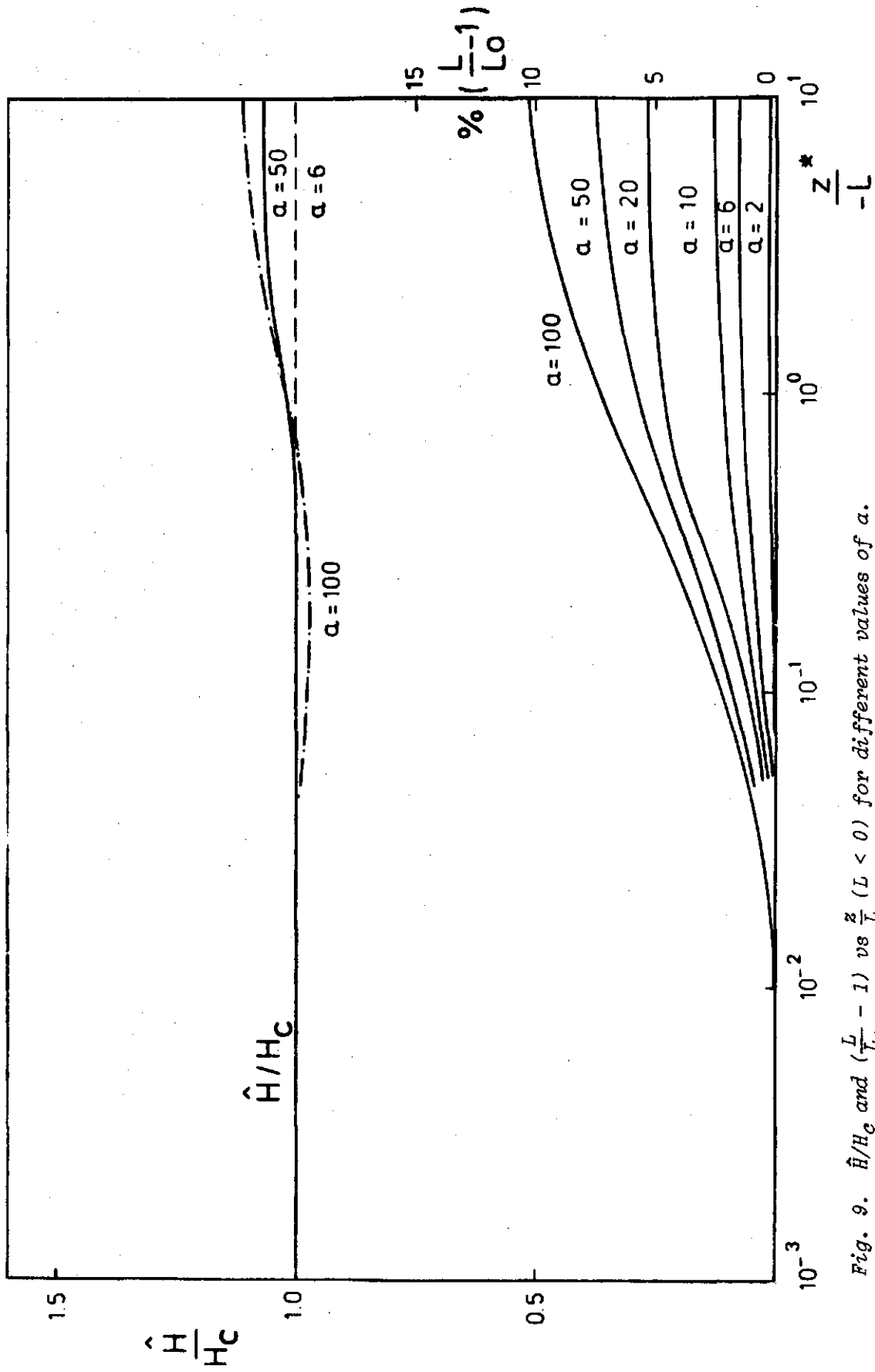


Fig. 9. \hat{H}/H_C and $\left(\frac{L}{L_0} - 1 \right)$ vs $\frac{Z}{L}$ ($L < 0$) for different values of a .

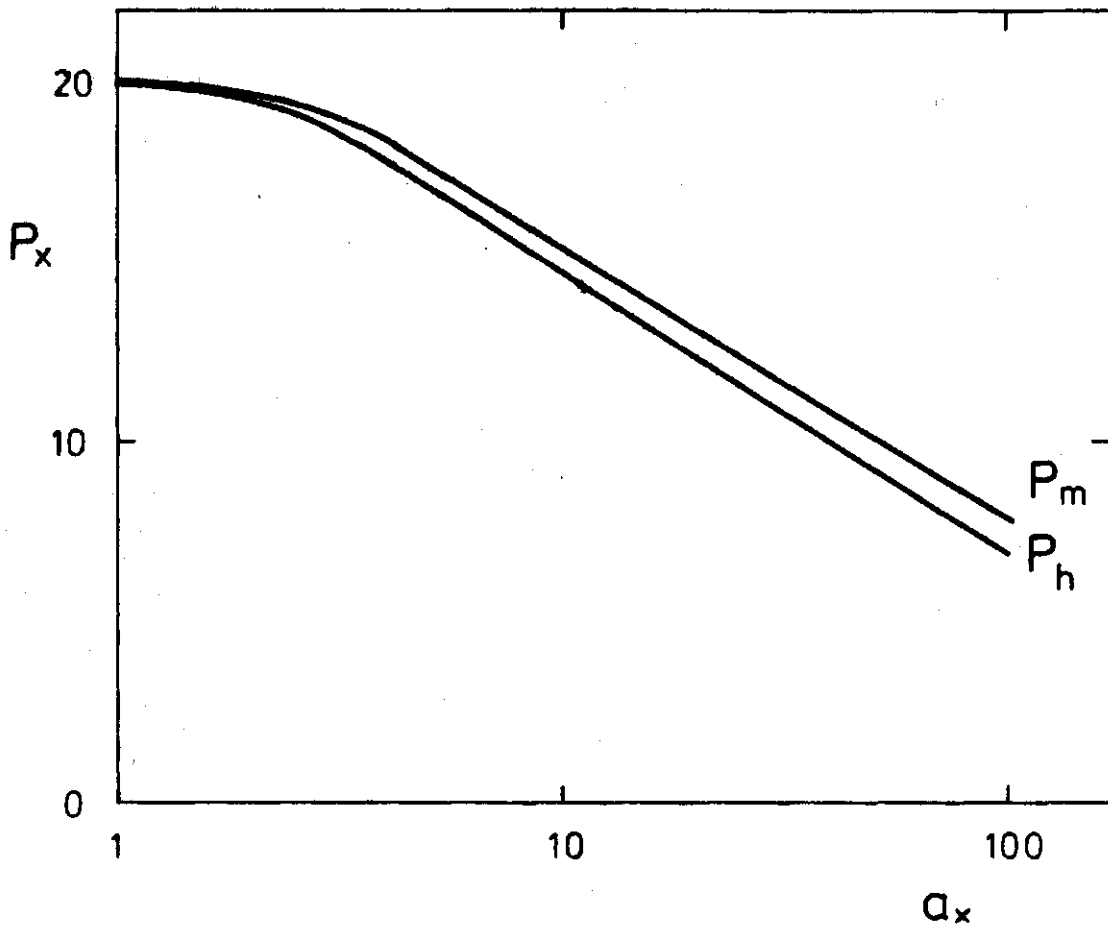


Fig. 10. Empirical parameter p_h and p_m vs a_h or a_m .

$$H = H_0 \left(1 - 16 \frac{z'}{L_0} \right)^{3/4}, \quad (54)$$

with

$$z' = \frac{1 - p_h \frac{z^*}{L_0}}{1 - 20 \frac{z^*}{L_0}} \quad (55)$$

The skill of these simple expressions, which holds for $a < 100$ and $-\frac{z^*}{L} \leq 5$ is very good. This is shown in Fig. 9 where H calculated with (54) and (55) (denoted as \hat{H}) is compared with H evaluated with the entire iteration scheme to solve the eqs. (18)-(24) (denoted as H_c). In this Figure we have only drawn the curves corresponding to $a = 6$, $a = 50$ and $a = 100$ because when $a \leq 20$ the deviations of \hat{H}/H_c from

1 are less than 3%, so that then the curves are almost covering each other. It can be concluded from Fig. 9 that (54) is a very good approximation; for $\frac{z^*}{|L|} < 1$ the deviations from the full iteration scheme are less than 3%.

3.3.2 Case b. Wind and temperature at different levels

When wind and temperature are not observed at the same levels the expressions derived above, generally, are not applicable. Only when $z_h^* \approx z_m^*$ and both a_h and a_m are smaller than 6 they can still be used.

In any case Eq. (44) is valid. With (9) this reads

$$\frac{L}{L_0} = \sqrt{\frac{1 - 16 \frac{z_m^*}{L}}{1 - 16 \frac{z_h^*}{L}}} \quad (L < 0). \quad (56)$$

This implies that

$$L_0 \leq L \leq L_0 \sqrt{\frac{z_m^*}{z_h^*}} \quad (57)$$

It is noted that for large values of $|L|$

$$L \approx L_0 - 8(z_m^* - z_h^*), \quad (58)$$

so that in the neutral limit L differs only a constant from L_0 .

For the limit $|L| \rightarrow 0$ we can make use of the empirical relation (52). With this we find that

$$L_0 \leq L \leq L_0 \sqrt{\frac{z_m^* p_m}{z_h^* p_h}} \quad (59)$$

Usually, the experimental set up will be so that the factor $\sqrt{z_m^* p_m} / \sqrt{z_h^* p_h}$ lies between about 0.5 and 1.5. For instance, at Cabauw, where temperature was observed at about 1 and 0.5 m and u at 2 m while $z_0 \approx 0.01$ m it equals about 0.5. Then we can take for L as first guess

$$\hat{L} = L_0 \frac{1 + \sqrt{\frac{z_m^* p_m}{z_h^* p_h}}}{2} \quad (60)$$

This estimate can be used to evaluate z_h' and z_m' with (52):

$$z_x' = \frac{1 - P_x \frac{z_x^*}{\hat{L}}}{1 - 20 \frac{z_x^*}{\hat{L}}} \quad (x = m \text{ or } h) \quad (61)$$

Then L follows from (56)

$$L = L_0 \sqrt{\frac{1 - 16 \frac{z_m'}{\hat{L}}}{1 - 16 \frac{z_h'}{\hat{L}}}}, \quad (62)$$

and subsequently H can be evaluated with

$$H = H_0 \left(1 - 16 \frac{z_h'}{L}\right)^{\frac{1}{2}} \left(1 - 16 \frac{z_m'}{L}\right)^{\frac{1}{4}}. \quad (63)$$

In Table 1 a verification of (63) is presented. It concerns about the "Cabauw configuration", namely $z_{h1} = 1.1$, $z_{h2} = 0.45$ and $z_{m1} = 2$ m, while $z_{m2} = z_0$ is taken 0.02 m. We may conclude that the results are very good.

$ \Delta\theta $	u_2	H_c	H_I	H_{II}	$\frac{z_h^*}{ L }$
0.1	0.5	8	8	(8)	0.346
0.1	1	8	8	(8)	0.069
0.1	2	11	11	11	0.015
0.1	3	16	16	16	0.007
0.1	5	26	26	26	0.002
0.3	0.5	52	52	(42)	1.210
0.3	1	41	40	(42)	0.242
0.3	2	43	43	43	0.050
0.3	3	54	54	53	0.021
0.3	5	80	80	80	0.007
0.5	0.5	125	128	(90)	1.82
0.5	1	95	93	(90)	0.455
0.5	2	88	86	(90)	0.089
0.5	3	100	99	98	0.036
0.5	5	140	139	140	0.012
0.7	0.5	223	232	(150)	2.42
0.7	1	167	165	(150)	0.661
0.7	2	142	140	(150)	0.132
0.7	3	153	152	(150)	0.052
0.7	5	204	203	204	0.017
0.9	0.5	342	361	(219)	3.64
0.9	1	256	254	(219)	0.851
0.9	2	208	205	(219)	0.177
0.9	3	215	213	(219)	0.069
0.9	5	273	272	273	0.023

Table 1. H computed for different values of u (at 2 m) and $\Delta\theta$ ($= \theta$ at 0.45 - θ at 1.1 m) with
 (i) the complete iteration scheme (H_c),
 (ii) eq. (63) (H_I) and (iii) eq. (71) or eq. (72) (H_{II});
 values between brackets are evaluated with (72). Also $-z_w^*/L$ is listed; $z_0 = 0.02$ m. (H in $W.m^{-2}$, $\Delta\theta$ in K and u_2 in $m.s^{-1}$).

When $\sqrt{z_m^* p_m / z_h^* p_h}$ differs more than 0.5 from 1 it is possible that one or two extra iterations must be included in order to obtain a more accurate value of L with eqs. (61) and (62). (Then after (62) one recalculates z_h' and z_m' with the new value of L). This limited iteration process is considerably easier than the original complete calculation schema.

3.4 The free convection scaling

3.4.1 Introduction

A further simplification of the standard flux profile method can be obtained making use of the so-called free convection scaling. This is based on the fact that under very unstable conditions H becomes independent of u_* and is determined by the temperature gradient only. In this section we will discuss the theoretical background of free convection, while also the practical applicability will be considered.

3.4.2 Theory

Free convection is the state in which the vertical transfer of heat (or momentum and water vapor) is maintained solely by convectively produced turbulence. Dimensional analysis shows (Lumley and Panofsky, 1964, pp. 108-110; Monin and Yaglom, 1971, Chapter 4) that in the regime of free convection H becomes H_f given by

$$H_f = h_0^* \rho c_p z^2 \sqrt{\frac{g}{T}} \left| \frac{\partial \bar{\theta}}{\partial z} \right|^{3/2}, \quad (64)$$

where h_0^* is a constant.

It is seen that H does not depend on u_* and is determined by $\partial \bar{\theta} / \partial z$ only.

Assuming that H is constant with height (64) can be integrated which leads to

$$H_f = \frac{h_o^* \rho c_p \sqrt{\frac{g}{T}} |\Delta\theta|^{3/2}}{[3 |z_{h1}^{-1/3} - z_{h2}^{-1/3}|]^{3/2}} \quad (65)$$

When the free convection formulations (64) and (65) are valid, ϕ_h , introduced in the previous section, must become proportional to $(-z/L)^{-1/3}$. This can be shown in the following way. From eqs. (1), (4) and (6) it follows that H can be written as

$$H = \rho c_p k^2 z^2 \left| \frac{\partial\theta}{\partial z} \right|^{3/2} \sqrt{\frac{g}{T}} \left(\frac{z}{|L|} \right)^{-1/2} \phi_h^{-3/2}. \quad (66)$$

This expression can be presented in a dimensionless form:

$$h^* = k^2 \left(\frac{z}{|L|} \right)^{-1/2} \phi_h^{-3/2}, \quad (67)$$

where the dimensionless heat flux h^* is defined by

$$h^* = \frac{H}{\rho c_p z^2 \sqrt{\frac{g}{T}} \left| \frac{\partial\theta}{\partial z} \right|^{3/2}}. \quad (68)$$

According to the free convection theory we must require that for $\frac{-z}{L} \rightarrow \infty$ h^* becomes constant. Thus

$$\lim_{\frac{-z}{L} \rightarrow \infty} h^* = h_o^* = \lim_{\frac{-z}{L} \rightarrow \infty} k^2 \left(\frac{z}{|L|} \right)^{-1/2} \phi_h^{-3/2} = \text{constant}. \quad (69)$$

As a consequence ϕ_h must become proportional to $\left(\frac{-z}{L} \right)^{-1/3}$ for $\frac{-z}{L} \rightarrow \infty$.

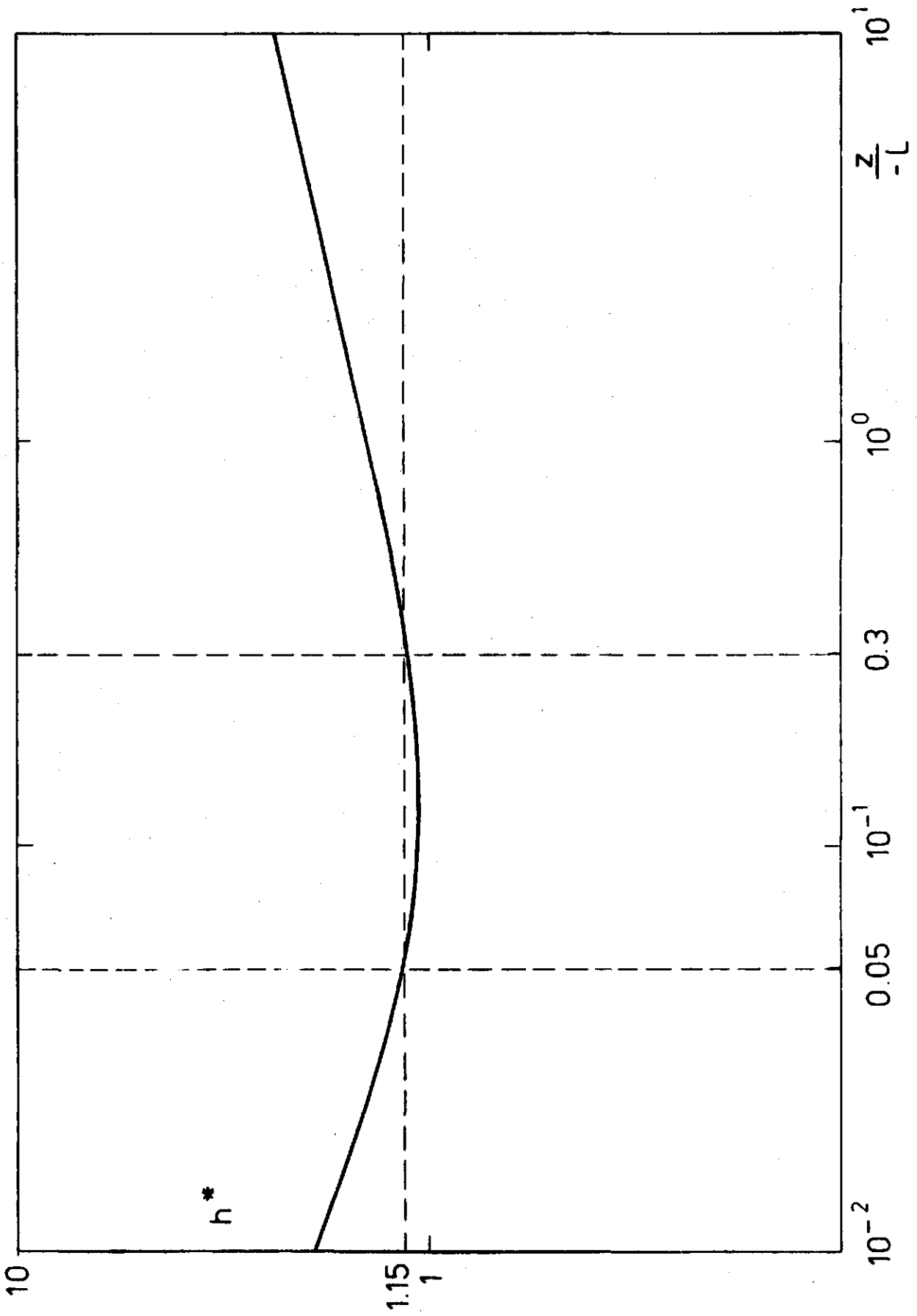


Fig. 11. Dimensionless heat flux h^* vs $\frac{z}{L}$ ($L < 0$).

The functions for ϕ_h proposed by Dyer (1974) (= eq. 9) and Businger et al. (1971) do not have this behavior. Hence the data sets analysed by these authors do not confirm the free convection formulations given by (64) and (65). On the other hand there are also authors e.g. Crawford (1965) who substantiate the "1/3-power law". The validity of (64) and (65) is therefore still uncertain.

In spite of the fact that the Businger-Dyer form of ϕ_h does not satisfy (69) there is still a region for $-z/L$ in which H , evaluated with this ϕ_h , is almost independent of u_* . This is shown in Fig. 11 in which h^* is depicted as determined with (34) using the Dyer form of ϕ_h given by (9). It is seen that in the region $-0.05 \geq z/L \geq -0.3$ h^* is fairly constant at about 1.15. Close to the ground, in the first 2 m or so, z/L is seldom less than -0.3 . This implies that in that case H can be evaluated with (65) with $h_0^* = 1.15$ when $z/L \leq -0.05$. From this feature use will be made in the next section.

3.5 Measurements close to the ground

When the measurements are done close to the ground, as was the case in the Cabauw experiment, the stability parameter z/L is seldom less than -0.3 . This can be seen from Table 1. Only at very low wind conditions, which are very rare, this is the case.

Thus we can make use of the results of the previous section referring to the free convection scaling. Herein we found that in the region $-0.05 \geq z/L \geq -0.3$ the dimensionless heat flux h^* is fairly constant, so that then H can be evaluated with eq. (64) using $h_0^* = 1.15$. On the other hand for small z we will be not far from the neutral limit when $z/L \geq -0.05$. From the foregoing it follows that then $L \approx L_0$ and $z_x' \approx z_x^*$. Moreover, for small values of z/L

$$\left(1 - 16 \frac{z}{L}\right)^{\frac{1}{2}} \approx 1 - 8 \frac{z}{L} \quad (70a)$$

and

$$\left(1 - 16 \frac{z}{L}\right)^{\frac{1}{4}} \approx 1 - 4 \frac{z}{L}. \quad (70b)$$

These considerations lead with (63) to the following simple expressions

$$H = H_0 \left(1 - \frac{8z_h^* + 4z_m^*}{L_0} \right) \quad \text{for } \frac{z_x^*}{L_0} > -0.05 \quad (71)$$

where $z_x^* = \max(z_h^*, z_m^*)$, while for $\frac{z_x^*}{L_0} < -0.05$ H is given by (65):

$$H = \frac{1.15 \rho c_p \sqrt{\frac{g}{T}} |\Delta\theta|^{3/2}}{[3 |z_{h1}^{-1/3} - z_{h2}^{-1/3}|]^{3/2}} \quad (72)$$

In the last column of Table 1 the results of this very simple approach are shown.* It is seen that they are very satisfactory, except under very low wind conditions ($u < 1 \text{ m.s}^{-1}$). But these are very rare.

3.6 Daytime mean values

Until now we did not define precisely the time interval Δt over which $\Delta\theta$ and u are averaged in the application of the profile-method. We used half an hour which is a good compromise between the requirements of (a) stationarity and (b) a good statistical accuracy of the means of θ and u .

When daily or daytime means of the fluxes are needed a time step of half an hour is rather inconvenient. Therefore it is worthwhile to investigate if it is possible to apply the expressions derived above to e.g. daytime mean averages of $\Delta\theta$ and u in order to obtain directly a daytime mean of H .

For this we analysed the data of July 1977 (which contains the dry fortnight) and we restricted ourselves to the simple method to determine H given by (71) and (72).

Because around local noon the fluxes are greatest these will be contribute significantly to the daytime mean. Then mostly the "free

* Page II.39

convection" formula (72) must be used. Therefore it is to be expected that instead of $\overline{\Delta\theta}^d$ we must take

$$\tilde{\Delta\theta}^d \equiv \left\{ \frac{\overline{\Delta\theta}^d}{|\Delta\theta|^{3/2}} \right\}^{2/3} \quad (73)$$

as input. As before the index d refers to the period of the day that $Q^* \geq 0$.

We found that

$$\tilde{\Delta\theta}^d \approx 1.15 \overline{\Delta\theta}^d \quad (74)$$

We applied (71) and (72) with this "mean" temperature difference and \overline{u}^d as input. In Fig. 12 the results are shown for \overline{H}^d , and in Fig. 13 those for $\overline{\lambda E}^{24}$ obtained with (29) and this estimate of \overline{H}^d .

The evaporation data of the dry period are encircled again. It is seen that the results are promising.

For practical routine observations this "day-mean" approach is very important because it simplifies the data handling considerably; only the daytime means of $\Delta\theta$, u and Q^* are needed, while further the calculation scheme is very simple.

The latter can be applied with a micro-processor system which contains the arithmetic operation $+$, $-$, \times , \div and $\sqrt{\quad}$.

3.7 Summary of section 3

In this section simplifications of the standard flux profile method are presented. The most important results are summarized briefly in the following. For convenience the numbering of the equations is that used in the text.

- (i) θ is observed at $z = z_{h1}$ and z_{h2} , and u at z_{m1} and z_{m2} , while a_x is defined by $a = z_{x1}/z_{x2}$ ($x = m$ or h ; level 1 > level 2, so that $a > 1$). Also $\Delta\theta = \overline{\theta}_1 - \overline{\theta}_2$ and $\Delta u = \overline{u}_1 - \overline{u}_2$, and

$$z_x^* = \frac{z_{x1} - z_{x2}}{\ln(a_x)}.$$

- (ii) We define

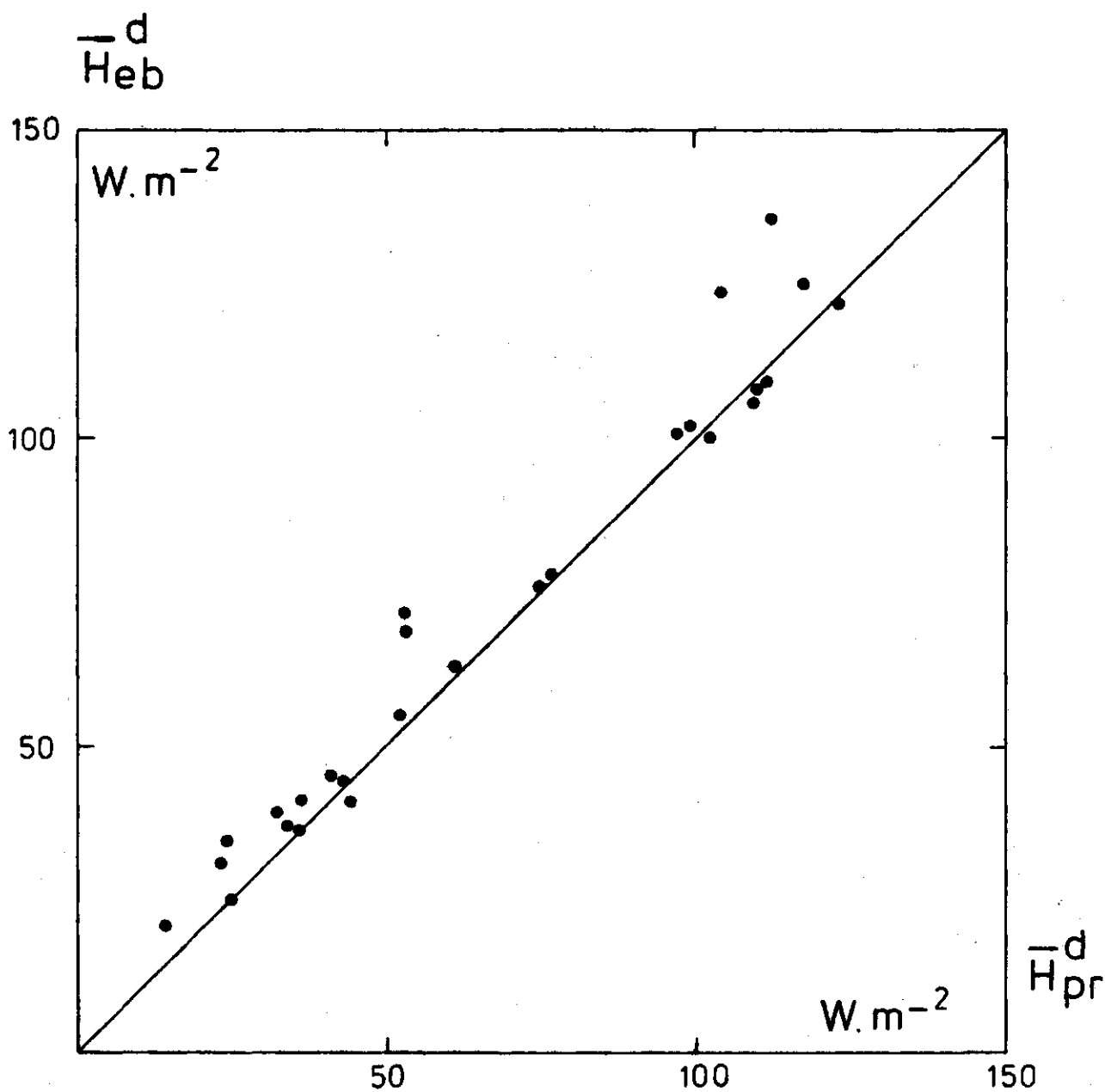


Fig. 12. \bar{H}^d as computed with (71) or (72) from the daytime mean $\tilde{\Delta\theta}^d$ and \bar{u}^d vs the energy-balance measurements; July 1977. The data from the dry period 3-17 July are encircled.

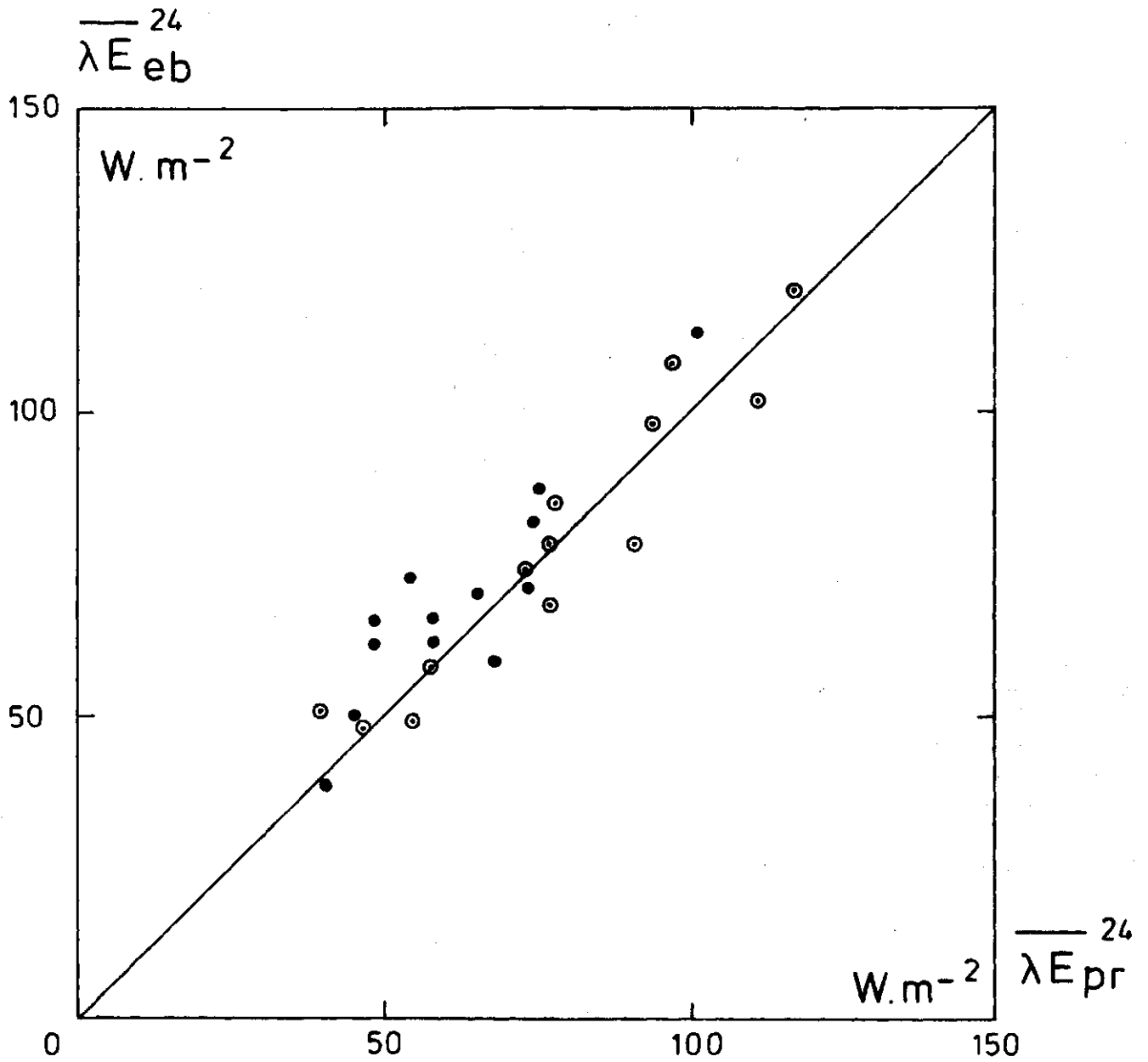


Fig. 13. As Fig. 12 but for $\overline{\lambda E}^{24}$ evaluated with (29).

$$H_o = \frac{k^2 \rho c_p |\Delta\theta| \Delta u}{\ln(a_h) \ln(a_m)} \quad (37)$$

and

$$L_o = \frac{T}{g} \frac{(\Delta u)^2}{\Delta\theta} \frac{\ln(a_h)}{\ln^2(a_m)} \quad (38)$$

I. Half-hourly values

Case a $z_{m1} = z_{h1} \equiv z_1$, $z_{m2} = z_{h2} \equiv z_2$.

Then the Obukhov length is approximately

$$L = L_o, \quad (L < 0) \quad (46)$$

and the sensible heat flux density

$$H = H_o \left(1 - 16 \frac{z'}{L_o}\right)^{3/4}, \quad (L < 0) \quad (54)$$

where z' follows from

$$z' = \frac{1 - p_h \frac{z_h^*}{L_o}}{1 - 20 \frac{z_h^*}{L_o}} \quad (L < 0) \quad (55)$$

Parameter p_h is a function of a_h . Its value is depicted in Fig. 10. When $a \leq 6$ (55) can be replaced by

$$z' = \sqrt{z_1 z_2} \quad (50)$$

Case b. θ and u observed at different levels.

A first estimate of L is

$$\hat{L} = L_0 \frac{1 + \sqrt{\frac{z_m^* p_m}{z_h^* p_h}}}{2}, \quad (L < 0) \quad (60)$$

where p_m and p_h can read from Fig. 10.

Next L is obtained with

$$L = L_0 \sqrt{\frac{1 - 16 \frac{z_m'}{\hat{L}}}{1 - 16 \frac{z_h'}{\hat{L}}}}, \quad (L < 0) \quad (62)$$

where

$$z_x' = \frac{1 - p_x \frac{z_x^*}{\hat{L}}}{1 - 20 \frac{z_x^*}{\hat{L}}}, \quad (L < 0; x = m \text{ or } h) \quad (61)$$

Subsequently H follows from

$$H = H_0 \left(1 - 16 \frac{z_h'}{L}\right)^{\frac{1}{2}} \left(1 - 16 \frac{z_m'}{L}\right)^{\frac{1}{4}}. \quad (L < 0) \quad (63)$$

Case c. Observations close to the ground, i.e. z_{m1} and $z_{m2} < 2$ m.

In this case H can be obtained from

$$H = H_0 \left(1 - \frac{8z_h^* + 4z_m^*}{L_0}\right), \quad \text{for } 0 \geq \frac{z_x^*}{L_0} \geq -0.05 \quad (71)$$

and

$$H = \frac{1.15 \rho c_p \sqrt{\frac{g}{T}} |\Delta\theta|^{3/2}}{\{ 3|z_{h1}^{-1/3} - z_{h2}^{-1/3}| \}^{3/2}}, \quad \text{for } \frac{z_x^*}{L_o} \leq -0.05 \quad (72)$$

$$(z_x^* = \max(z_h^*, z_m^*))$$

II. Daytime mean values.

Observations in the first 2 m.

Defining \bar{X}^d as the daytime mean of a certain quantity X the \bar{H}^d can be obtained from

$$\bar{H}^d = \bar{H}_o^d \left(1 - \frac{8z_h^* + 4z_m^*}{L_o^d} \right), \quad \text{for } 0 > \frac{z_x^*}{L_o^d} > -0.05 \quad (71')$$

or

$$\bar{H}^d = \frac{1.15 \rho c_p \sqrt{\frac{g}{T}} |\tilde{\Delta\theta}^d|^{3/2}}{\{ 3|z_{h1}^{-1/3} - z_{h2}^{-1/3}| \}^{3/2}} \quad \text{for } \frac{z_x^*}{L_o^d} \leq -0.05 \quad (72')$$

Here $\tilde{\Delta\theta}^d \approx 1.15 \bar{\Delta\theta}^d$,

$$\bar{H}_o^d = \frac{k^2 \rho c_p |\tilde{\Delta\theta}^d| \bar{u}^d}{\ln(a_h) \ln(a_m)} \quad (37')$$

and

$$L_o^d = \frac{T}{g} \frac{(\bar{\Delta u}^d)^2}{\tilde{\Delta\theta}^d} \frac{\ln(a_h)}{\ln^2(a_m)} \quad (38')$$

When the roughness length of the terrain of interest is known $z_{m2} = z_0$ and $u_2 = 0$, so that $\Delta u = u_1$.

Usually, the approximations are accurate enough for practical calculations; the errors are smaller than those introduced by measuring errors or imperfections of the flux profile method itself.

4. The temperature fluctuation method

4.1 Introduction

In this section a method for determining the sensible heat flux density during daytime is considered, which requires observations at a single level only. The method is based on the relation between temperature fluctuations and the vertical transfer of sensible heat. It can be regarded as a sister of the flux profile method; the difference is that $\partial\bar{\theta}/\partial z$ is replaced by σ_T/z , where σ_T is the standard deviation of the temperature.

A verification of the method is presented. This consists of a comparison with the energy-balance technique, using Bowen's ratio.

The applicability of the approach for routine observations of H during daytime and mean daily evaporation will be discussed.

4.2 Theoretical background

Close to the ground turbulent fluctuations are responsible for vertical transfer processes. Therefore we may expect that the standard deviation of the temperature σ_T , which is a suitable measure for the intensity of the temperature fluctuations, is related to the sensible heat flux. From dimensional arguments it can be shown that in the case of free convection H and σ_T are related as follows (Monin and Yaglom, 1971):

$$H = h_\sigma^* \rho c_p z^{\frac{1}{2}} \sqrt{\frac{g}{T}} \sigma_T^{3/2}, \quad (L < 0) \quad (75)$$

where h_σ^* is a constant. Eq. (75) is similar to (64). The only dif-

ference is that $\overline{\partial\theta/\partial z}$ is replaced by σ_T/z . There is no disagreement on the validity of (75), while we have seen that it is uncertain whether (64) holds.

The constant h_σ^* is given by

$$h_\sigma^* = \frac{k^{\frac{1}{2}}}{C_1^{3/2}}, \quad (76)$$

where C_1 follows from the form in which (75) often is presented in literature

$$\frac{\sigma_T}{|\theta_*|} = C_1 \left(\frac{z}{|L|}\right)^{-1/3}. \quad (L < 0) \quad (77)$$

Wyngaard et al. (1971) reported a value of $C_1=0.95$, which they derived from the well-known Kansas data. It should be noted that C_1 remains unaltered when the corrections for θ_* , u_* , L and k proposed by Wieringa (1980) are applied. With $k = 0.41$ this leads to $h_\sigma^* = 0.7$. Recent measurements in Cabauw (see the Appendix) substantiate this value, which means that it applies also to less homogeneous terrain. Wyngaard et al. also found that (77) holds already for $\frac{z}{L} \leq -0.1$.

At $\frac{z}{L} > -0.1$ mechanically produced turbulence will also play a part in the transfer processes and then the influence of u_* must be taken into account. This has been done by Tillman (1972) who proposed instead of (77) the interpolation formula

$$\frac{\sigma_T}{|\theta_*|} = C_1 \left(C_2 + \frac{z}{|L|}\right)^{-1/3}, \quad (L < 0) \quad (78)$$

where C_2 is another constant. As a result

$$H = h_{\sigma}^* \rho c_p z^{\frac{1}{2}} \sqrt{\frac{g}{T}} \sigma_T^{3/2} C_2^{\frac{1}{2}} \left(1 + \frac{1}{C_2} \frac{z}{|L|}\right)^{\frac{1}{2}} \left(\frac{z}{|L|}\right)^{-\frac{1}{2}} \quad (L < 0) \quad (79)$$

C_2 follows from

$$\lim_{\frac{z}{|L|} \rightarrow 0} \frac{\sigma_T}{|\theta_*|} = C_3, \quad (80)$$

$$\text{with } C_3 = \frac{C_1}{C_2^{1/3}}.$$

The value of C_3 is rather uncertain. This is due to the fact that when $\frac{z}{|L|} \rightarrow 0$ both σ_T and θ_* vanish. Tillman (1972) suggested $C_3 = 2.5$, which leads to $C_2 \approx 1/18$. When the Kansas-data are reevaluated according to Wieringa (1980) C_3 becomes somewhat higher, about 2.9.

For our calculations we will use $C_3 = 2.5$, so that (79) becomes

$$H = \frac{0.7}{\sqrt{18}} \rho c_p |L|^{\frac{1}{2}} \sqrt{\frac{g}{T}} \left(1 + 18 \frac{z_T}{|L|}\right)^{\frac{1}{2}} \sigma_T^{3/2}, \quad (L < 0) \quad (81)$$

where z_T is the level at which σ_T is observed.

For the evaluation of L additional measurement of the wind speed are needed. When it is assumed that the roughness length of the terrain of interest is known we can use the flux-profile relation for momentum to determine u_* (eq. 19):

$$u_* = \frac{k u}{\ln\left(\frac{z_u}{z_0}\right) - \psi_m\left(\frac{z_u}{L}\right)} \quad (82)$$

(z_u is the level at which u is measured).

With $H = -\rho c_p u_* \theta_*$ and (78) written as (using $C_3 = C_1 C_2^{-1/3}$ and $C_2 = 1/18$)

$$|\theta_*| = \frac{\sigma_T}{C_3} \left(1 + \frac{18 z_T}{|L|}\right)^{1/3} \quad (L < 0) \quad (83)$$

we then have obtained a set of equations which can be solved iteratively when u and σ_T are known. However, as was the case with the flux-profile relations, such a calculation procedure is too complicated for many practical applications. Therefore we searched for a more simple solution.

For this we rewrite (82) using (42):

$$u_* = \frac{k u}{\ln\left(\frac{z_u}{z_0}\right) \phi_m\left(\frac{z'_m}{L}\right)}, \quad (84)$$

where z'_m is a level between z_u and z_0 .

With the Dyer relation (9) for ϕ_m , and eqs. (83) and (4) we then find for L

$$|L| = \frac{T}{g} \frac{k C_3}{\ln^2\left(\frac{z_u}{z_0}\right)} \frac{u^2}{\sigma_T} \frac{\left(1 + 16 \frac{z'_m}{|L|}\right)^{1/2}}{\left(1 + 18 \frac{z_T}{|L|}\right)^{1/3}} \quad (L < 0) \quad (85)$$

For $\frac{z}{L} \lesssim -0.1$ the free convection formulation (75) holds, which implies that then H is not sensitive to an error in L , because L disappears in (75). On the other hand, when $\frac{z}{L} > -0.1$ we are so close to neutral stability that the factor

$\left(1 + 16 \frac{z'_m}{|L|}\right)^{1/2} / \left(1 + 18 \frac{z_T}{|L|}\right)^{1/3}$ will be close to 1.

As a result it is safe to ignore this factor in (85), so that we can estimate L with

$$|\hat{L}| = \frac{T}{g} \frac{k C_3}{\ln^2\left(\frac{z_u}{z_o}\right)} \frac{u^2}{\sigma_T} \quad (86)$$

Inserting (86) into (79) we get with (76) and $C_3 = C_1 C_2^{-1/3}$:

$$\hat{H} = \frac{k \rho c_p}{C_3 \ln\left(\frac{z_u}{z_o}\right)} u \sigma_T \left(1 + \frac{C_3^2 \ln^2\left(\frac{z_u}{z_o}\right)}{k C_1^3} \frac{g}{T} z_T \frac{\sigma_T}{u^2}\right)^{\frac{1}{2}} \quad (87)$$

The error we make with (87) can be evaluated from

$$\frac{H}{\hat{H}} = \left[\frac{1 + 18 \frac{z_T}{|\hat{L}|}}{\left(1 + 18 \frac{z_T}{|\hat{L}|}\right)^{1/3} + 18 \frac{z_T}{|\hat{L}|}} \right]^{\frac{1}{2}} \quad (88)$$

which follows from (81), (85) and (86).

In the case that $z_m = 2$ m, $z_o = 0.01$ m and $z_T = 0.9$ m (which is about the configuration used at Cabauw) H/\hat{H} deviates never more than 3% from 1 (see Table 2). We conclude that (87) is accurate enough for practical use.

It is remarked that when z_m' differs too much from z_T (86) possibly is too crude. Then a better approximation of L can be obtained using expressions similar to eqs. (61) and (62).

σ_T (K)	u_2 (m.s ⁻¹)	H/\hat{H}	$-z_T/L$	\hat{H} (W.m ⁻²)
0.1	0.5	.98	.14	5
	1	.97	.10	6
	2	.98	.02	9
	3	.99	< 10 ⁻³	12
	5	.99	< 10 ⁻³	19
0.3	0.5	.99	1.33	25
	1	.97	0.32	27
	2	.97	0.07	33
	3	.97	0.03	42
	5	.99	0.01	62
0.5	0.5	.99	2.17	53
	1	.98	0.55	56
	2	.97	0.12	65
	3	.97	0.05	77
	5	.98	0.02	108
0.7	0.5	.99	2.9	88
	1	.98	0.78	91
	2	.97	0.18	101
	3	.97	0.07	117
	5	.98	0.02	158
0.9	0.5	.99	3.66	127
	1	.98	1.00	131
	2	.97	0.23	143
	3	.97	0.10	162
	5	.98	0.03	212

Table 2. H/\hat{H} for different values of u (at 2 m) and σ_T (at 0.9 m). Also z_T/L and \hat{H} (W.m⁻²) are given; $z_0 = 0.01$ m.

4.3 Experimental

For the verification of the temperature fluctuation method data were collected during some days in August-September 1980 at the micrometeorological field at Cabauw. The standard deviation of the temperature was measured at about 0.8 m with a small thermocouple system developed by the instrumental division of the Royal Netherlands Meteorological Institute. The sensor has a diameter of about 100 μm . The thermometer was unshielded and was not ventilated artificially. For comparison purposes the surface fluxes were measured with the energy-balance method described in section 2.3. The instrumental details are given in section 2.4. Unfortunately the measurement of the soil heat flux was not reliable. This quantity was estimated as one-tenth of the net radiation, which is a rather good approximation during daytime (De Bruin and Holtslag, 1982).

All data were handled by a Hewlett and Packard 21MX minicomputer. The sample frequency was 1 Hz. With a standard program the 10 min averages and the corresponding standard deviations of all measured quantities were determined and stored on magnetic disk and later on magnetic tape. For this study we constructed from the 10 min values hourly fluxes. Because of all measured quantities the standard deviation per 10 min was determined the data set includes also σ_T observed with the thermometers used to determine the Bowen ratio (at the lowest level (0.45 cm) the absolute temperature is observed). From this we will estimate H also with the σ_T method (see next section). The thermometer is developed for operational use (Slob, 1978). It is shielded and is ventilated artificially. The sensor is a thermo-couple with a diameter of about 2 mm.

We analysed the data of four days, namely 15, 17 and 25 September and 3 September 1980. On these days the wind speed conditions were different; the two meter wind covered a range between about 1.5 and 5 m.s^{-1} .

4.4 Results

In Fig. 14 the hourly and daytime mean values of H evaluated with the temperature fluctuation method (eq. 87) are plotted versus the energy-balance observations. We recall that σ_T was observed with a small thermocouple at about 0.8 m, that the roughness length of the field is about

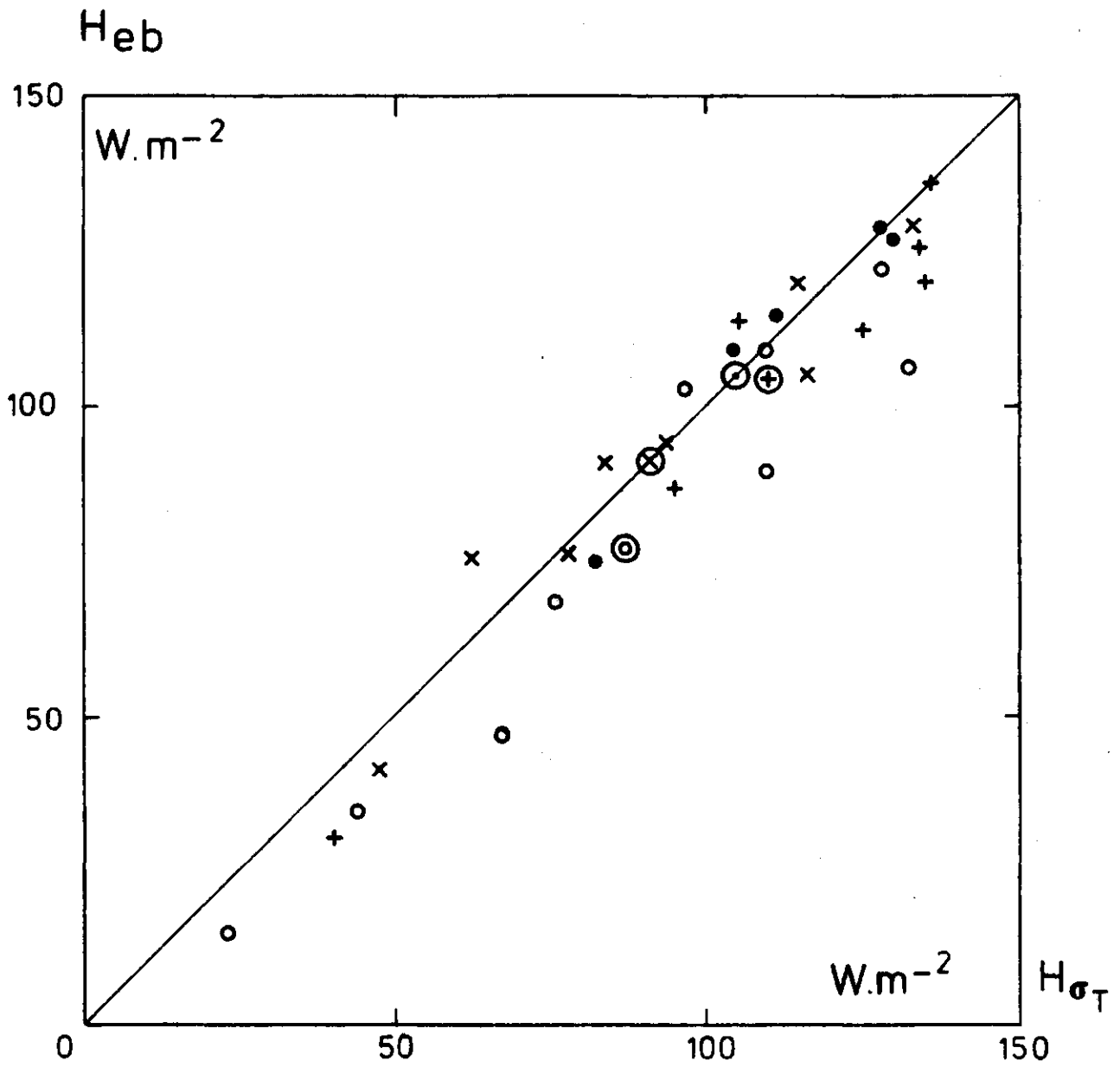


Fig. 14. Hourly and daytime mean values of H computed with (87) compared with the energy-balance measurements.
 (● 15 Aug., + 17 Aug., x 25 Aug., ○ 3 Sept., ⊙ daytime mean).

1 cm, while the hourly and daytime means are constructed from 10 min averages. Also in the energy-balance data the soil heat flux density is taken as one-tenth of the net radiation. The results presented in Fig. 14 are very promising; the scatter shown is of the same order as that caused by measuring errors.

To illustrate that the influence of the wind speed cannot be neglected we plotted in Fig. 15 for each day separately H , computed with the free convection formula (75), versus the energy-balance measurements. At the top of each sub-figure the course of the observed wind speed at 2 m is indicated. On 25 August 1980 u_2 was low ($\leq 2 \text{ m.s}^{-1}$) and then the free convection formula yields good results. But on the other days, when $u_2 > 2 \text{ m.s}^{-1}$ eq. (75) underestimates H considerably. The evidence given in Figs. 14 and 15 reveals that the interpolation formula (87) accounts satisfactorily for the influence of u on H .

The results shown in Figs. 14 and 15 are obtained from measurements of σ_T carried out with a thermometer that is about 100 μm in diameter. Such a sensor is very sensitive to destruction by e.g. hail, rain and animals. Therefore it is not very attractive for operational use. For that reason we investigated whether the σ_T method is applicable with a thermometer of the type that is used for the determination of the Bowen ratio. As reported in the previous section this instrument has a diameter of a few mm and therefore it is slower. But it can be used operationally. We found experimentally that the σ_T of this robust thermometer is about 2/3 of that observed with the fast 100 μm thermocouple. With this conversion factor we corrected the data of the slow thermometer, after which we applied with these corrected values the temperature fluctuation method. The results are depicted in Fig. 16. We conclude that they are very satisfactory; also now the deviations are of the same order as those caused by measuring errors. This result is very important for practical applications. When on a routine weather station the temperature is observed with a thermometer similar to the robust instrument used in this experiment, reliable estimates of H during daytime can be obtained.

Then with (28) the daily mean evaporation can be evaluated. For this we need the net radiation. When this is not measured directly, it can be estimated from standard weather data using well-known semi-empirical expressions (see e.g. Monteith and Szeicz, 1961; De Bruin and Kohsiek, 1977; Van Ulden and Holtslag, 1982; Nielsen et al., 1981).

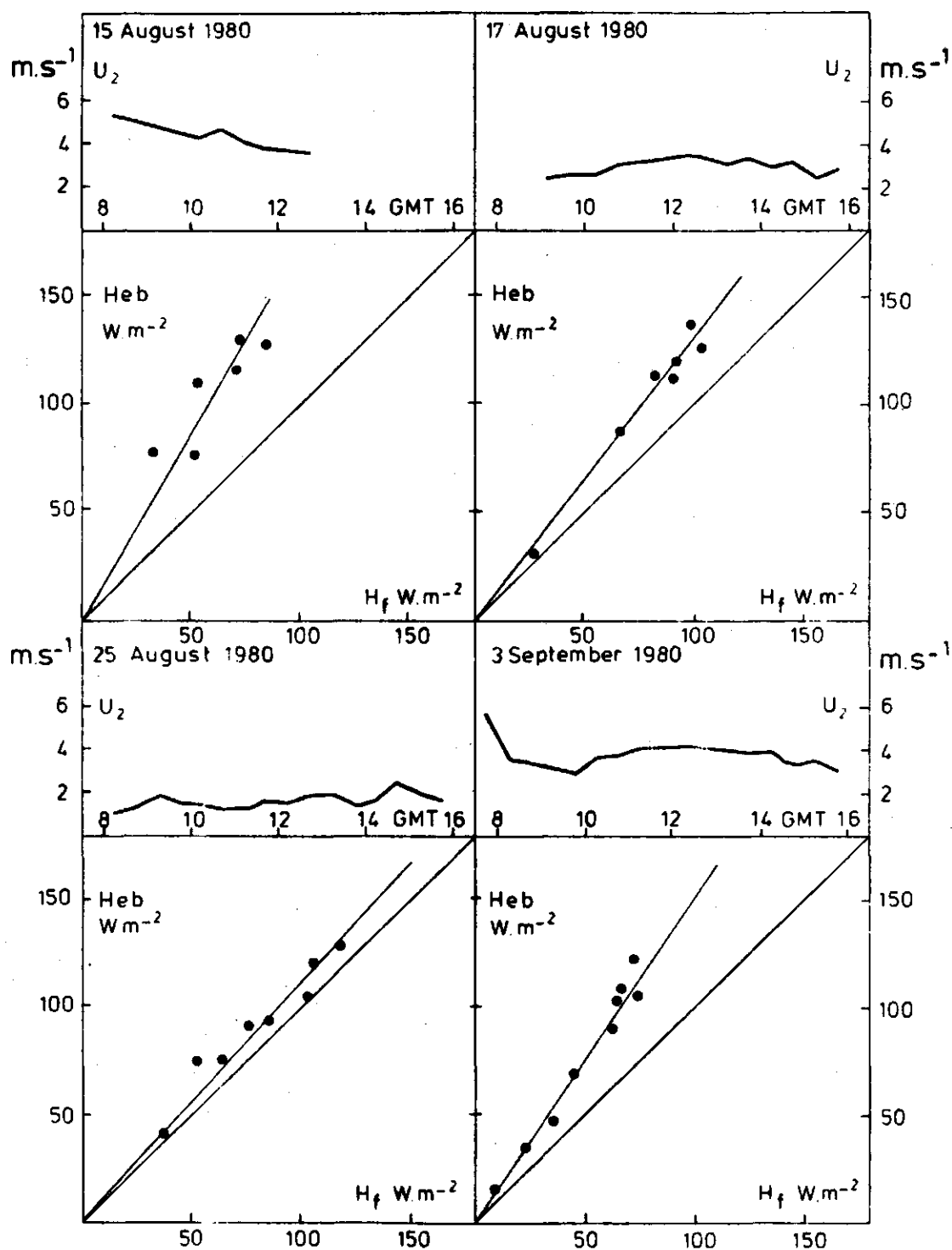


Fig. 15. Free convection estimate of H (hourly values) evaluated with (75) compared with the energy-balance observations for 15, 17 and 25 August and 3 September. Also the course of the 2 wind speed at 2 m (u_2) is given.

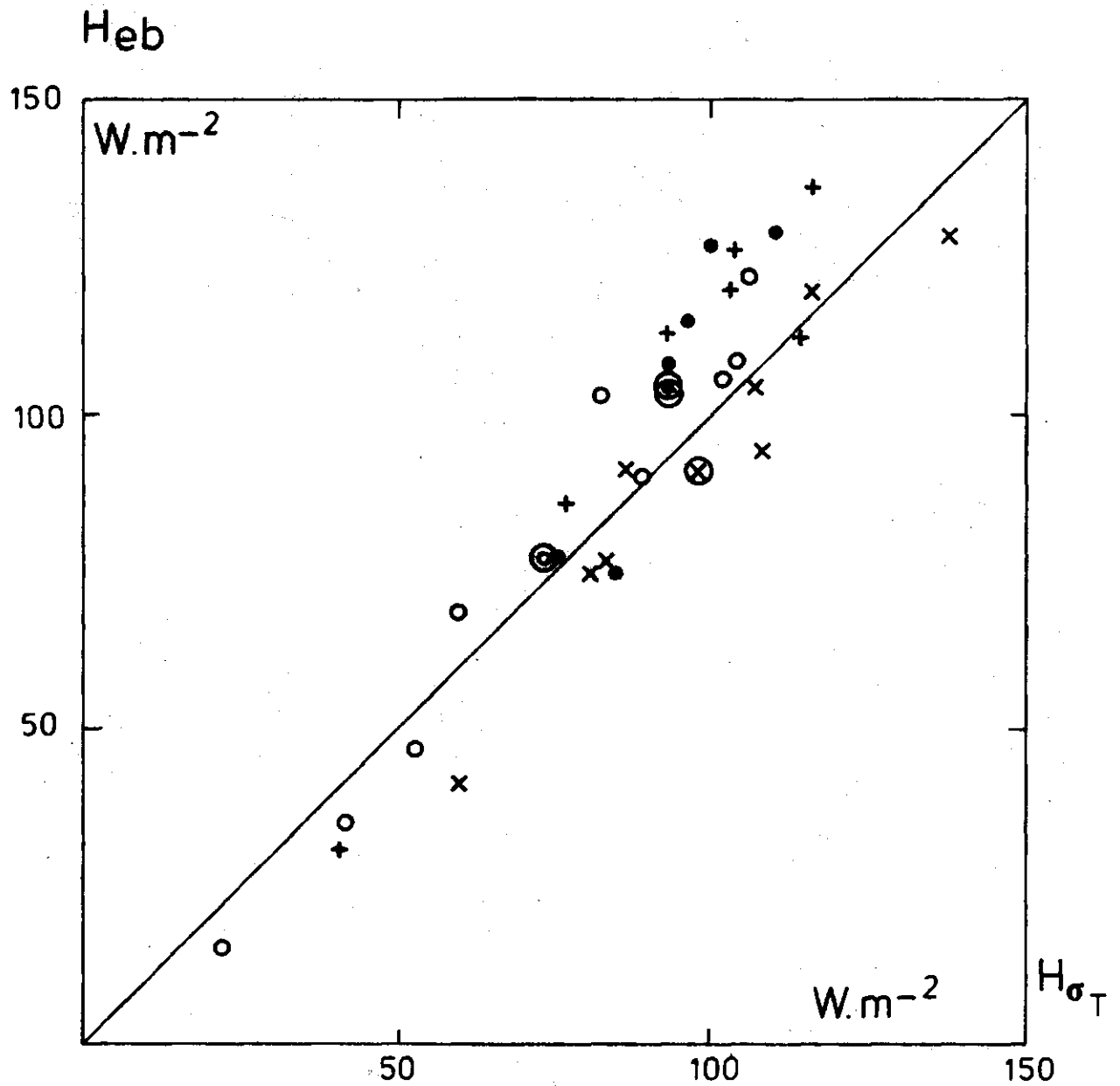


Fig. 16. As Fig. 14, except σ_T observed with a robust, but relatively slow, thermometer.

4.5 Discussion and conclusion

In this section it is shown that the temperature fluctuation method is a very suitable technique for the determination of the sensible heat flux during daytime. With the results of section 2, in which it is shown that reliable estimates of the daily mean evaporation can be obtained from the daytime mean of H_s , this also implies that with the temperature fluctuation method the evaporation can be evaluated. Then additionally net radiation must be observed (see eqs. (28) and (29)), but this can be done directly, while also Q^* can be estimated from standard weather data (see e.g. De Bruin and Kohsiek, 1979, and Van Ulden and Holtslag, 1982). Our results implies that at a standard weather station evaporation can be observed when additionally σ_T is measured. The extra costs of this are relatively low.

The determination of σ_T can be done in several ways. It is the best to use a microprocessor. This can execute the entire data handling, so that H and E can be obtained on the site. A more simple way is to registrate T with a X-Y recorder. Then σ_T can be estimated from the peak-to-peak values of the recorded T -signal (Businger, 1973). This is rather laborious, but most data collected at a routine weather station are still processed manually.

Under some circumstances the temperature averaged over 5 min or so changes rapidly. Then σ_T must be corrected for time trend, because very low frequencies in the T -spectrum influence clearly σ_T , but do not contribute to the vertical exchange processes. Trend corrections can be made rather easily. When the manual procedure is used one can correct for trend visually, while when the data handling is done by a microprocessor linear regression techniques can be applied. Usually, the time trend in T is the most pronounced in the early morning and in the late afternoon. But then the fluxes are small. In our opinion, therefore a trend correction can be omitted when σ_T is determined over 10 min. This period is so short that the trend of T cannot be large, while it is long enough to obtain σ_T with sufficient statistical accuracy.

The great advantage of the temperature fluctuation method is that it requires observations at a single level only, while it is also not very sensitive to irregularities in the terrain (see the Appendix). This makes the method very attractive for application in agriculture for which often the surface fluxes from small fields are needed. We have seen before that then it is difficult to satisfy the requirements that the observations must be done (a) in the internal boundary layer and (b) at a level much greater than the roughness length. With the temperature fluctuation method these requirements can be fulfilled much easier than with a profile approach.

Appendix

The temperature fluctuation method is based on the free convection scaling leading to eqs. (75) and (77). These expressions are obtained with dimensional analysis, assuming that the terrain is horizontal and homogeneous. The theory does not predict the numerical values of the constants C_1 and h_σ^* involved in (75) and (77). These must be determined experimentally. We used $C_1 = 0.95$ (resulting in $h_\sigma^* = 0.7$ with $k = 0.41$) as derived by Wyngaard et al. (1971) from the Kansas data. In Kansas the terrain is very homogeneous. Usually the Dutch land scape is less uniform. For instance at Cabauw the terrain consists of pastures separated by ditches with at intervals trees and houses. These irregularities influence the profiles of wind and temperature. Wieringa (1980) reported that at 20 m the Cabauw wind profiles show a kink. This feature reflects on the applicability of e.g. the flux profile method. Therefore it is very interesting to investigate whether (75) and (77) (or the related expressions) are sensitive to disturbances of the flow.

In 1981 an experimental program was carried out at Cabauw to investigate the behavior of u_* , H and E in a disturbed surface layer. At Cabauw the disturbances are largest at easterly and northern winds. In this Appendix some preliminary results of these experiments will be presented.

H and u_* were observed at 3.4 and 22.5 m with the eddy-correlation method, thus with

$$H = \rho c_p \overline{w'T'} \quad (89)$$

and

$$u_*^2 = -\overline{u'w'} \quad (90)$$

where u and w are the wind components in the x and z direction respectively and a prime denotes a deviation from a mean value.

At 3.4 m u and w were observed with a sonic anemometer and T with a small thermocouple (of the same type as described in section 4.3).

At 22.5 m this was done with a trivane and a thermocouple system described by Driedonks (1981).

The data handling was done by a H.P. 21MX minicomputer; a sample frequency of 5 Hz was used. All samples are stored on magnetic tapes. Data are available of about 75 periods of 10 min.

In Figs. 17a and b the eddy-correlation observations of σ_T/θ_* are plotted against z/L for 3.4 and 22.5 m respectively. Also the lines corresponding to (77) and (78) with

$C_1 = 0.95$ (as found by Wyngaard et al., 1971),

$C_2 = 2.5$ (proposed by Tillman, 1972) and

$C_3 = 2.9$ (following from the reevaluation of the Kansas data as suggested by Wieringa, 1980).

From Fig. 17 it is seen that for $z/L < -0.2$ (75) with $C_1 = 0.95$ fits the Cabauw data well, taking into account that the random scatter of 10 min fluxes is always large. For $z/L > -0.2$ the data points deviate from the free convection formulation. But then u_* determines H also and (78) must be applied. It is seen that the curves corresponding to this expression with $C_3 = 2.5$ and $C_3 = 2.9$ both fit well to the data points in the region $-0.05 > z/L > -0.5$. Then also the difference between these two curves is small. In the nearly neutral case ($z/L > -0.05$) there is a tendency to underestimate $\sigma_T/|\theta_*|$, so that $C_3 = 2.9$ or even a greater value must be preferred. However, we recall that under nearby neutral conditions σ_T and θ_* both are small. As a consequence their ratio cannot be determined with great accuracy. So it is dangerous to draw definitive conclusions on the numerical value of C_3 from our results. Because for $z/L < -0.05$ the curves corresponding to $C_3 = 2.5$ and $C_3 = 2.9$ do not differ significantly (in view of the experimental scatter) and because the fluxes are small for $|z/L| < 0.05$ the uncertainty of C_3 has no great practical consequences.

As pointed out by Hicks (1980) the validity of (77) is not a sufficient condition for the validity of (75). Therefore we verified separately the latter expression. In Fig. 18a and b we plotted $\overline{w'T'} (\equiv H/\rho c_p)$ vs $z^{\frac{1}{2}} \sigma_T^{3/2}$ for convective days, while also the line following from (75) with $h_o^* = 0.7$ is shown. It is seen that the agreement is good.

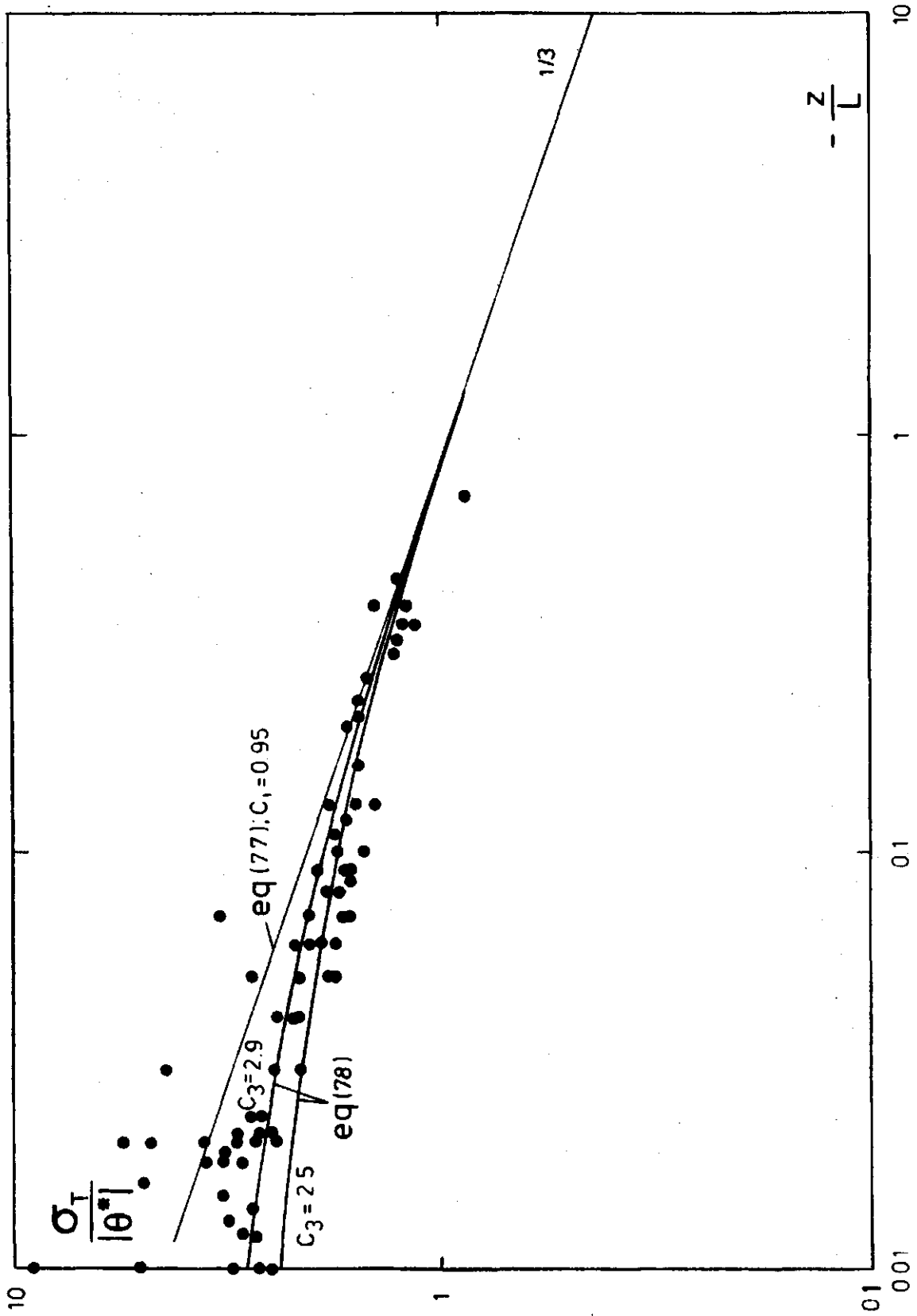


Fig. 17a. Eddy-correlation measurements of $\sigma_T/|\theta^*|$ vs z/L ($L < 0$); 10 min values, Cabauw, summer 1981, $z = 3.4$ m.

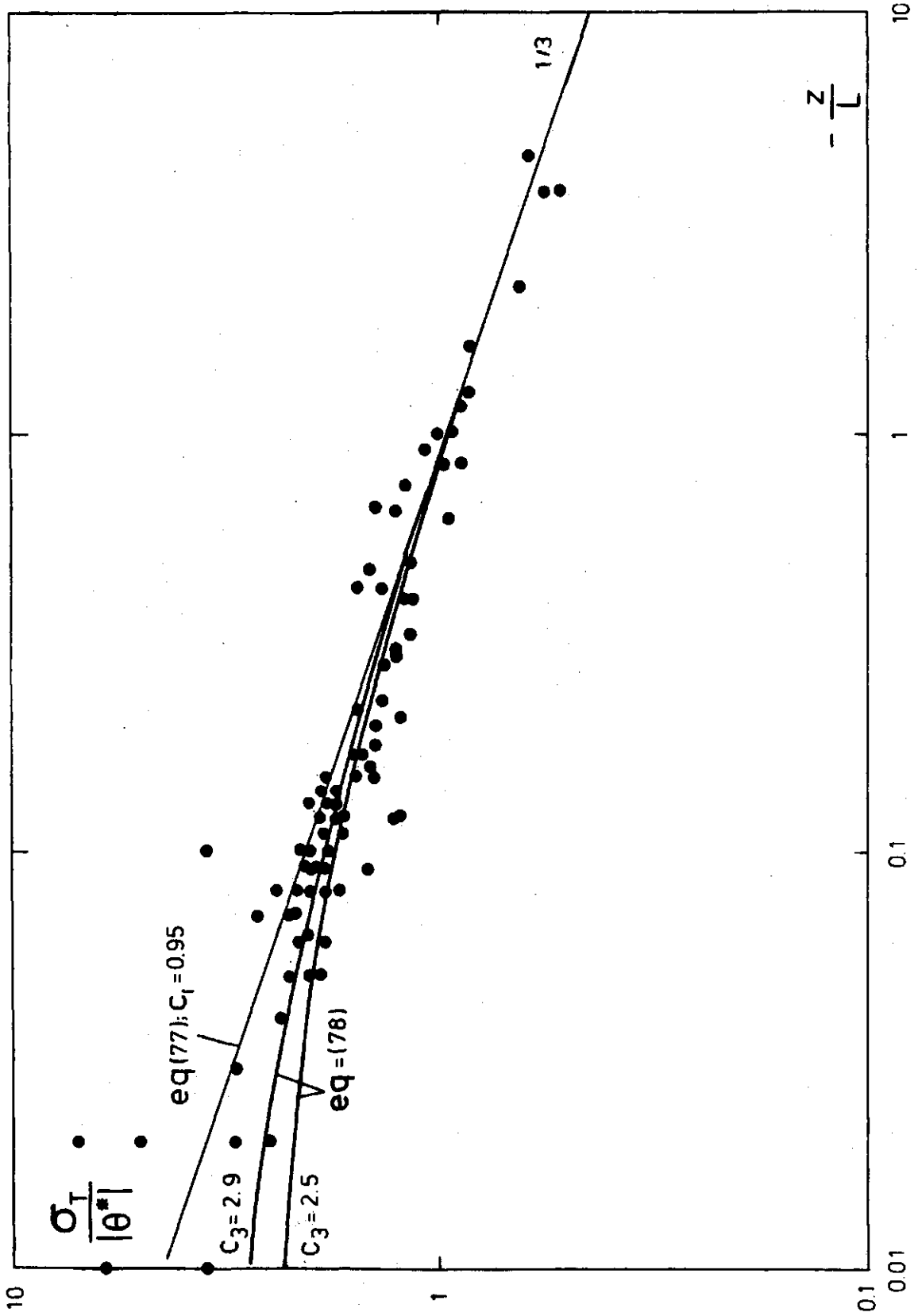


Fig. 17b. As Fig. 17a, but $z = 22.5$ m.

The evidence shown in Figs. (17) and (18) refers to a wide range of wind directions, including the "disturbed" easterly and northern sectors. Because the Cabauw eddy correlation measurements are well described by (77) and (78) derived from the Kansas data collected over homogeneous terrain, we conclude that (77) and (78) are not very sensitive to irregularities at the surface. This means that the temperature fluctuation method is attractive for many practical purposes.

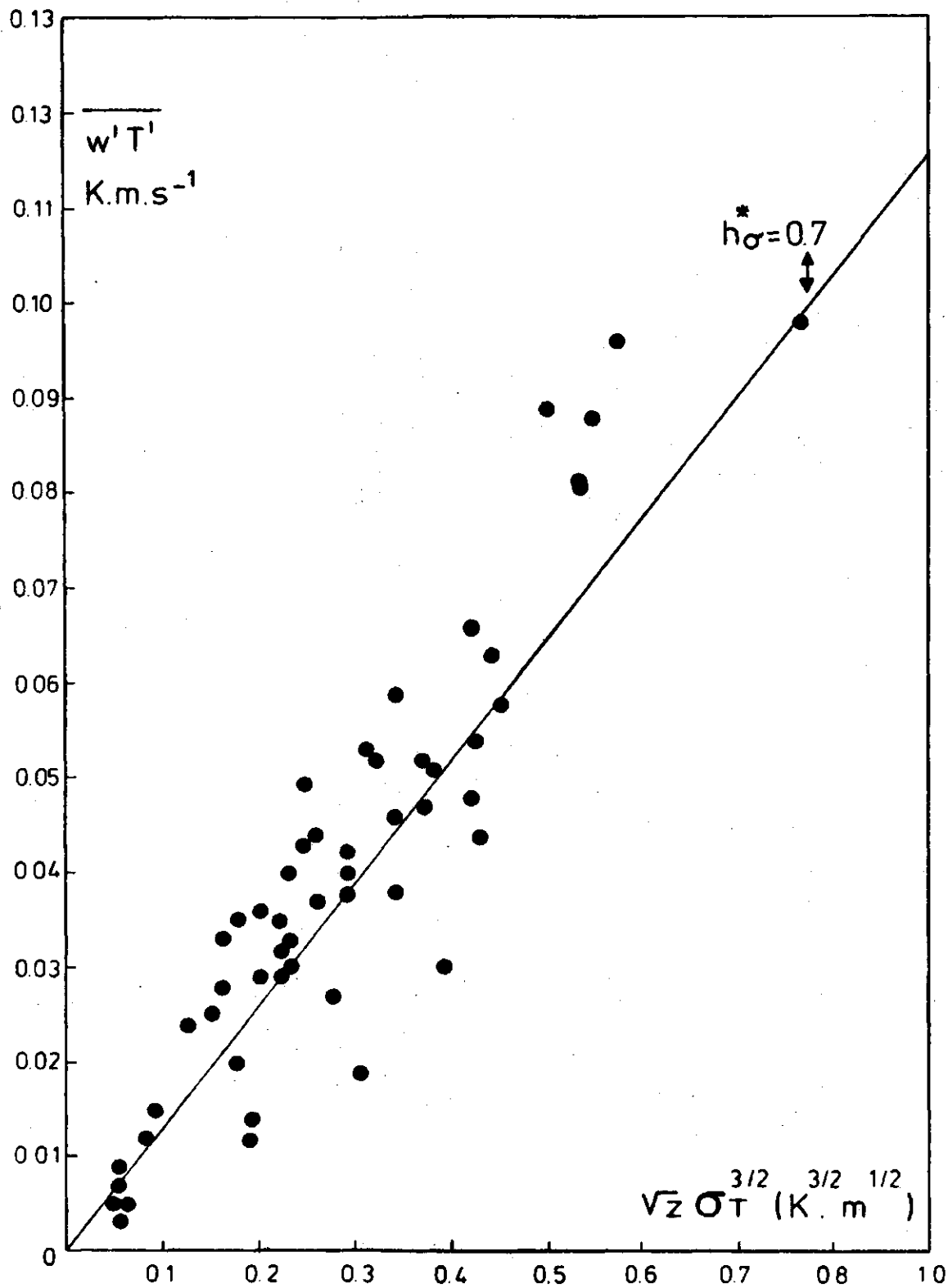


Fig. 18a. $\overline{w'T'}$ (10 min values) vs $z^{1/2} \sigma_T^{3/2}$; Cabauw, summer 1981, $z = 3.4$ m. Convective days.

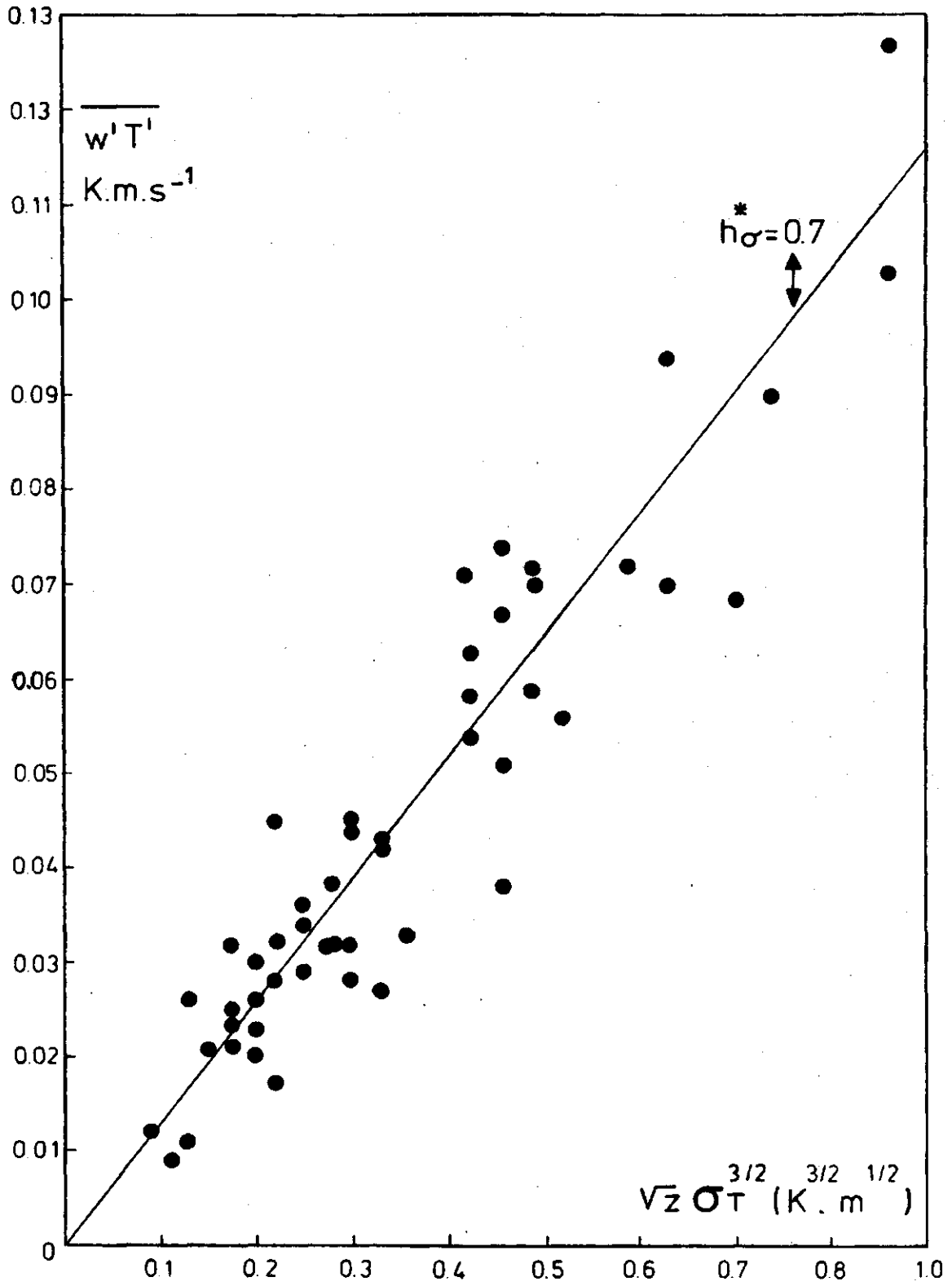


Fig. 18b. As Fig. 18a, but $z = 22.5$ m.

- III. A simple parameterization of the surface fluxes of sensible and latent heat during daytime compared with the Penman-Monteith concept. †

Abstract

In this paper a comparison is made between two methods to determine the surface fluxes of sensible and latent heat during daytime. The first method, known as the Penman-Monteith approach, incorporates a more complete description of the physics. However, it needs a relatively large number of input parameters, which is inconvenient in many applications. The second method is a modification of the Priestley-Taylor evaporation model, which needs only net radiation, air temperature and an indication of the moisture condition at the surface. Both models are compared on basis of hourly micro-meteorological data obtained in the Netherlands during the summer of 1977. It appears that the models have a similar skill for a short vegetation. Therefore, the simple parameterization is preferred for practical purposes. It reveals that this result can be explained partly by the fact that the so-called equilibrium latent heat flux density (LE_{EQ}) and vapor pressure deficit are correlated.

† Submitted to Journal of Applied Meteorology
A.A.M. Holtslag as co-author.

III.2

List of symbols

c_p	specific heat of vaporization	$(\text{J} \cdot \text{kg}^{-1} \cdot \text{K}^{-1})$
e_a	water vapor pressure	(mb)
e_s	saturation water vapour pressure	(mb)
r_a	aerodynamic resistance	$(\text{m} \cdot \text{s}^{-1})$
r_c	surface resistance for water vapor	$(\text{m} \cdot \text{s}^{-1})$
s	de_s/dT at $T = T_a$	$(\text{mb} \cdot \text{K}^{-1})$
u	wind speed	$(\text{m} \cdot \text{s}^{-1})$
z	height	(m)
z_0	roughness height	(m)
B	the Bowen ratio	(-)
E	evaporation	$(\text{kg} \cdot \text{m}^{-2} \cdot \text{s}^{-1})$
E_{EQ}	equilibrium evaporation	$(\text{kg} \cdot \text{m}^{-2} \cdot \text{s}^{-1})$
G	soil heat flux density	$(\text{W} \cdot \text{m}^{-2})$
H	sensible heat flux density	$(\text{W} \cdot \text{m}^{-2})$
L	latent heat of vaporization	$(\text{J} \cdot \text{kg}^{-1})$
Q^*	net radiation	$(\text{W} \cdot \text{m}^{-2})$
α	Priestley-Taylor parameter	(-)
α'	modification of α	(-)
β	constant	(-)
γ	psychrometric constant	$(\text{mb} \cdot \text{K}^{-1})$
δe	saturation deficit	(mb)
ρ	density of air	$(\text{kg} \cdot \text{m}^{-3})$

1. Introduction

A simple description of the surface fluxes of heat and water vapor in terms of routine variables is useful for many purposes, such as:

- the determination of evapo(transpi)ration from the surface, which is required by hydrology and agriculture.
- the description of the convective atmospheric boundary layer.
- the estimation of the stability of the air near the ground, e.g. for air pollution problems.
- the determination of the input of heat and moisture at the ground into the atmosphere for weather-forecast purposes.

For some of these applications the fluxes must be described in terms of variables which can be forecast, while for others a parameterization is needed in terms of routine weather data observed in the past at standard meteorological stations. In this paper a parameterization of the surface fluxes will be treated which has the capability to be useful for both categories. It is a modification of the evaporation model of Priestley and Taylor (1972).

It is the aim of this paper to compare the skill of this simple model with that of the Perman-Monteith approach (Monteith, 1965). This description contains the most complete physics; however, it has the disadvantage that it needs a relatively large number of input parameters. For the comparisons a set of micro-meteorological data collected at Cabauw, the Netherlands in the summer of 1977 is used. We will consider hourly values during daytime.

2. Experimental data

For this study we analysed a set of micro-meteorological data collected at Cabauw, in the centre of the Netherlands, in the period May through August 1977. The measurements were carried out at a field of 100 x 100 m covered with short grass kept about 8 cm high. The surface fluxes of sensible and latent heat were determined with the well-known energy-budget method, using Bowen's ratio (e.g. Sellers, 1965). The latter was evaluated with ventilated psychrometers (Slob, 1978) at 0.45 and 1.10 m respectively. The vertical differences of dry- and wet-bulb temperature were measured directly with thermocouples. The net radiation was measured with a net

pyrradiometer of the type Funk (1959). The soil heat flux was observed with heat flux plates at a depth of 5 and 10 cm at three locations. With the aid of the temperature difference between 0 and 2 cm in the ground the soil heat flux at the surface was obtained with a method developed by Slob (see Appendix). The wind speed was observed with a cup anemometer at 2 m.

For this study we transformed the 10-min means into hourly averages. Unreliable values were excluded; these mostly refer to situations with rain and fog.

3. The models

a. Introduction

According to the energy balance equation for the earth's surface the sum of sensible and latent heat flux densities (H and LE respectively) is given by

$$H + LE = Q^{\star} - G, \quad (1)$$

where Q^{\star} is the net radiant flux density, generally denoted as net radiation, G the soil heat flux density, L the latent heat of vaporization and E the evaporation. For a land surface G is mostly small with respect to Q^{\star} during daytime. A good estimate for G is (e.g. Burridge and Gadd, 1977)

$$G = 0.1 Q^{\star}. \quad (2)$$

This is confirmed by our measurements (see later).

Since net radiation can be evaluated from cloud cover (or duration of bright sunshine), air temperature and solar elevation using semi-empirical relations (e.g. Van Ulden and Holtslag, 1982), our problem is reduced to the determination of the partitioning of the available energy ($Q^{\star} - G$) into sensible and latent heat.

b. The Penman-Monteith model

The most complete expression for the partitioning of ($Q^{\star} - G$) into H and LE is Penman's equation applied to a cropped surface as done e.g.

III.5

by Monteith (1965) and Rijtema (1965) resulting in

$$LE = \frac{s(Q^* - G) + \rho c_p \delta e / r_a}{s + \gamma (1 + r_c / r_a)}, \quad (3)$$

where s is the slope of the saturation vapor-pressure temperature curve, ρ and c_p the density and specific heat at constant pressure of air, γ the psychrometric constant, r_a the aerodynamic resistance for sensible heat (and water vapor) of the air layer between the ground and the height of observation z , r_c the surface resistance, and δe the saturation deficit at z defined by

$$\delta e = e_s(T_a) - e_a, \quad (4)$$

where $e_s(T_a)$ is the saturation vapor pressure at air temperature T_a and e_a the actual vapor pressure at z .

Eq. (3) applies to extensive areas covered with a uniform vegetation fully shading the ground. Then the surface resistance is mainly determined by physiological factors, except when the foliage is wet. In that case $r_c = 0$. A detailed survey on the different features of Eq. (3) has been given recently by Monteith (1981). The counterpart of (3) for sensible heat is

$$H = \frac{\gamma(1 + r_c / r_a)(Q^* - G) - \rho c_p \delta e / r_a}{s + \gamma(1 + r_c / r_a)}. \quad (5)$$

From (1) and (3) it follows that the surface resistance r_c is given by

$$r_c = \left(\frac{s}{\gamma} B - 1 \right) r_a + \frac{\rho c_p}{\gamma} \frac{\delta e}{(Q^* - G)} (1 + B), \quad (6)$$

where B is the Bowen ratio ($= H/LE$).

With this relation r_c can be determined from micro-meteorological observations. Then the aerodynamic resistance r_a must be specified. In this study the semi-empirical expression proposed by Thom and Oliver (1977) is used, which is a modification of a relation given before by Penman (1948):

$$r_a = \frac{4.72 \left[\ln\left(\frac{z}{z_0}\right)^2 \right]}{1 + 0.54u}, \quad (7)$$

where u is the wind speed, z is the height and z_0 the surface roughness length for momentum. Thom and Oliver showed that in this expression stability effects on r_a are taken into account empirically^x. In the deduction of (7) it is assumed that the "surface roughness lengths" for heat and water vapor are equal to z_0 . This is not correct, but the errors introduced that way are small because the Bowen ratio often is of the order γ/s (see later). Then the first term in the right hand side of (6) can be ignored and r_c is independent of r_a .

For our purposes Eqs. (3) and (5) are rather inconvenient, since they contain a relatively large number of variables. Therefore, it is worthwhile to search for a simplification of the Penman-Monteith's formula. Before doing so, it must be emphasized that although this formula has some empirical elements (notably the determination of r_c is fully empirical) it is a physical reality that the surface fluxes depend on so many variables. The only chance we have to arrive at a simplification of Eqs. (3) or (5) is that some variables are either dominating, are interrelated or have a fairly narrow range of values in practice.

^x Eq. (7) suggests that z can be varied. However, since Penman's wind function is valid only for $z = 2$ m eq. (7) can only be applied to this height.

c. The modified Priestley-Taylor model

The best known simplification of Penman's formula is the concept of Priestley and Taylor (1972), who found for saturated surfaces^{xxx} that

$$LE = \alpha \frac{s}{s+\gamma} (Q^x - G) \quad (8)$$

where α is the so-called Priestley-Taylor parameter. When saturated air passes over a wet surface^x α will reach 1 (this has been noticed already by Schmidt in 1915 and follows directly from Eq. (3) with $r_c = \delta e = 0$). LE then equals $\frac{s}{s+\gamma} (Q^x - G)$. In literature this quantity often is denoted as the *equilibrium* latent heat flux density (LE_{EQ}), because some authors believe that when unsaturated air passes over an extensive wet surface it finally will become saturated. However, air seldom is saturated and for saturated surfaces α is found to be about 30 per cent greater than 1 when daily values are concerned (e.g. Priestley and Taylor, 1972, Brutsaert and Stricker, 1979). Eqs. (1) and (6) lead to

$$H = \frac{(1 - \alpha)s + \gamma}{s + \gamma} (Q^x - G). \quad (9)$$

In the moderate climatological regions $LE > H$, which implies that a relative small deviation of the Priestley-Taylor concept causes a relatively large error in H. Evidence given by e.g. De Bruin and Keijman (1979) reveals that a two parameter model of the type

$$LE = \alpha' \frac{s}{s+\gamma} (Q^x - G) + \beta \quad (10)$$

^{xxx} This refers to water surfaces as well as to cropped land surfaces not short of water.

^x A water surface or a land surface covered with a thin water layer.

III.8

is a somewhat better description of LE, where β is a small constant (see later).

Then H is given by

$$H = \frac{(1 - \alpha')s + \gamma}{s + \gamma} (Q^{\mathbb{K}} - G) - \beta \quad (11)$$

As noticed before, The Priestley-Taylor concept originally was restricted to saturated surfaces. In our study it will be applied also to non-saturated cases. Then the parameters α , α' and β will depend on the soil moisture conditions, the soil type, etcetera. Herein we follow authors like Davis and Allen (1973).

We found that the Priestley-Taylor approach becomes more transparent by writing

$$\beta = \frac{\frac{\rho_c p}{\gamma} \frac{\delta e}{r_c} - \left[\alpha' - (1 - \alpha') \frac{r_a}{r_c} \frac{s + \gamma}{\gamma} \right] \frac{s}{s + \gamma} (Q^{\mathbb{K}} - G)}{\frac{s}{\gamma} \frac{r_a}{r_c} + \frac{r_a}{r_c} + 1}, \quad (12)$$

which follows directly from Eqs. (3) and (10). This equation shows clearly that in reality parameter β depends on several independent variables such as δe , r_a and $(Q^{\mathbb{K}} - G)$. Consequently, the Priestley-Taylor model can only yield useful results when on the average β is small with respect to the first term in the right-hand side of Eq. (10). Then a variation of β of, say a factor 2, which certainly must be expected when we look at Eq. (12), results in a much smaller change of LE.

A reason why β will be small is that the two terms in the numerator of (12) have about the same magnitude, hence when

$$\frac{\rho_c p}{\gamma} \frac{\delta e}{r_c} \sim \left[\alpha' - (1 - \alpha') \frac{r_a}{r_c} \frac{s + \gamma}{\gamma} \right] \frac{s}{s + \gamma} (Q^{\mathbb{K}} - G). \quad (13)$$

It is seen that the first term of (13) contains δe and the second term $s/(s+\gamma)(Q^x - G)$.

Now, both these quantities have a pronounced diurnal variation. (That of δe is mainly due to the diurnal cycle of the air temperature). To illustrate this δe and LE_{EQ} are shown in Fig. 1 as function of time at a clear day in June 1977. This effect will lead to a positive correlation between the two terms in (13) and thus to the diminishing of β . In the next section more experimental evidence for (13) will be given.

4. Model comparison.

From the above description of the two models under consideration it follows that both contain at least one parameter which is determined by soil and plant factors. These are r_c in the Penman-Monteith model and α , α' and β in the (modified) Priestley-Taylor approach. Generally, these quantities depend upon many factors, such as availability of soil moisture, stage of development of the canopy, carbondioxide concentration, irradiance etc.* Models have been developed to describe e.g. r_c as a function of these physiological and environmental factors (e.g. Rijtema, 1965), but for the practical problems we are dealing with these procedures are not useful, not at least because the necessary information about canopy and soil often is missing. Therefore in real life the best we can do is to choose appropriate values for r_c , α etcetera under classes of circumstances, e.g. under *wet*, *normal* and *dry* conditions. Our available data set does not cover a range of soil conditions wide enough to define these classes very precisely. But, since it is our purpose to compare several models here this is not a serious problem.

It appears that during July 3 till 17 there was a significant shortage of soil moisture. In the next this period will be denoted as *dry* while the remaining days will be characterized as being *normal*.

* For a review in recent literature on the dependence of r_c on these factors see Ziemer (1979).

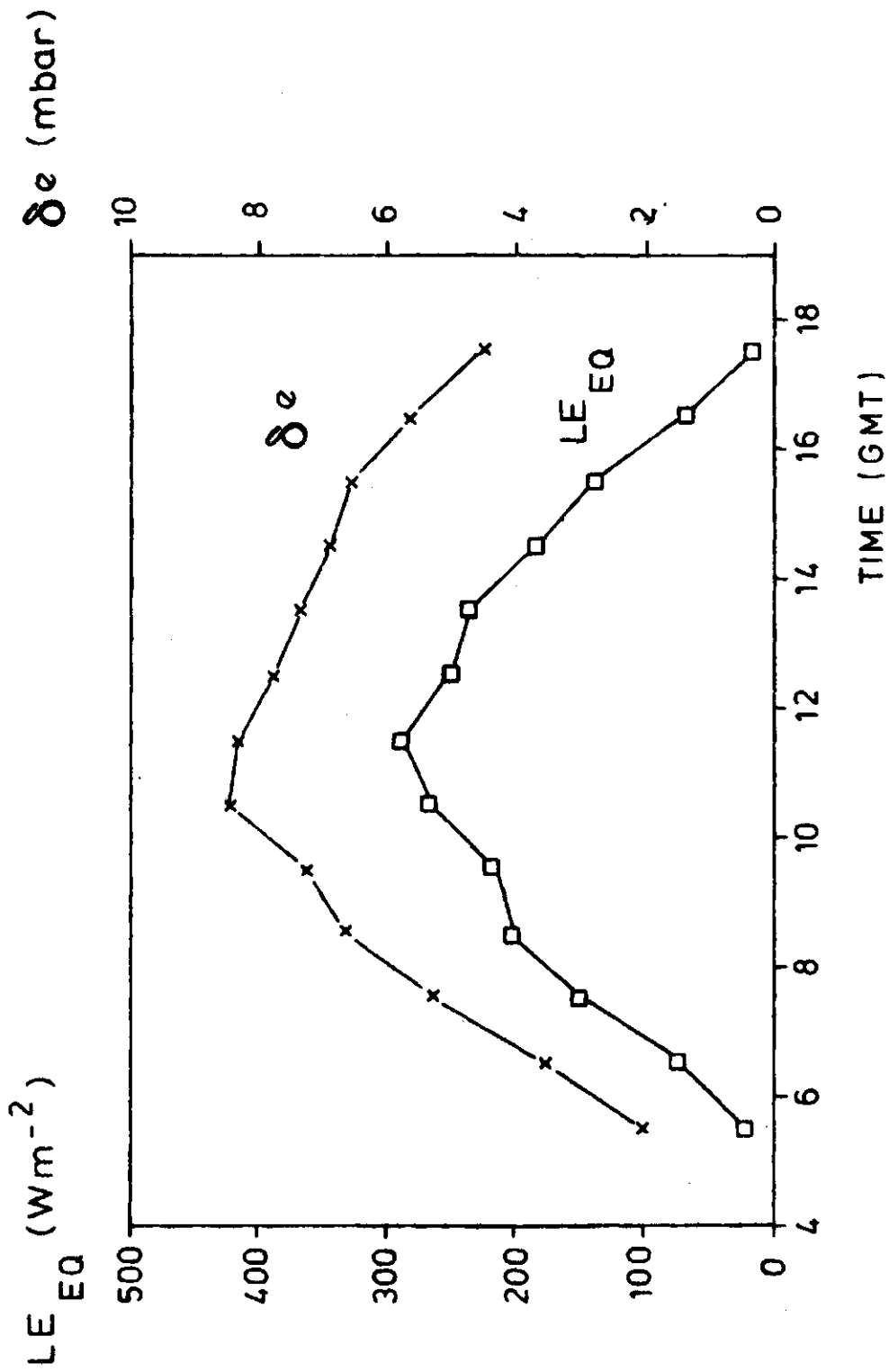


Fig. 1. Diurnal cycle of the water vapor deficit δ_e and the equilibrium latent heat flux density LE_{EQ} for a day in June 1977.

For the model comparison the following strategy is chosen. Firstly the model parameters will be adjusted for the *dry* and *normal* period, then the surface fluxes will be evaluated with the different models using these parameters. Finally a comparison will be made with the measured fluxes.

5. Results

Firstly, we will investigate the skill of Eq. (2) for the determination of the soil heat flux density (G). In Fig. 2 the hourly values of G , determined with the procedure described in the Appendix, are plotted against the corresponding observations of the net radiation (Q^{x}). A visual inspection of this figure reveals that on the average Eq. (2) is a rather good approximation, but there is a large random scatter. From a statistical analysis it follows that $\overline{Q^{\text{x}}} = 196 \text{ Wm}^{-2}$ and $\overline{G} = 16 \text{ Wm}^{-2}$ (a bar denotes a mean value of the entire data set), the correlation coefficient is 0.85, while for the regression parameter \underline{a} from $G = \underline{a} Q^{\text{x}}$ a value of 0.09 is found. Practically this does not differ significantly from $\underline{a} = 0.1$, used by Burridge and Gadd (1977). Taking $\underline{a} = 0.1$ a standard error for G of 9 Wm^{-2} is obtained. This is more than 50% of \overline{G} , however it is 5% of $Q^{\text{x}} - G$ which is an acceptable scatter for our practical calculations.

In order to get an impression of the variability of the model parameters r_c , α and α' from Eqs. (3), (8) and (10) respectively and in order to be able to adjust these quantities for the *normal* and *wet* period in Fig. 3 the daytime mean hourly values of r_c , α and α' are shown. Only those days were considered from which a complete data set of at least four hours are available.

From Fig. 3a it is seen that r_c has a considerable variation; it varies between, say, 20 and 280 s.m^{-1} . In the normal period it has a typical value of 60 s.m^{-1} , while in the dry July fortnight it rises continuously from 100 to 260 s.m^{-1} with a mean of about 160 s.m^{-1} .

Also the parameters α and α' (Figs. 3b and c) show a considerable scatter; α varies between 0.6 and 1.5 with a mean of about 1.15 in the *normal* and 0.8 in the *dry* period. The parameter α' from the modified Priestley-Taylor formula (10) shows a very similar behavior. Its mean

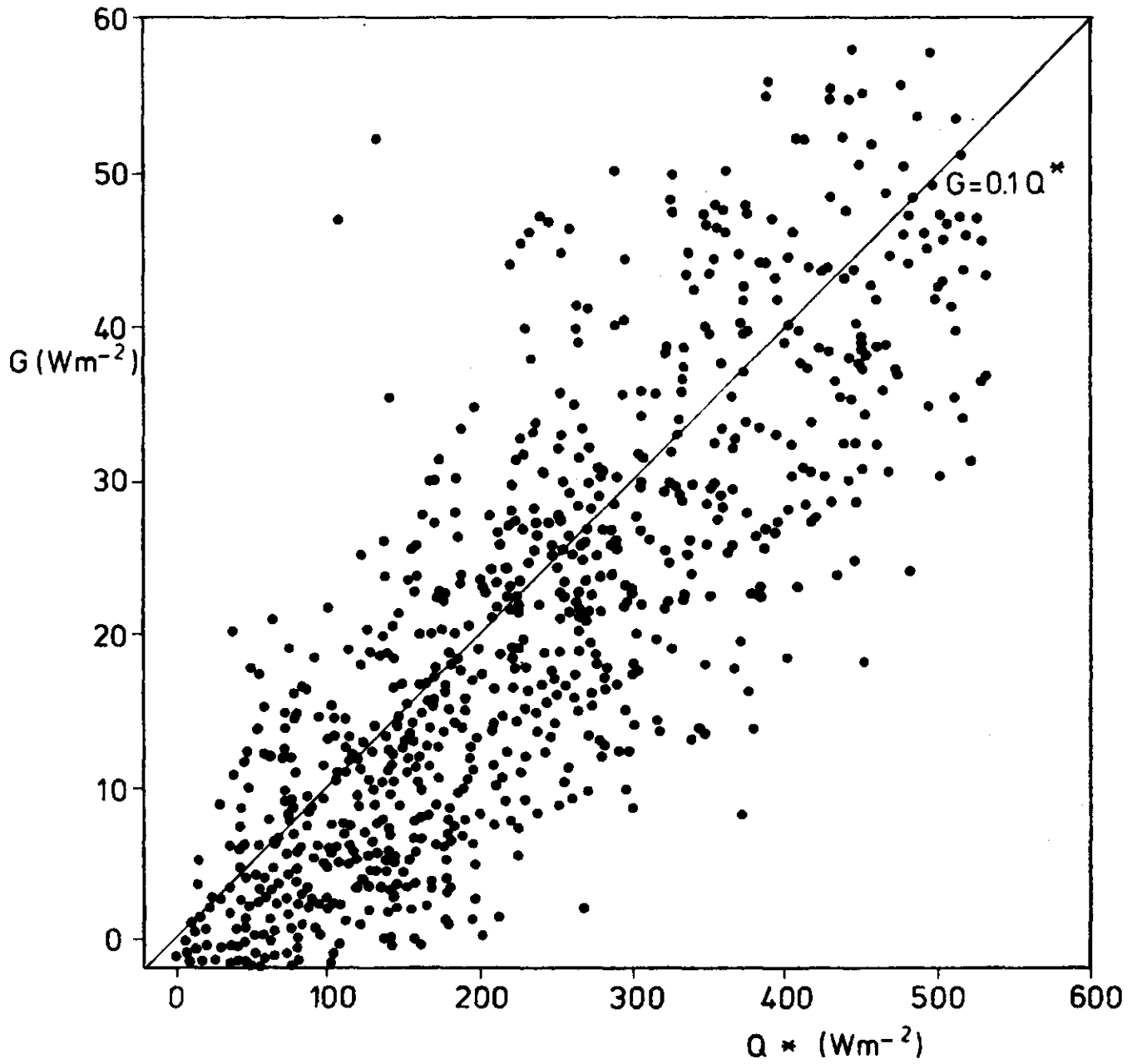


Fig. 2. Soil heat flux density G plotted against net radiation for 1040 hourly values during daytime.

r_c (sm^{-1})

III.13

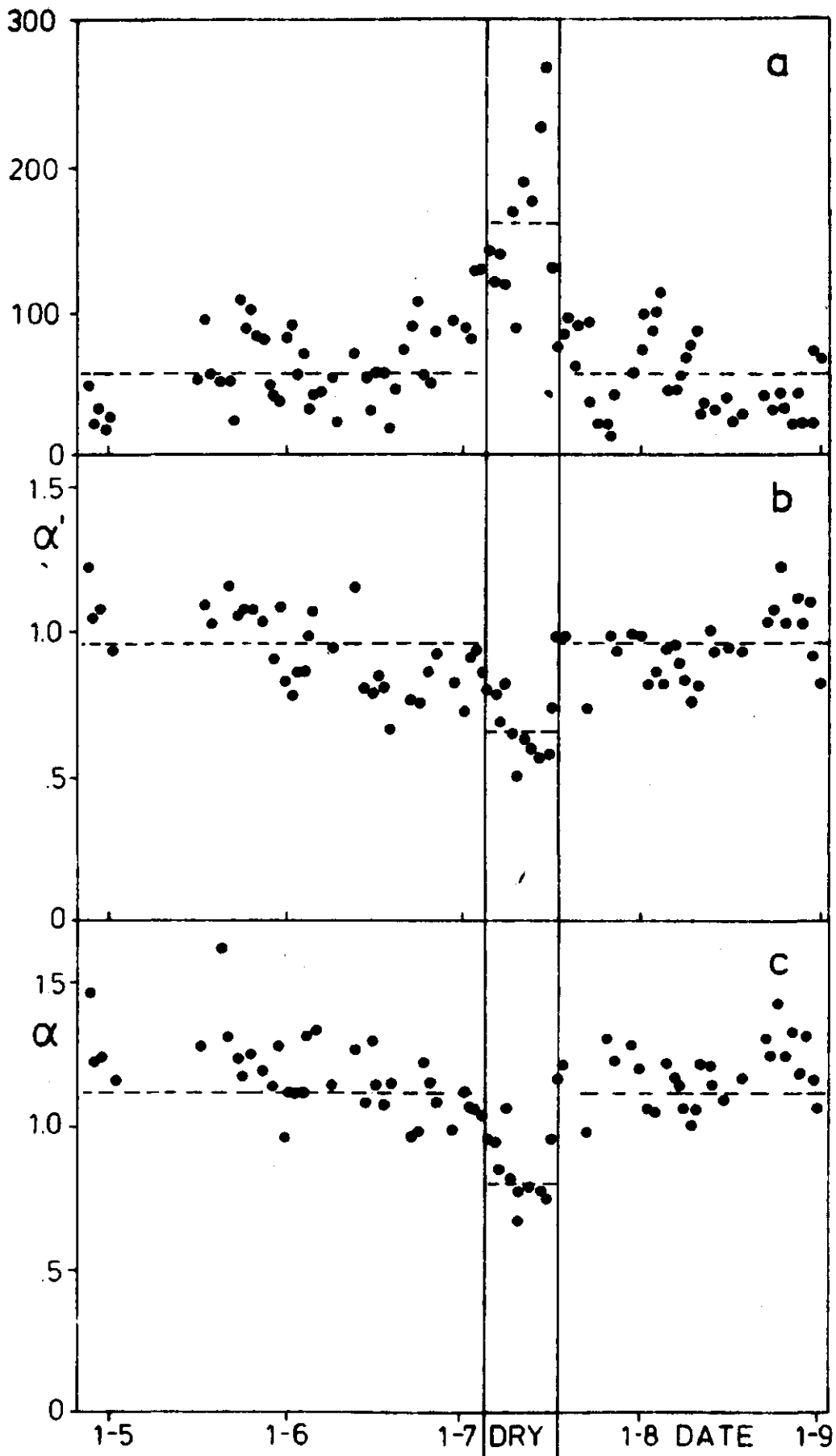


Fig. 3. Daytime averages of: a: the surface resistance r_c of Eq. (15).
b: the modified Priestley-Taylor parameter α' of Eq. (8).
c: the Priestley-Taylor parameter α of Eq. (6).

Quantity	\bar{Y}	\bar{X}	r	SE	SE/ \bar{Y}
LE ₁	125.4	125.1	0.97	23.8	0.19
LE ₂	125.4	125.3	0.97	21.2	0.17
LE ₃	125.4	126.2	0.95	26.3	0.21
H ₁	55.3	55.5	0.92	23.8	0.43
H ₂	55.3	55.3	0.92	21.2	0.38
H ₃	55.3	54.4	0.90	26.3	0.48

Table 1. Comparison of observed values (Y) and calculated values (X) of the fluxes of sensible (H) and latent heat (LE) of 1040 hours with $H + LE > 0$. (H, LE, Y, X and SE in $W.m^{-2}$).

- \bar{Y}, \bar{X} the average values of Y, X respectively.
- r correlation coefficient between Y and X.
- SE $\{(X-Y)^2\}^{\frac{1}{2}}$
- H₁, LE₁ refer to the unmodified Priestley-Taylor model, with $\alpha = 1.12$ for the normal and $\alpha = 0.8$ for the dry period.
- H₂, LE₂ refer to the modified Priestley-Taylor model with $\alpha' = 0.95$ for the normal period and $\alpha' = 0.65$ for the dry period and $\beta = 20 Wm^{-2}$ for the entire period.
- H₃, LE₃ refer to the Penman-Monteith model with $r_c = 60 sm^{-1}$ for the normal period and $r_c = 160 sm^{-1}$ for the dry period.

value in the *normal* and *wet* period is about 0.95 and 0.65 respectively. It is noted that α' is evaluated after β is chosen at 20 W.m^{-2} for the entire data set. This mean value of β is visually obtained by plotting the observed values of LE against LE_{EQ} .

After having obtained these results it was decided to choose the following values for r_c , α and α' to be used in the model comparisons:

(a) *normal* period: $r_c = 60 \text{ s.m}^{-1}$, $\alpha = 1.12$ and $\alpha' = 0.95$,

(b) *dry* period: $r_c = 160 \text{ s.m}^{-1}$, $\alpha = 0.8$ and $\alpha' = 0.65$.

(As noted before parameter β is kept at 20 W.m^{-2} for the entire period).

Using these values the surface fluxes were evaluated with the Penman-Monteith model and the, modified and unmodified Priestley-Taylor formula. For LE some results are shown in Fig. 4. In Table 1 statistical information is given about the skill of the models, referring to the entire data set and including also the sensible heat flux.

From the evidence given in Fig. 4 and Table 1 it can be seen that the skill of the modified Priestley-Taylor model is certainly as good as that of the Penman-Monteith equation. This leads to the conclusion that for many practical problems the modified Priestley-Taylor model must be preferred.

As to be expected the results of both models for evaporation are better than for the sensible heat flux, mainly due to the fact that mostly LE is greater than H during day-time.

From Table 1 it is seen that the modification of the Priestley-Taylor model by adding the constant $\beta = 20 \text{ Wm}^{-2}$ improves the skill, especially with respect to H. This can partly be explained by the fact that during the transition hours around sunrise and sunset H and $(Q^* - G)$ do not change sign at the same time. Especially, at the end of the day it is often observed that H becomes zero earlier than $(Q^* - G)$.

In section 3c it is noticed that a good skill of the Priestley-Taylor model can be explained by the fact that the two terms of (13) are positive correlated. That this is the case indeed is shown in Fig. 5, where a scatter diagram between these two terms is given. The correlation coefficient is found to be 0.65. For this relatively high value is no direct physical reason. It is mainly due to the fact that δe and $\frac{s}{s+\gamma} (Q^* - G)$ both have a diurnal (and also an annual) cycle. The corre-

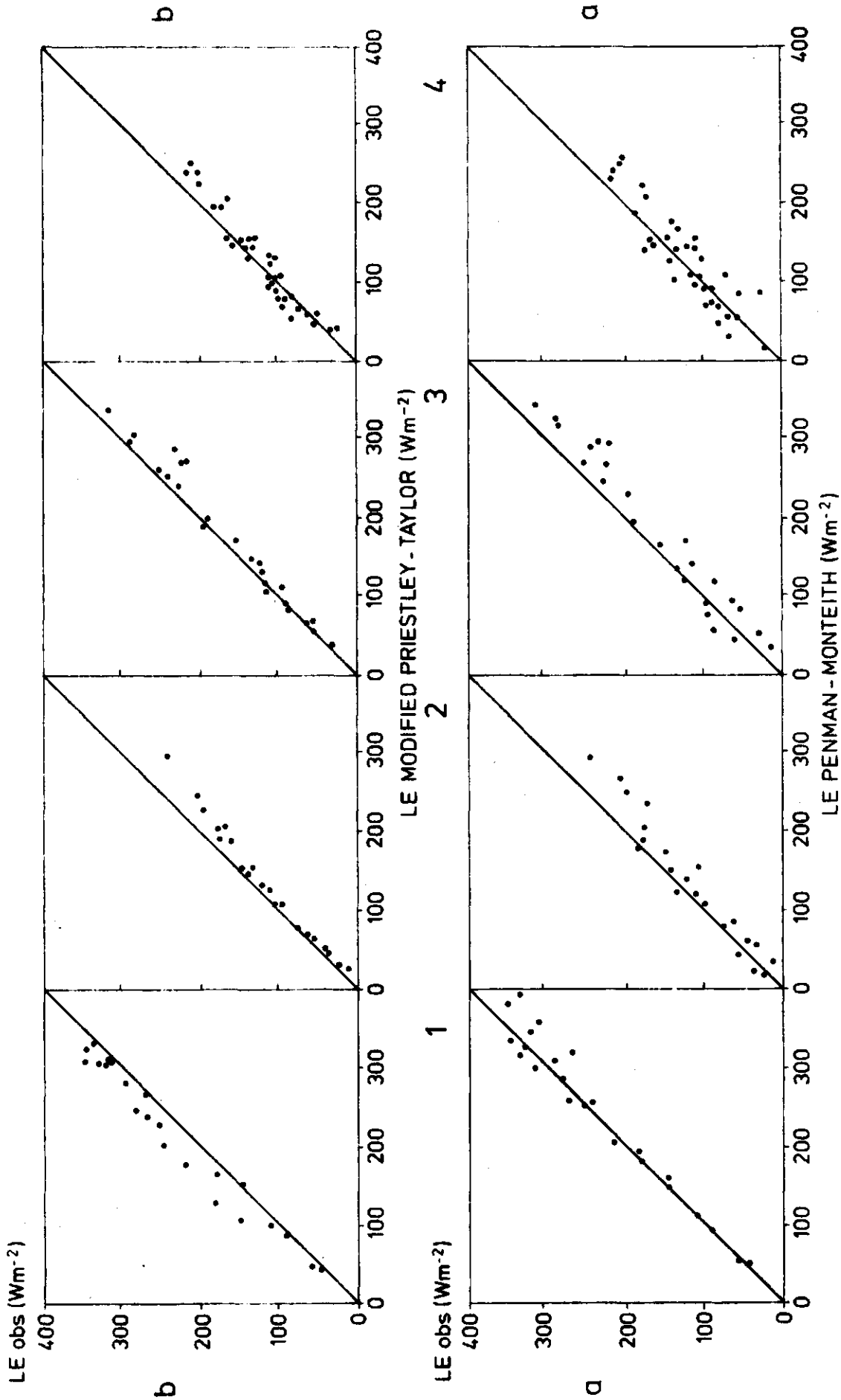


Fig. 4. Comparison of observed hourly averages of the latent heat flux (LE obs) with: a: The Penman-Monteith concept of Eq. (3). b: The modified Priestley-Taylor model of Eq. (8) for the following days: 1: May 19 and 25 (normal period) 2: June 4 and 30 (normal period) 3: July 3 and 22 (normal period) 4: July 9, 10 and 16 (dry period).

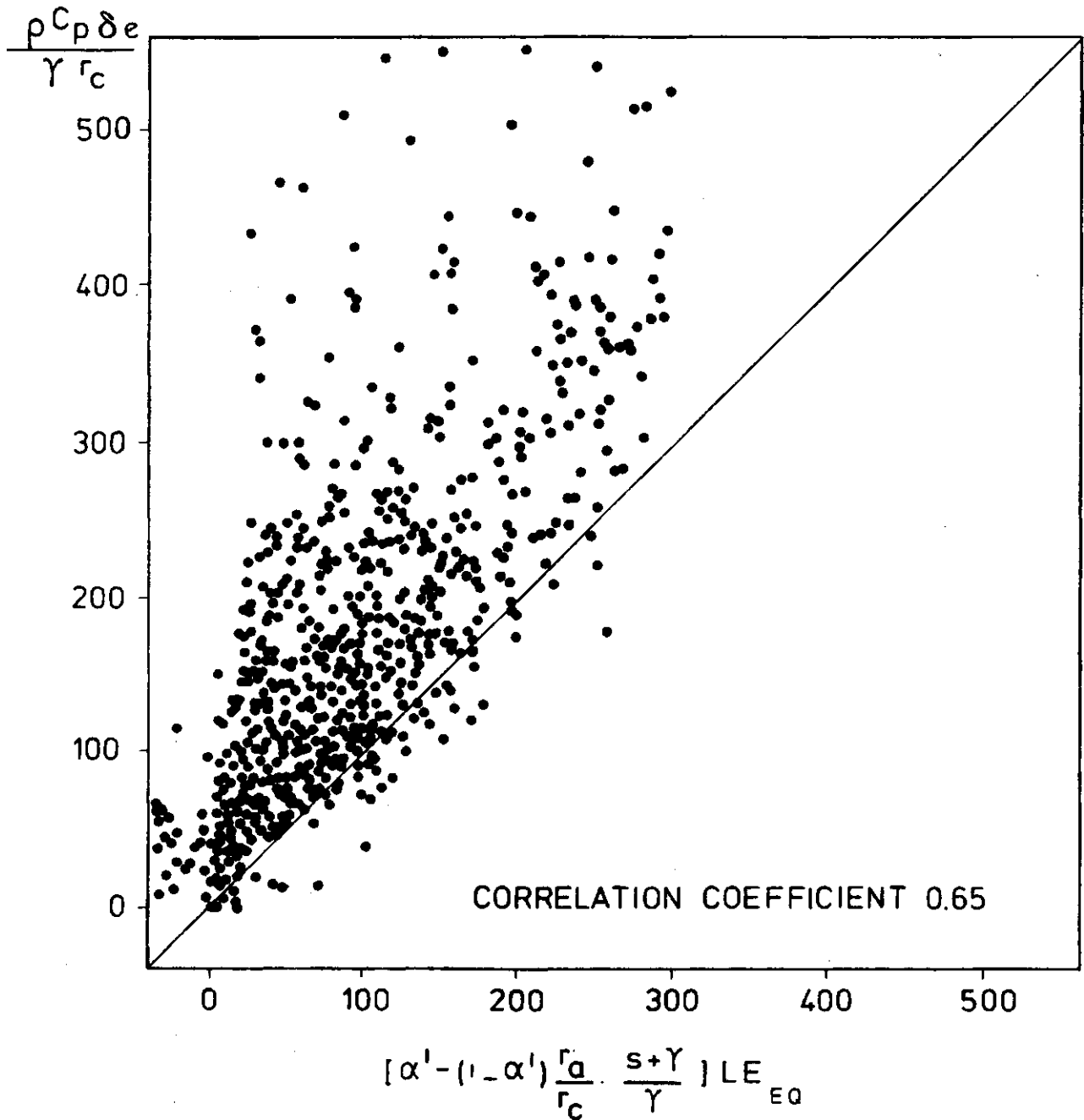


Fig. 5. Scatter diagram of the two terms of (13) for 1040 hourly values during daytime.

lation coefficient between these quantities appears to be 0.7. From Fig. 5 it is seen further that the first term of (13) mostly exceeds the second, resulting in a mean value of β greater than zero. The scatter present in Fig. 5 illustrates the statistical character of the Priestley-Taylor model; in reality β has a relatively large variation. When α' is fixed at 0.95 in the *normal* and at 0.65 in the *dry* period it appears that β for our data set can vary between -10 and +100 W.m^{-2} . Excluding the extreme values we obtain $\bar{\beta} = 23 \text{ W.m}^{-2}$ with about the same standard deviation.

The final step which must be made, but which falls outside the scope of this paper, is the determination of the net radiation. The way in which this must be done depends upon the available data. As an example we present here the results of an estimation scheme developed by Holtslag et al. (1980). They determine the net radiation from the air temperature, the total cloud cover and the incoming shortwave radiation. Using further Eq. (2), $\beta = 20 \text{ Wm}^{-2}$ and $\alpha' = 0.95$ in the *normal* and $\alpha' = 0.65$ in the *dry* period H is evaluated with Eq. (11) for 152 randomly selected hours. The results are shown in Fig. 6. It is seen that the agreement with the measured values is good.

6. Discussion

From the evidence given above it can be concluded that from a practical point of view the modified model of Priestley-Taylor has about the same skill as the more complete, but also more complicated, model of Perman-Monteith. We arrived at this result after adjustment of the model parameters which depend on soil- and plant factors. The available data set does not allow us to develop complete empirical rules for the determination of these parameters under different soil moisture conditions. In, what is denoted in this paper as *normal* period, the parameter α' from the modified Priestley-Taylor model appears to be about 1 (0.95 to be more precisely), while it equals about 0.65 in the so-called *dry* period. The best estimate of β appears to be 20 Wm^{-2} during the entire period.

An explanation for the fact that the Perman-Monteith model can be simplified to the modified Priestley-Taylor formula is the fact that the water vapor deficit δe is positive correlated with $L E_{FD}$. This correlation

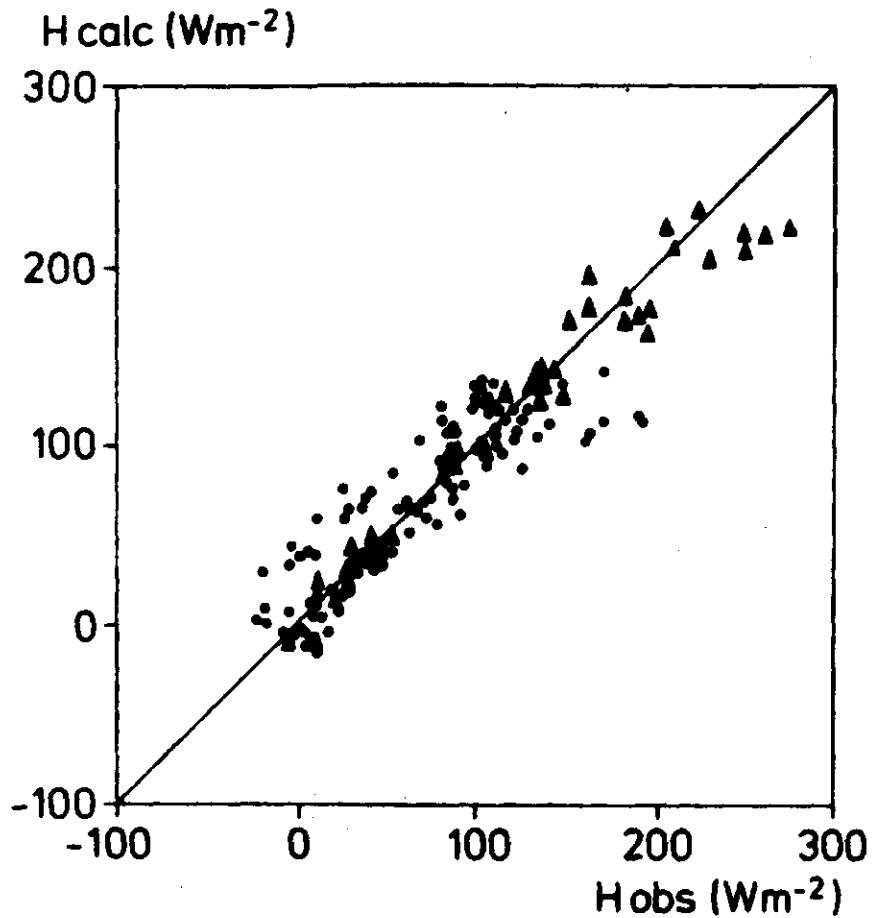


Fig. 6. Comparison of observed hourly averages of the sensible heat flux (H_{obs}) and calculated values (H_{calc}) with Eqs. (9), (2) and a semi-empirical procedure for the net radiation taken from Holtslag et al. (1980). Dots represent hours in normal periods and triangles represent hours in the apparently dry fortnight of July.

is mainly based on the diurnal cycle of both quantities. As a result the two terms in the numerator of Eq. (12) are counteractive, by which on the average β is small and H and LE become insensitive to variations of δe , r_c and r_a (and thus to variations of wind speed).

We have seen that in the *normal* period α' is found to be 1 and $\beta \approx 20 \text{ W.m}^{-2}$. On a clear summerday LE is of the order of several hundreds of W.m^{-2} , so that then β can be neglected, by which

$$LE \approx LE_{EQ}, \quad (14)$$

and consequently the Bowen ratio equals

$$B = \frac{Y}{S} \quad (15)$$

As noted before this result is also obtained when saturated air passes over a wet surface. On the other hand in literature often experimental evidence is reported for (14) for non-saturated circumstances, but this refers mostly to daily mean values. A review of these observations is given by McNaughton (1976). This author deduced Eq. (15) theoretically for the case of a sudden step in surface wetness, assuming that the reciprocal eddy diffusivities becomes indefinitely large with height.

In this study it is shown clearly that $\alpha' \approx 1$ on the average but that there is a large random scatter, while furthermore (14) and (15) are not valid in the dry July period.

Nevertheless, there remains some intriguing questions: Is there a tendency for (short) crops not short of water to evaporate at its equilibrium rate LE_{EQ} ? and: Is there a physical or physiological reason for this? If there is a physical cause for (14) and (15) then, in our opinion, this must be searched in the mechanism of turbulent exchange of heat and mass. It is suggested that in unstable air the vertical transfer of heat, mass and momentum is maintained by so-called *convective plumes* (Kaimal and Businger, 1970). Possibly, within these plumes the partitioning of the available energy at the surface ($Q^* - G$) into H and LE is described by (15). If this is true there can be an interaction between the plant-cover and the thermal. Does the canopy play an active role, e.g. by opening

its stomata when a plume is passing? Or, reverse: Does the occurrence of a plume be triggered by a plant cover opening its stomata and causing a local instability due to the water vapor injected into the atmosphere? These are intriguing questions indeed on which at the moment we do not know the answer. But it is worthwhile to look at the energy-exchange process in this way.^x

It is noted before that for so-called saturated surfaces parameter α from the unmodified Priestley-Taylor model is often found to be 1.26 for daily means of LE. This is not in contradiction with our $\alpha = 1.12$ obtained for daytime hourly values. Namely, when it is assumed that during nighttime LE is negligible small, while $(Q^x - G)$ is significantly less than zero, it can be shown that the daily mean of α is about 10 per cent greater than its hourly value during daytime. Indeed, it is found that $\alpha = 1.26$ yields good results for daily values in the summer months (De Bruin and Stricker, 1982).

Our results applies to a short vegetation for which the aerodynamic and the surface resistance are of the same order. This is illustrated in Fig. 7 where the ratio r_c/r_a is given. Except for the dry July period, r_c/r_a is of the order 1.5 which is in good agreement with the value found by Thom and Oliver (1977) for a similar surface in England. In the case of a tall vegetation with a dry foliage, r_c/r_a is much larger since r_a is than small due to the great surface roughness. In the limit $r_a \rightarrow 0$ LE reaches (Thom and Oliver, 1977)

$$LE = \frac{\rho c_p}{\gamma} \frac{\delta e}{r_c}, \quad (16)$$

so that LE does not depend anymore upon $(Q^x - G)$ explicitly. Thus for tall vegetations it is not to be expected that the Priestley-Taylor model is applicable. Nevertheless, the correlation between δe and $\frac{s}{s+\gamma} (Q^x - G)$ remains to exist also in the case of a tall crops, so that the Priestley-Taylor concept still may be useful. But then one should account for the contribution of evaporation of intercepted water to the total evaporative losses (Shuttleworth and Calder, 1979).

^x We found afterwards that the behavior of α and B can be understood with a coupled boundary layer-surface layer model (see next chapter).

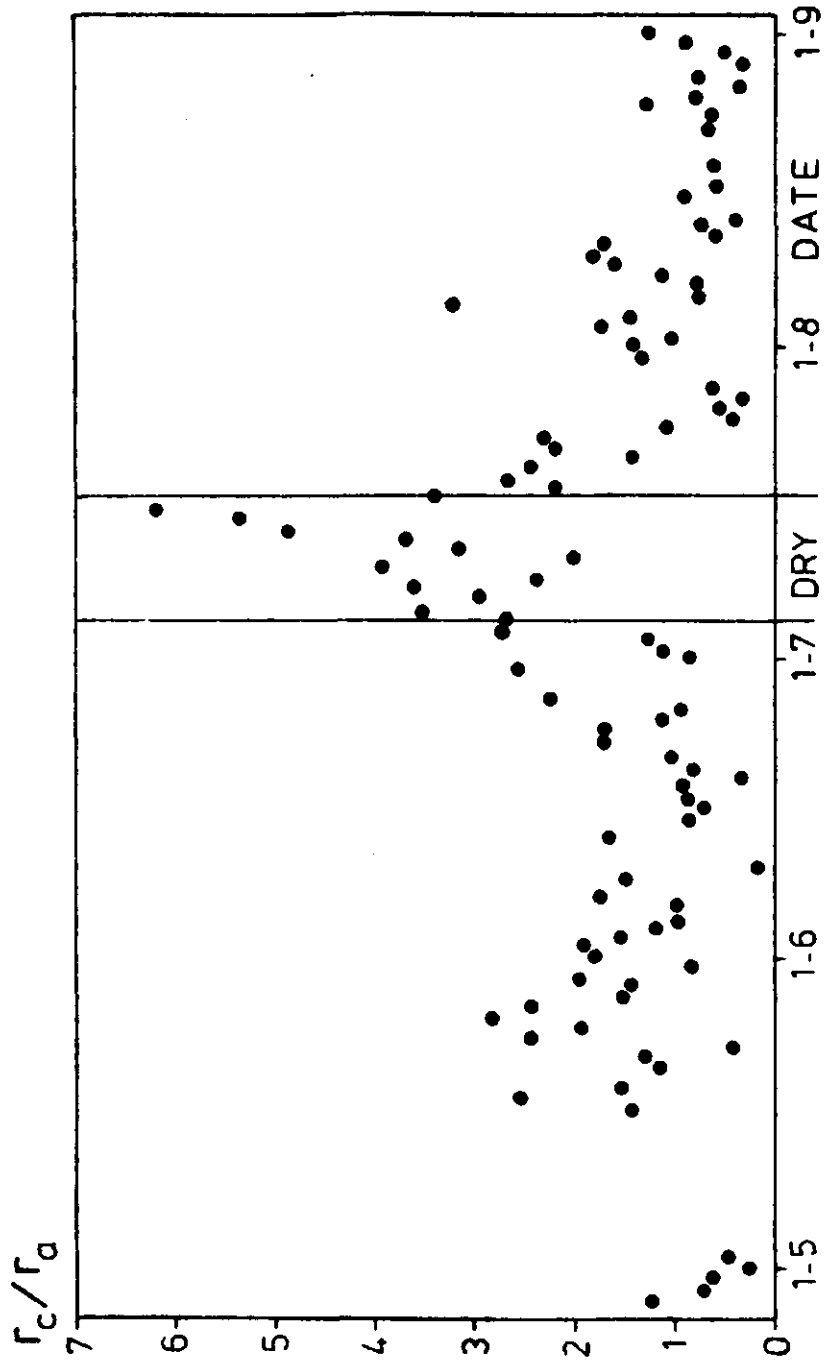


Fig. 7. Daytime averages of the surface aerodynamical resistance ratio r_c/r_a .

Finally, it must be emphasized that our results refer to the summer months. Then $(Q^* - G)$ is relatively large. In winter this is no longer true and it must be expected that then the (modified) Priestley-Taylor model will yield unrealistic results.

7. Conclusions

In this paper it is shown that for a short vegetation the hourly fluxes of latent and sensible heat can appropriately described by a modified Priestley-Taylor model Eq. (10) and (11). It has the same skill as the Penman-Monteith equation, which is more complete from a physical point of view but which requires more input data. An important reason why the Penman-Monteith equation can be simplified to the Priestley-Taylor formula is the fact that the saturation deficit and the equilibrium latent heat flux density (LE_{EQ}) are correlated, due to the fact that both have a diurnal cycle.

APPENDIX

The determination of the soil heat flux

The soil heat flux density G is described by:

$$G(z) = - \lambda \frac{\partial T}{\partial z} , \quad (A1)$$

where λ is the thermal conductivity of the soil, T is the soil temperature and z is the depth. In our experimental set-up G is measured at 5 and 10 cm simultaneously with the soil temperature at 0 and 2 cm in the ground.

The soil heat flux at the surface ($z = 0$) must be evaluated. For this Slob (unpublished) uses the following procedure:

It is assumed that $\partial T / \partial z$ at the surface can be approximated by:

$$\left(\frac{\partial T}{\partial z} \right)_s = \frac{\Delta T}{\Delta z} , \quad (A2)$$

where ΔT is the difference between the soil temperature at 2 and 0 cm and $\Delta z = 2$ cm. Furthermore the assumption is made that λ in the top layer of 2 cm is constant during a period of approximately one day taken from 4.00 GMT till 4.00 GMT the next day. The unknown value of λ during the period is obtained as follows: Firstly, the quantity $I(z)$ is introduced, which is defined by:

$$I(z) = \int_{t_0}^{t_0+\tau} \left| G(z,t) - \frac{G(z,t_0) - G(z,t_0+\tau)}{\tau} (t-t_0) \right| dt , \quad (A3)$$

where t is the time, $t_0 = 4.00$ GMT and $\tau = 1$ day. It is seen that $I(z)$ is the time integral of the absolute value of $G(z)$ minus the trend over 1 d. It is a measure for the diurnal amplitude of the soil heat flux density.

Now it is assumed that $I(z)$ decreases exponentially with depth. This is the case when $\lambda/(\rho_s c)$ (ρ_s is the density and c the specific heat capacity of the soil) is constant with the depth and when there is no trend. This leads to:

$$\frac{I(0)}{I(5)} = \frac{I(5)}{I(10)}. \quad (4)$$

Then $I(5)$ and $I(10)$, these are the values of I at 5 cm and 10 cm respectively, can be evaluated from the available data.

Since λ is assumed to be constant over τ it can be obtained from Eqs. (A1)-(A3) by taking $z = 0$. This yields:

$$\lambda = - I(0) \Delta z \left[\int_{t_0}^{t_0+\tau} \left| \Delta T(t) - \frac{\Delta T(t_0) - \Delta T(t_0+\tau)}{\tau} (t-t_0) \right| dt \right]^{-1} \quad (A5)$$

Then G follows from (A1).

IV. A boundary layer model coupled to the Penman-Monteith equation †

Abstract

A model is presented that describes the evolution of air temperature, humidity and the surface fluxes of sensible heat and water vapor, when the initial profiles of temperature and humidity are known together with the radiative forcing and the surface wetness. The model can be regarded as an extension of the one by Perrier. In our study the description of the atmospheric boundary layer is more complete, e.g. the boundary layer height varies in time, while at its top the fluxes of sensible heat and water vapor are parameterized. For this a simple description is used by which a relaxation equation for the specific humidity deficit is obtained. With our model the Priestley-Taylor parameter α is calculated as a function of the surface wetness and other parameters. Good agreement with observations is found.

† Submitted to Journal of Applied Meteorology.

IV.2

List of symbols

a	entrainment parameter for sensible heat	(-)
b	entrainment parameter for moisture	(-)
c	constant in Swinbank formula	(K ⁻²)
h	boundary layer height	(m)
p	air pressure	(N.m ⁻²)
q	specific humidity	(kg.kg ⁻¹)
q _m	specific humidity of the well-mixed layer between $z = z_L$ and $z = h$	(kg.kg ⁻¹)
q _w	saturation specific humidity	(kg.kg ⁻¹)
r _a	aerodynamic resistance	(s.m ⁻¹)
r _c	surface resistance for water vapor	(s.m ⁻¹)
s	$\frac{dq_w}{dT}$ at $T = \theta_m$	(K ⁻¹)
s _r	idem at $T = \theta_r$	(K ⁻¹)
t	time	(s)
t ₀	initial time	(s)
t ₀ [*]	idem	(s)
u	wind speed	(m.s ⁻¹)
z	height	(m)
z _L	height of the surface layer	(m)
A	albedo	(-)
B	the Bowen ratio	(-)
E	evaporation	(kg.m ⁻² .s ⁻¹)
G	soil heat flux density	(W.m ⁻²)
H	sensible heat flux density	(W.m ⁻²)
I	heat-input integral	(m.K)
K	turbulent exchange coefficient	(m ² .s ⁻¹)
K [↓]	incoming shortwave radiation	(W.m ⁻²)
L [↓]	incoming longwave radiation	(W.m ⁻²)
Q [*]	net radiation	(W.m ⁻²)
T	air temperature	(K)
T _d	dew point	(K)
Y	dew point depression	(K)

IV.3

Y_e	quantity defined by eq. (8)	(K)
α	Priestley-Taylor parameter	(-)
γ	$= c_p/\lambda$	(K ⁻¹)
γ^*	$= \gamma(1 + \frac{r_a}{r_c})$	(K ⁻¹)
γ_θ	$= \frac{d\theta}{dz}$ for $z > h$	(K.m ⁻¹)
γ_q	$= \frac{dq}{dz}$ for $z > h$	(m ⁻¹)
δ_0	quantity defined by eq. (19)	(K.m)
δq	saturation specific humidity deficit	(kg.kg ⁻¹)
$(\delta q)_e$	quantity defined by eq. (35)	(kg.kg ⁻¹)
θ	potential temperature	(K)
θ_m	potential temperature of the well-mixed layer between $z = z_L$ and $z = h$	(K)
θ_s	potential temperature at the surface	(K)
θ_{∞}	defined by eq. (20)	
λ	latent heat of vaporization	(J.kg ⁻¹)
ρ	density of air	(kg.m ⁻³)
σ	the Stefan Boltzmann constant	(W.m ⁻² .K ⁻⁴)
τ	time lag	(s)
$\Delta\theta$	jump in θ -profile at $z = h$	(K)
Δq	jump in q -profile at $z = h$	(kg.kg ⁻¹)

1. Introduction

The Penman-Monteith equation (Monteith, 1981) describes the surface flux densities of water vapor (E) and sensible heat (H) as functions of air temperature (θ) and specific humidity (q). In this concept θ and q are assumed to be independent variables, i.e. they do not depend on H and E .

On the other hand, models have been developed that describe the evolution of the temperature and humidity of the lowest layer of the atmosphere as a function of E and H (e.g. Driedonks, 1981). In these models H and E are assumed to be independent quantities. In reality there is an interaction between θ and q on the one side and H and E on the other. When at the surface heat and water vapor are supplied to the atmosphere the temperature and moisture content of the air will be influenced. In turn this reflects on the surface fluxes.

In a recent paper Perrier (1980) pointed out this interaction in the Penman-Monteith equation. He constructed a simple model in which the relation between θ and q and the surface fluxes is taken into account. In this paper a model is presented which can be regarded as an extension of that by Perrier.

The behavior of the soil-atmosphere system is determined also by external factors. Among other things, these are the amount of energy and the amount of water available at the surface. We will confine ourselves to extensive homogeneous cropped terrains during daytime conditions. Then the surface wetness can be described by the surface resistance r_c (Monteith, 1965, 1981). Furthermore, a vegetation insulates the surface efficiently, so that usually the soil heat flux density (G) is small compared to the net radiation (Q^*). During daytime G can be taken as a small fraction of Q^* . Then the sum of the sensible and latent heat flux densities $H + \lambda E$ (λ = latent heat of vaporization) is determined by Q^* only. This quantity depends mainly on solar radiation and, in first order, it can be regarded as a purely external factor. For that reason we will describe with our model the partitioning of $Q^* - G$ into H and λE rather than the surface fluxes H and E themselves.

For this we will use the Priestley-Taylor parameter α , defined by

$$\lambda E = \alpha \frac{s}{s+\gamma} (Q^* - G) , \quad (1)$$

where $\gamma = c_p/\lambda$, c_p the specific heat of air at constant pressure and s the slope of the saturation specific humidity-temperature curve at air temperature.

We prefer to use α rather than the Bowen ratio $B \equiv H/\lambda E$ as a measure for the partitioning of $(Q^* - G)$ into H and λE (i) for practical reasons: in the last several years a large number of papers have been published on α and (ii) for physical reasons: in the case that saturated air passes over a wet surface (i.e. $r_c = 0$) $\alpha = 1$ and $B = \gamma/s$ (this follows directly from the Penman-Monteith equation treated in section 3.2). Since s depends on θ this implies that for that case B still varies with θ , while α is constant for all temperatures.

Another external factor is the wind speed. The influence of this weather variable on the surface fluxes can be described by the aerodynamic resistance r_a (Monteith, 1981).

The main differences between the model of Perrier and ours are (i) in our model the height of the boundary layer h varies as a function of H and time, whereas Perrier took h constant, and (ii) in the model of Perrier there is no air exchange at the top of the boundary layer. In our model there is a flux of heat and moisture at $z = h$ due to the entrainment from above of warm and generally dry air into the boundary layer. Because Perrier assumed that the boundary layer is closed at the top, while heat and moisture are supplied continuously to the atmosphere at the surface θ and q can reach unrealistically high values in his model.

For the development of our model we will use a boundary layer model recently published by Driedonks (1981, 1982).

We intend to calculate α as a function of the surface resistance r_c for different values of the aerodynamic resistance r_a and for different entrainment rates of dry air at the top of the boundary layer. This will be done for a typical summer day in the Netherlands.

Finally comparisons between observed and calculated values of α will be made.

2. The model of Perrier

Perrier (1980) started from a schematic picture of the atmosphere-soil-plant system as shown in Fig. 1. Above the canopy there is a surface sub-layer (Perrier used the French denoting sous-couche limite de surface) to which an exchange coefficient ($1/r_a$) can be assigned.

Above this sub-layer there is a turbulent layer (couche turbulente) characterized by temperature T , dew point T_d and wind speed u . The height of this layer (h) is constant, while at $z = h$ the system is closed, so that there vertical fluxes of heat and water vapor are zero.

Perrier ignores further details of the structure of the turbulent layer and the surface sub-layer.

He states without derivation that the evolution of T and T_d are described by

$$\rho c_p h \frac{d[T(t) - T(t_0)]}{dt} = H \quad (2)$$

and

$$\rho c_p h \frac{s}{\gamma} \frac{d[T_d(t) - T_d(t_0)]}{dt} = \lambda E, \quad (3)$$

where ρ is the air density and t_0 the initial time.

From (2) and (3) a differential equation for the dew point depression

$$Y = T - T_d \quad (4)$$

is obtained:

$$\frac{dY}{dt} = \frac{H - \gamma/s \lambda E}{\rho c_p h} \quad (5)$$

Finally, using the Penman-Monteith equation for E and H , Perrier arrives at a relaxation equation for Y , which we present here in the form

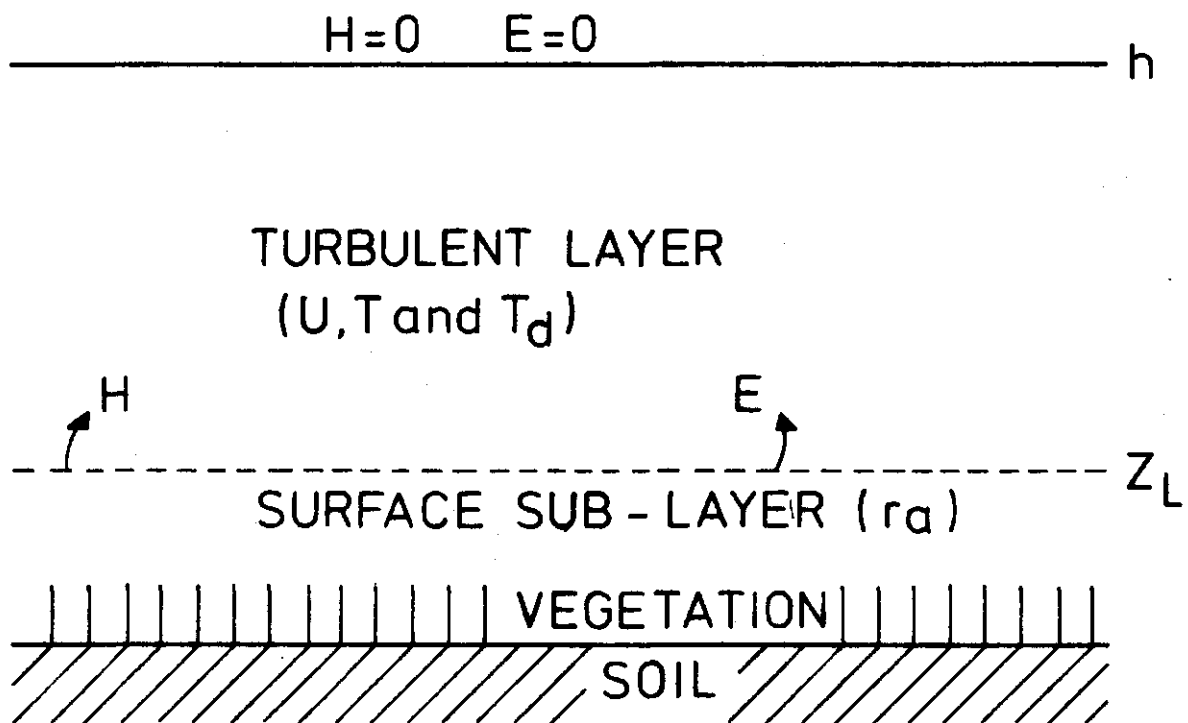


Fig. 1. Schematic picture of the soil-plant-atmosphere system used by Perrier (1980).

$$\frac{dY}{dt} + \frac{Y}{\tau} = \frac{Y_e}{\tau} \quad , \quad (6)$$

where the time lag τ is given by

$$\tau = (r_a + \frac{\gamma}{s+\gamma} r_c) h \quad (7)$$

and

$$Y_e = \frac{\gamma}{s+\gamma} \frac{Q^* - G}{\rho c_p} r_c \quad (8)$$

Perrier assumes that r_c is independent on weather variables. Although Perrier's description, especially that of the atmospheric boundary layer, is not complete, it is a very elegant first step to model the interaction between θ and q and the surface fluxes. The main imperfection of the model of Perrier is the fact that in his description the temperature and humidity of the air can reach unrealistically high values. This is due to the assumption made concerning the atmospheric boundary layer. As seen in the introduction this can lead to errors in the calculated surface fluxes. In our extension of the Perrier model a more realistic description of the boundary layer is used.

3. Our model

3.1 The boundary layer sub-model.

To describe the relevant boundary layer parameters we will use the recent papers by Driedonks (1981, 1982) concerning the dynamics of the well-mixed atmospheric boundary layer. On a clear day the profiles of the conservative quantities θ (= potential temperature)^x and q (specific humidity) have the approximative forms shown in Fig. 2.

^x Here θ is defined with respect to the surface air pressure in stead of 1000 mb generally used. By this θ equals the air temperature at $z = 0$.

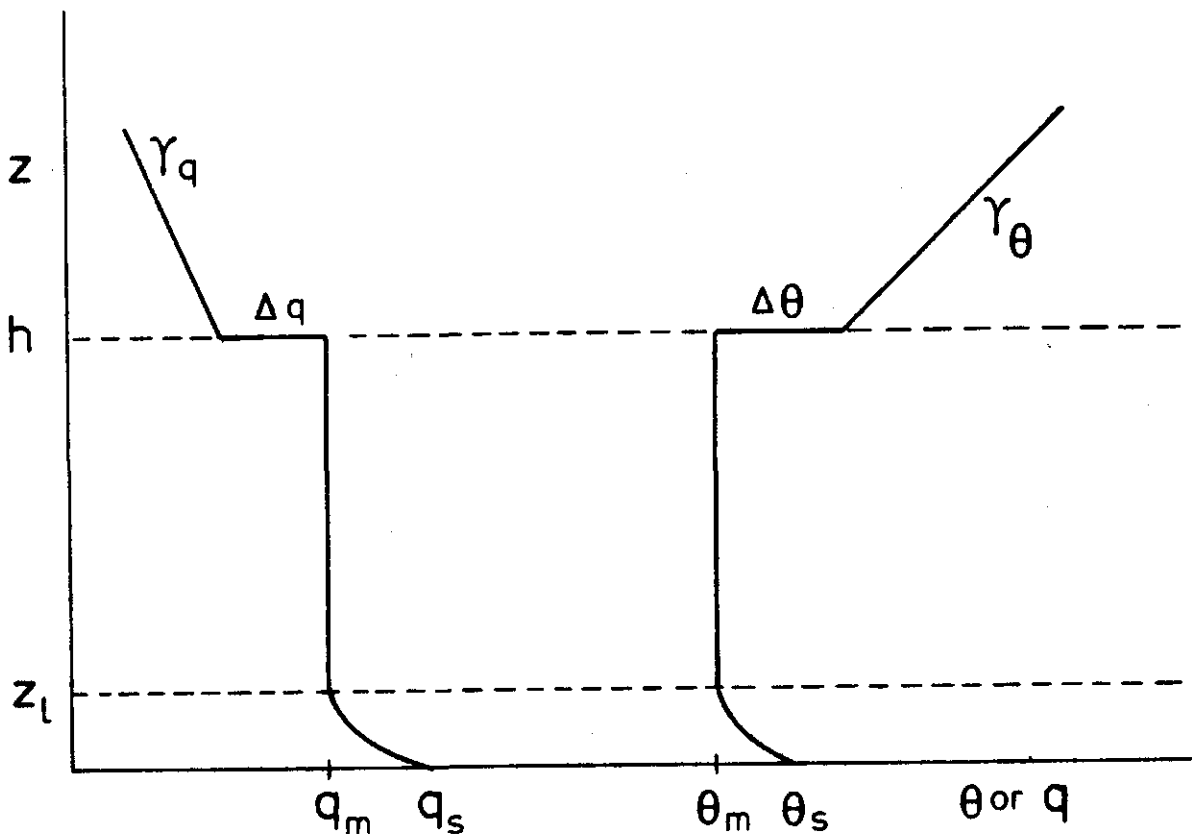


Fig. 2. Profiles of potential temperature (θ) and specific humidity (q) in the well-mixed atmospheric boundary layer.

Up to $z = h$ (= the height of the boundary layer) q and θ are constant at q_m and θ_m respectively due to turbulent mixing. At $z = h$ the boundary layer is capped by an inversion; for $z > h$ there is stable air characterized by $\gamma_\theta = (d\theta/dz)_{z > h}$ and $\gamma_q = (dq/dz)_{z > h}$. The transition layer between the well-mixed layer and the air aloft is usually small, so that the profiles can be approximated as shown in Fig. 2: at $z = h$ they have a jump characterized by $\Delta\theta$ and Δq .

In the surface layer (constant flux layer) the gradients of θ and q are sharp; going down from the top of this layer ($z = z_L$) to the ground θ and q increase rapidly during daytime from θ_m and q_m to their surface values θ_s and q_s , especially close to the ground.

Usually the thickness of the surface layer is small compared to h , so that its heat capacity can be neglected.

The dynamics of the atmospheric boundary layer can be described as follows. The atmosphere is transparent for shortwave (solar) radiation, implying that there is no direct heating of the air by the sun. The surface is heated by the sun, in its turn, the surface heats the air. This leads to convective production of turbulence in the boundary layer. If the wind speed is different from zero there is also mechanical production of turbulence due to wind shear. The turbulence maintains a vertical flux of heat. Since the heat flux decreases with increasing z the temperature of the air increases. On clear days with sufficient net radiation the turbulence is vigorous enough to maintain a well-mixed layer with vertical profiles as depicted in Figure 2.

In daytime the height of the boundary layer generally increases in time. The growth of h is caused by the entrainment of stable air above the inversion into the boundary layer. The entrainment is driven by turbulent eddies that intrude into the stable air aloft.

To simplify matters, we will restrict our study to cases in which only convectively produced turbulence is of importance. This condition is met most easily on clear summer days; also the early morning hours have to be avoided (Driedonks, 1981). Furthermore we neglect the influence on the temperature of the divergence of longwave radiation and the effects of horizontal advection.

3.1.1 Parameterization of the entrainment of dry and warm air at $z = h$.

When the boundary layer is growing stable air with a higher potential temperature enters it. As a result there is a downward heat flux at $z = h$. For practical applications good results are obtained when this flux is taken proportional to the flux at the surface (Tennekes, 1973; Driedonks, 1981). Together with the fact that (i) θ is constant in the boundary layer and (ii) the transition layers at the surface and the inversion are negligibly small, this leads to

$$\frac{d\theta_m}{dt} = \frac{a H}{\rho c_p h}, \quad (9)$$

where a is a constant equal to 1.2 (Driedonks, 1981).

The specific humidity q_m of the boundary layer is altered by (i) evaporation at the surface of liquid water and (ii) the entrainment of generally drier air at the top of the boundary layer. This implies that q_m depends on the rate of growth of h (dh/dt) and of the profile of q for $z > h$, i.e. on Δq and γ_q (Driedonks, 1981). In this study we will use a simplified parameterization for dq_m/dt , which corresponds to the simplified equation (9) for $d\theta_m/dt$. We thus approximate dq_m/dt by

$$\frac{dq_m}{dt} = \frac{b E}{\rho h}, \quad (10)$$

in which b is a parameter describing the rate of entrainment of dry air at the top of the boundary layer. When $b = 1$ there is no flux of moisture at $z = h$, while when $b = 0$ the humidity increase due to the surface evaporation is balanced by the humidity decrease at the top of the boundary layer caused by the entrainment of dry air. In that case q_m is constant. Also b can be negative. In that case the humidity decrease due to entrainment exceeds the effect of surface evaporation. We will assume that b is constant for any day, but we will allow it to vary from case to case.

Data on q_m are scarce. Driedonks (1981) published observations of q_m at Cabauw for 8 days. When variations of q_m of 15% or less are ignored, q_m was about constant on 4-5 days, implying that b was about 0 in those cases. Furthermore on one day q_m increased clearly, while on two others q_m tended to decrease. From this information we estimate that usually b varies between $-0.5 \lesssim b \lesssim 0.5$.

It will be shown in section 3.2 that the surface fluxes depend on the specific humidity deficit δq at the top of the surface layer (at $z = z_L$) defined by

$$\delta q = q_w(\theta_m, p_L) - q_m, \quad (11)$$

where q_w is the saturation specific humidity at $\theta = \theta_m$ and air pressure $p = p_L$ ($= p$ at z_L). We will assume that p_L is constant in time. Usually, the surface layer is so thin that the variation of p in this layer can be neglected. For these reasons we will omit the dependence of q_w on p in the following.

With these simplifications q_w is a function of θ_m only. This is a non-linear relationship. To simplify matters we now approximate $q_w(\theta_m)$ by

$$q_w(\theta_m) = q_w(\theta_r) + s_r(\theta_m - \theta_r), \quad (12)$$

where θ_r is a reference potential temperature which is the average of θ_m on a particular day, and s_r the derivative of q_w at $\theta = \theta_r$. In this way we get for δq :

$$\delta q = (q_w(\theta_r) - q_m) + s_r(\theta_m - \theta_r). \quad (13)$$

Here $q_w(\theta_r)$ and s_r are constant. Then $d(\delta q)/dt$ equals

$$\frac{d(\delta q)}{dt} = - \frac{dq_m}{dt} + s_r \frac{d\theta_m}{dt}. \quad (14)$$

With (9) and (10) this leads to

$$\frac{d(\delta q)}{dt} = \frac{a s_r H - b \gamma \lambda E}{\rho c_p h}. \quad (15)$$

We recall that $\gamma = \frac{c_p}{\lambda}$.

3.1.2 The evolution of θ_m and h

We are dealing with conditions under which the production of turbulence is purely convective. Then we can use the analytic expressions for the evolution of h and θ_m found by Driedonks (1981, 1982):

$$h(t) = \sqrt{\frac{2(2a-1) (I(t) - \delta_0)}{\gamma_\theta}} \quad (16)$$

and

$$\theta_m(t) = \theta_{\infty} + \gamma_\theta \frac{a}{2a-1} h(t) , \quad (17)$$

in which

$$I(t) = \int_{t_0}^t \frac{H}{\rho c_p} dt' , \quad (18)$$

where t_0 is the time of effective sunrise, i.e. the time at which H becomes positive. The quantities δ_0 and θ_{∞} are determined by the initial values of $\Delta\theta$, θ_m and h (denoted with an index 0):

$$\delta_0 = h_0 \Delta\theta_0 - \frac{1}{2} \gamma_\theta h_0^2 \quad (19)$$

and

$$\theta_{\infty} = \theta_{m0} + \Delta\theta_0 - \gamma_\theta h_0 . \quad (20)$$

In Fig. (3) the meaning of δ_0 and θ_{∞} is clarified. Eqs. (16) and (17) require that $I(t) > \delta_0$ and $h \geq 1.2 h_0$. In most cases these conditions are satisfied a few hours after t_0 . We will start our calculations at $t = t_0^*$ chosen such that we do not run into problems.

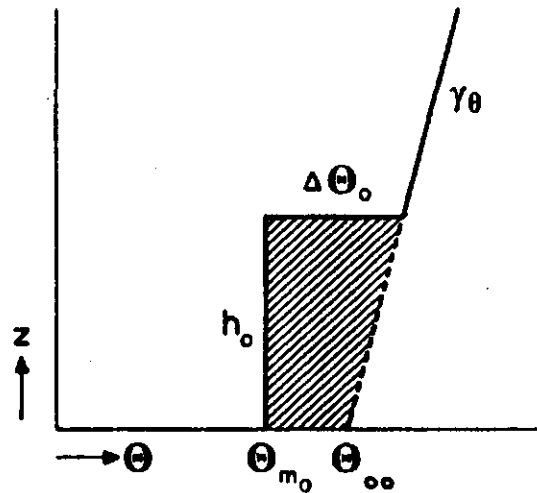


Fig. 3. Initial temperature profile. The shaded area represents δ_0 . Also θ_{∞} is indicated. (from Driedonks, 1981).

3.2 The surface fluxes.

3.2.1 The Penman-Monteith equation for E and H.

The simplest model for the fluxes of heat and water vapour from vegetative surfaces containing the essential physics is given by Monteith (1965, 1981) who applied Penman's equation to a vegetation. The Penman-Monteith equation reads

$$\lambda E = \frac{s(Q^* - G) + (\rho c_p / r_a) \delta q}{s + \gamma^*} \quad (21)$$

and

$$H = \frac{\gamma^*(Q^* - G) - (\rho c_p / r_a) \delta q}{s + \gamma^*}, \quad (22)$$

where $\gamma^* = \gamma(1 + \frac{r_c}{r_a})$. We recall that Q^* is the net radiation, G the soil heat flux density, $\gamma = c_p/\lambda$ and r_a and r_c are the aerodynamic and surface resistance respectively. As Perrier we assume that r_c depends not on weather variables and that it is determined only by soil moisture conditions.

In our study we will apply (21) and (22) to the entire surface layer, e.g. the level at which δq must be specified is $z = z_L$.

Then the aerodynamic resistance is

$$r_a = \int_{z_{oh}}^{z_L} \frac{dz}{K_h}, \quad (23)$$

in which z_{oh} is the roughness length and K_h the turbulent exchange coefficient for sensible heat and water vapor.

The specific humidity deficit is given by (11) and approximately by (13).

Eqs. (21) and (22) are derived from a set of equations which are also important for the following. These are

(i) The energy balance equation

$$Q^* - G = H + \lambda E \quad (24)$$

and

(ii) The bulk formulas for H and λE :

$$H = \rho c_p \frac{\theta_s - \theta_m}{r_a} \quad (25)$$

and

$$\lambda E = \lambda \rho \frac{q_w(\theta_s) - q_m}{r_a + r_c}. \quad (26)$$

In the model of Monteith the canopy is approximated by a hypothetical surface with a surface resistance r_c for water vapor, which is a result of the integrated effect of all stomata of the actual leaves of the canopy. Also it is assumed that this hypothetical surface has the same optical and aerodynamic properties as the actual surface, e.g. it has the same albedo and roughness length.

3.2.2 Net radiation and soil heat flux.

Because a vegetation insulates the surface efficiently from solar radiation the soil heat flux density G of a cropped surface is usually small compared to the net radiation Q^* . For practical calculations it is permitted to take it as a small fraction of Q^* . For a grass cover at Cabauw during daytime, De Bruin and Holtslag (1982) found:

$$G = 0.1 Q^* \quad (27)$$

We will adopt this empirical expression in this study.

Net radiation can be written as

$$Q^* = (1-A) K^\downarrow - \sigma \theta_s^4 + L^\downarrow, \quad (28)$$

where A is the albedo, K^\downarrow and L^\downarrow the incoming short- and longwave radiation and σ the Stefan-Boltzmann constant.

Furthermore θ_s is expressed in K. We recall that due to our definition of θ at the surface θ_s equals the surface temperature T_s . In (28) it is assumed that the surface is a black body in the longwave region.

For the time being we restrict ourselves to cloudless days and we approximate L^\downarrow by (Swinbank, 1963)

$$L^\downarrow = c \sigma \theta_m^6, \quad (29)$$

where θ_m is in K and c is a constant ($c = 9.4 \cdot 10^{-6} \text{ K}^{-2}$).

Next we use a series development for θ_s^4 which yields

$$\theta_s^4 = \theta_m^4 + 4 \theta_m^3 (\theta_s - \theta_m). \text{ Consequently}$$

$$Q^* = Q_m^* - 4 \sigma \theta_m^3 (\theta_s - \theta_m). \quad (30)$$

Here Q_m^* is defined by

$$Q_m^* = (1-A)K^{\downarrow} - \sigma \theta_m^4 + c \sigma \theta_m^6. \quad (31)$$

The last term of (30) is a relatively small correction term, which is estimated by us as follows.

By virtue of (22), (25) and (27) $(\theta_s - \theta_m)$ can be expressed in Q_m^* and δq

$$\theta_s - \theta_m = \frac{\frac{0.9 \gamma^*}{s + \gamma^*} Q_m^* - \frac{\rho c_p}{r_a} \frac{\delta q}{s + \gamma^*}}{\frac{\rho c_p}{r_a} + \frac{0.9 \gamma^*}{s + \gamma^*} 4 \sigma \theta_m^3}. \quad (32)$$

This expression will be used for the calculations of Q^* . In this way the influence of θ_s and θ_m on Q^* are taken into account. This is another extension of the model of Perrier (1980), because he assumed that $Q^* - G$ is given.

3.3 Relaxation equation for δq

Substitution of the Perman-Monteith formulas (21) and (22) into the differential equation (15) for δq leads, after some algebra, to the following relaxation equation

$$\frac{d(\delta q)}{dt} + \frac{\delta q}{\tau} = \frac{(\delta q)_e}{\tau}, \quad (33)$$

in which

$$\tau = r_a h \frac{s + \gamma^*}{a s_r + b \gamma} \quad (34)$$

and

$$(\delta q)_e = \frac{(Q^* - G) r_a (s_r a \gamma^* - b \gamma s)}{\rho c_p (a s_r + b \gamma)}, \quad (35)$$

It should be noted that when we take $a = b = 1$ and $s_r = s$ we retrieve the eqs. (6)-(8) which were derived firstly by Perrier.^x However, in our concept h is variable.

The lag time τ is proportional to h . Because usually h grows in the morning relatively rapidly τ will have the same behavior.

The quantity $(\delta q)_e$ represents the external forcing, since it contains $(Q^* - G)$. When the resistances r_c and r_a are constant, $(\delta q)_e$ will approximately behave as a sine wave with its maximum at about local noon.

4. Comparison with the model of Perrier.

In order to get an impression of the differences between the model of Perrier and ours we will consider here the simple case, also treated by Perrier (1980), that all variables are constant, except $(Q^* - G)$. The latter jumps at time $t = 0$ from one constant value to another. Then δq will reach the new value of $(\delta q)_e$, while $d(\delta q)/dt$ will become zero. Consequently the Bowen ratio $B(\equiv H/\lambda E)$ goes to:

$$B \rightarrow \frac{b}{a} \frac{\gamma}{s_r}. \quad (36)$$

^x $s \gamma \approx \delta q$.

This follows directly from (15). In the "closed boundary layer" concept of Perrier $a = b = 1$ (and $s = s_p$), so that $B \rightarrow \gamma/s$, which implies that the Priestley-Taylor parameter $\alpha \rightarrow 1$ (This in virtue of (1) and (24)). In our approach $a = 1.2$, while we found for b that it can vary between about -0.5 and 0.5 . Therefore B lies between about $-0.4 \gamma/s$ and $+0.4 \gamma/s$.

This example illustrates that our extensions of the Perrier model can have significant effects.

The example used here, however, is not realistic. This can be seen as follows. When we take $s = s_p \approx 10^{-3} \text{ K}^{-1}$, $r_a = 50 \text{ s.m}^{-1}$, $h = 500 \text{ m}$, $b = 0$ and $a = 1.2$ the time constant τ is at least 7 h ($r_c \geq 0$). Due to the properties of the relaxation equation (32) δq will reach a new equilibrium state at about $t = 3\tau$. This implies that this is the case after at least 20 h . In reality, therefore, an equilibrium never will be reached.

In the next section we will treat more realistic examples.

5. Results from model calculations.

In this section we will apply our model under conditions typical for a clear summerday in the Netherlands. We will calculate the Priestley-Taylor parameter α for different values of (i) the parameter b which determines the entrainment of dry air at the top of the boundary layer (ii) the surface resistance r_c and (iii) the aerodynamic resistance r_a . The main lines of our calculation scheme are given in the Appendix. As initial conditions we used the data observed at Cabauw on 31 May 1978 (Driedonks, 1981). These are at about 7 GMT: $h = 180 \text{ m}$, $\theta_{mo} = 18.5 \text{ }^\circ\text{C}$, $\delta q = 5 \text{ g/kg}$ and $\gamma_\theta = 5 \cdot 10^{-3} \text{ K.m}^{-1}$ *. We also used the observed solar radiation data ($\frac{1}{2}$ hourly values). 31 May 1978 was a typical summerday. In Fig. 4 the diurnal variation of the calculated α is shown for different values of r_c . The aerodynamic resistance r_a is taken 50 s.m^{-1} and $b = 0$ (i.e. $q_m = \text{constant}$). It is seen that α has a diurnal variation, but during the midday hours, when the fluxes are largest, α is fairly constant. Also the curves referring to different values of r_c are very similar. Therefore, they

* In fact γ_θ was not constant on 31 May 1978, we took a mean value.

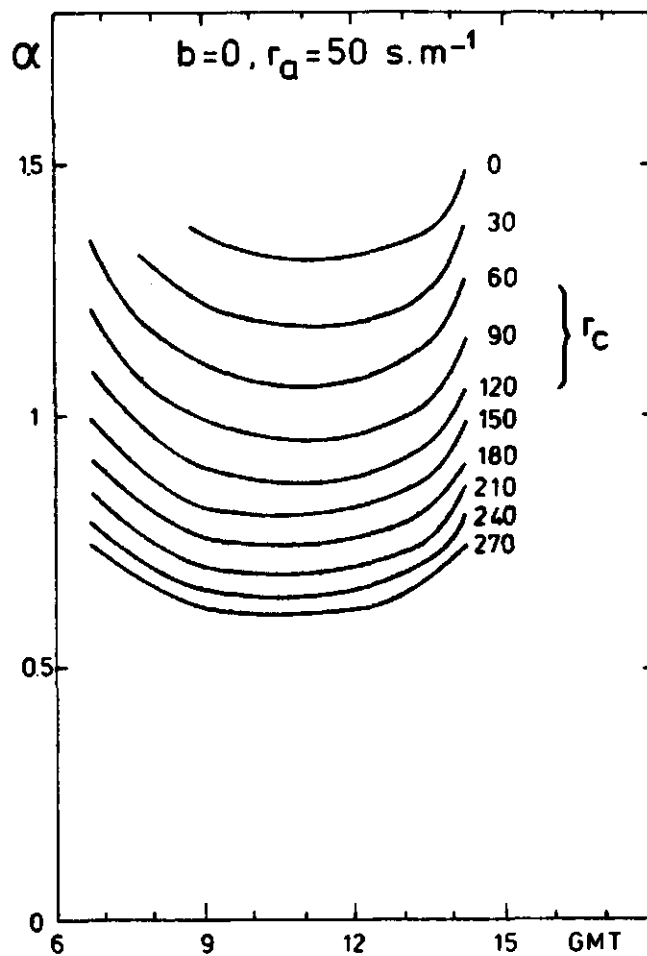


Fig. 4. Daytime variation of the computed α for different values of r_c ; $b = 0$ and $r_a = 50 \text{ s.m}^{-1}$.

can be characterized by one point. For this we chose α_{11} which is the value of α at 11 GMT. This reduces the information to be presented considerably.

In Fig. 5 α_{11} is shown as a function of r_c for different values of b , while r_a is taken constant at $r_a = 50 \text{ s.m}^{-1}$. The main features are:

(i) α_{11} varies between 1.2 and 1.45 at $r_c = 0$ and equals about 0.6 at $r_c = 270 \text{ s.m}^{-1}$. In the region between $r_c = 30$ and $r_c = 120 \text{ s.m}^{-1}$ (a typical range under normal conditions in the Netherlands) α_{11} varies between 0.85 and 1.25. These results are in good agreement with the α values found by De Bruin and Holtslag (1982).

(ii) The dependence of α on b is relatively weak and is insignificant for $r_c > 150 \text{ s.m}^{-1}$.

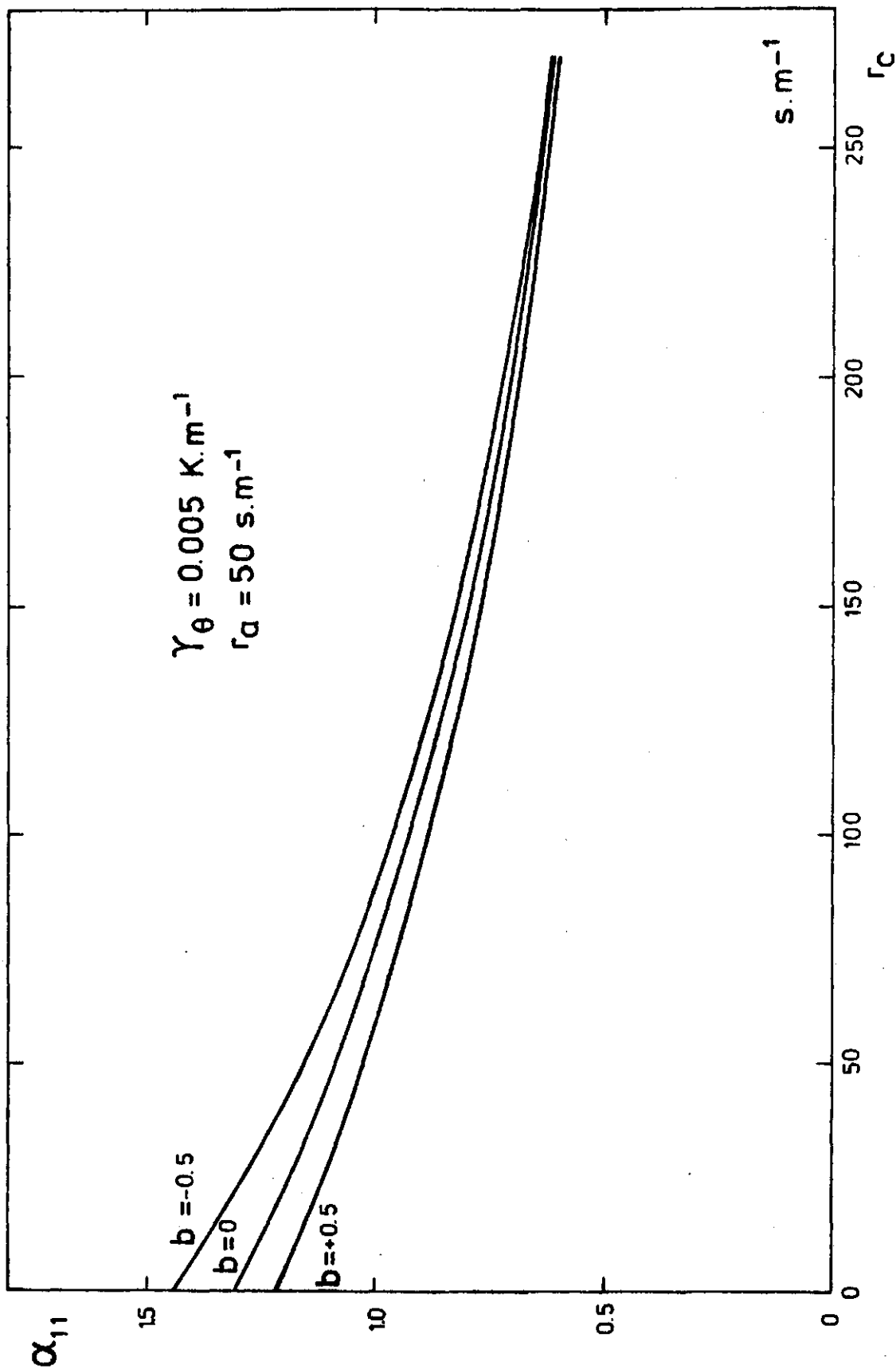


Fig. 5. Calculated α_{11} as a function of r_c for different value of b ; $r_a = 50 \text{ s.m}^{-1}$.

- (iii) When $r_c = 30 \text{ s.m}^{-1}$ which is about the minimum value of r_c for grass when the root zone is well supplied with water and when the foliage is dry, α_{11} is found to be about 1.2 which agrees well with $\alpha \approx 1.3$ often observed for well-watered surfaces. (see e.g. De Bruin and Keijman, 1978, and Monteith, 1981).
- (iv) A typical summer value of r_c for a pasture in a moderate climate is 60 s.m^{-1} (Thom and Oliver, 1977; De Bruin and Holtslag, 1982). Then α_{11} is about 1, a value often reported in the literature (McNaughton, 1976; Perrier, 1980).

In Fig. 6 the dependence of the calculated α_{11} on r_a and r_c is shown. This Figure refers to $b = 0$. We can conclude that for $r_c < 120 \text{ s.m}^{-1}$ α_{11} depends only slightly on r_a , but for $r_c > 120 \text{ s.m}^{-1}$ α is more sensitive to variations of r_a . Generally, r_a increases with decreasing wind speed. Thus the model predicts that when the surface is dry α decreases with increasing wind speed.

Usually, $r_c < 120 \text{ s.m}^{-1}$ so that in most cases the wind speed has a minor influence on α and thus on the surface fluxes. This agrees with the findings of De Bruin and Holtslag (1982).

In Fig. 7 the calculated and observed values of Q^* , H and λE are depicted for 31 May 1978. For the calculations we used $b = 0$, $r_a = 50 \text{ s.m}^{-1}$ and $r_c = 60 \text{ s.m}^{-1}$.

It is seen that Q^* is simulated well by the model. Reasonable results are obtained also for H and λE . At the end of the day the calculated fluxes deviate from the observed one; the measured H 's then are greater. An explanation for this is that often r_c increases at the end of days with a relatively high evaporation rate.

At the end of such days the water supply in the root zone stagnates after which the plants close their stomata.

The analysis given above reveals that on clear days α is mainly determined by r_c . It is interesting to investigate whether observations of α and r_c behave as predicted by the model. In Fig. 8 α_{11} and the cor-

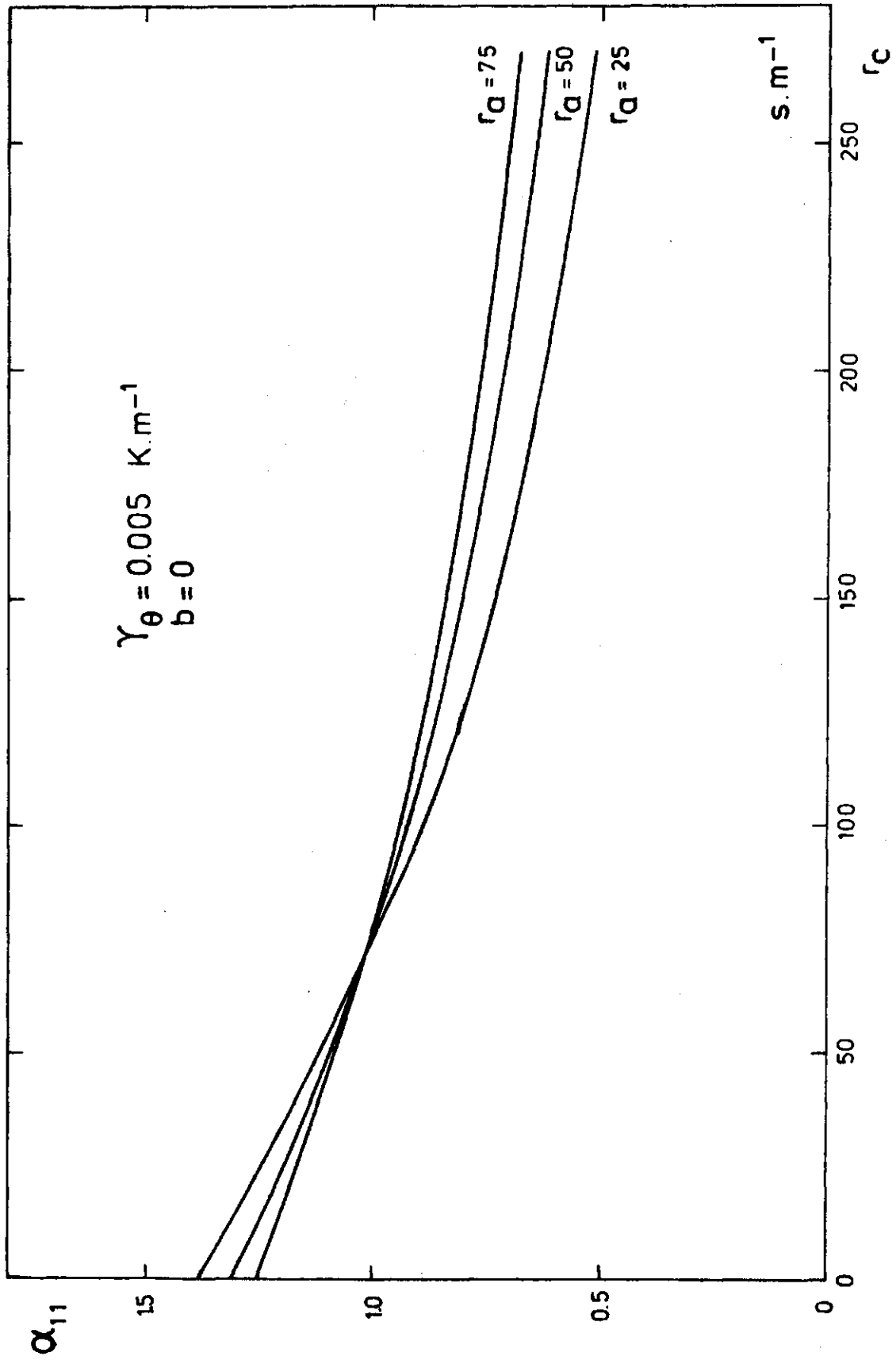


Fig. 6. Calculated α_{11} as a function of r_c for different values of r_a ; $b = 0$.

IV.24

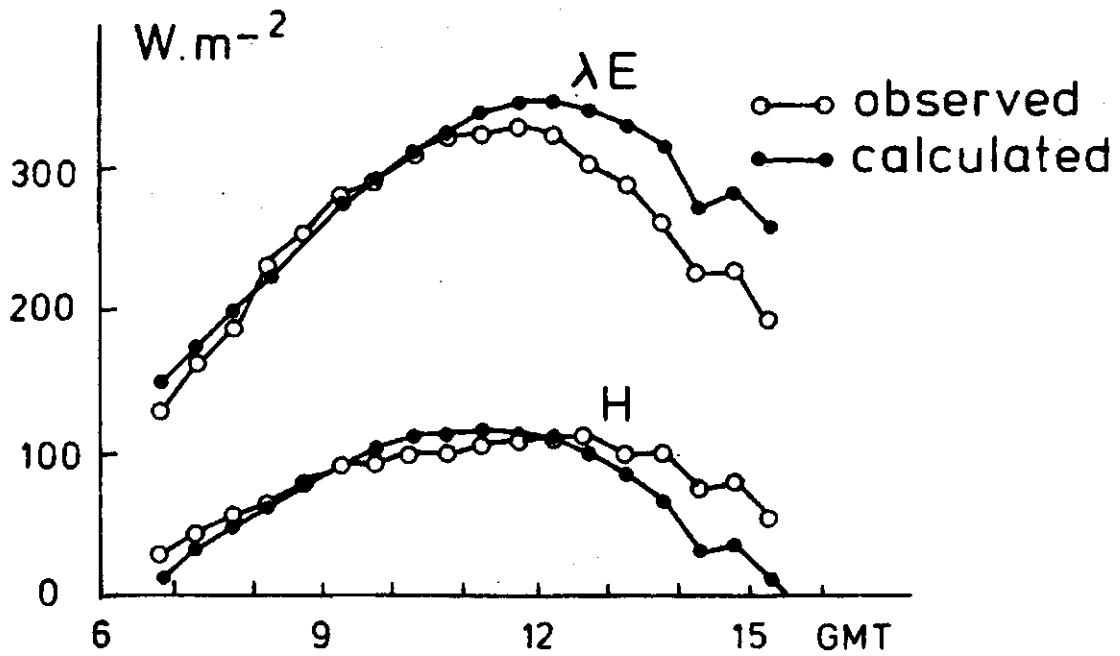
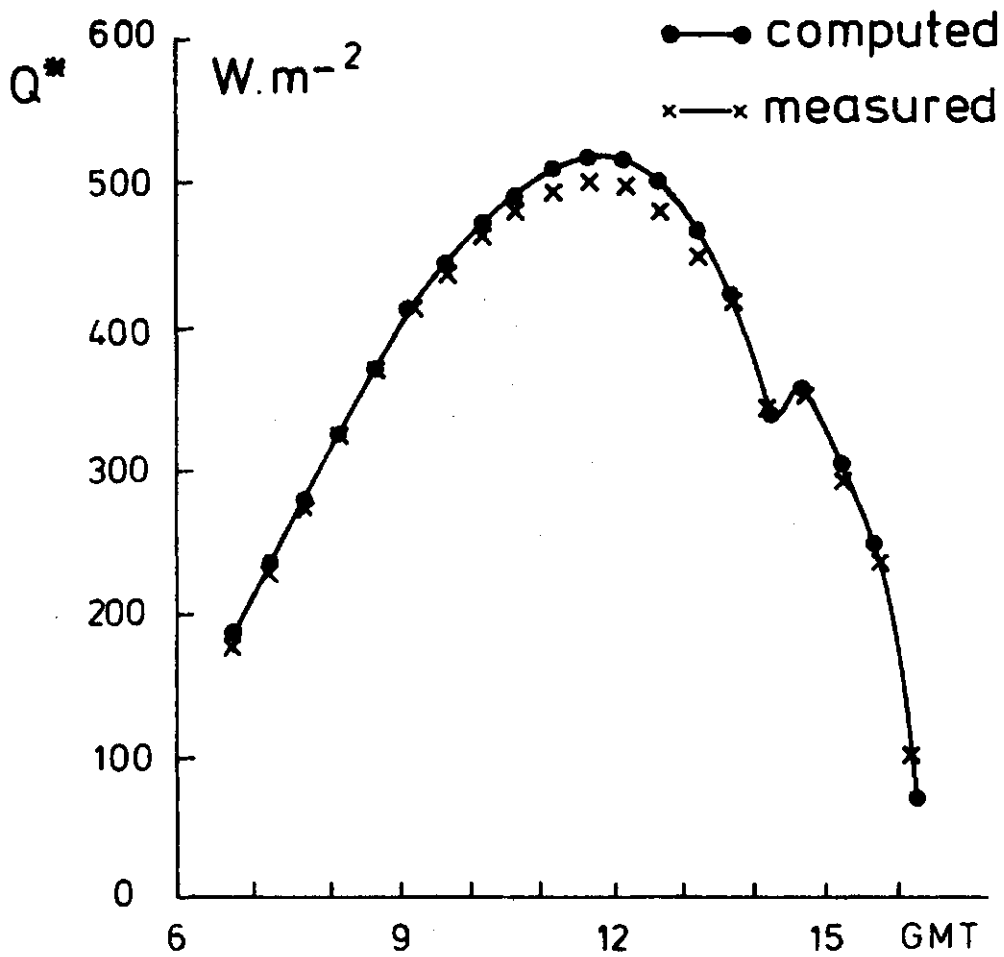


Fig. 7. Calculated and observed Q^* (top) and H and λE (bottom); Cabauw 31 May, 1978.

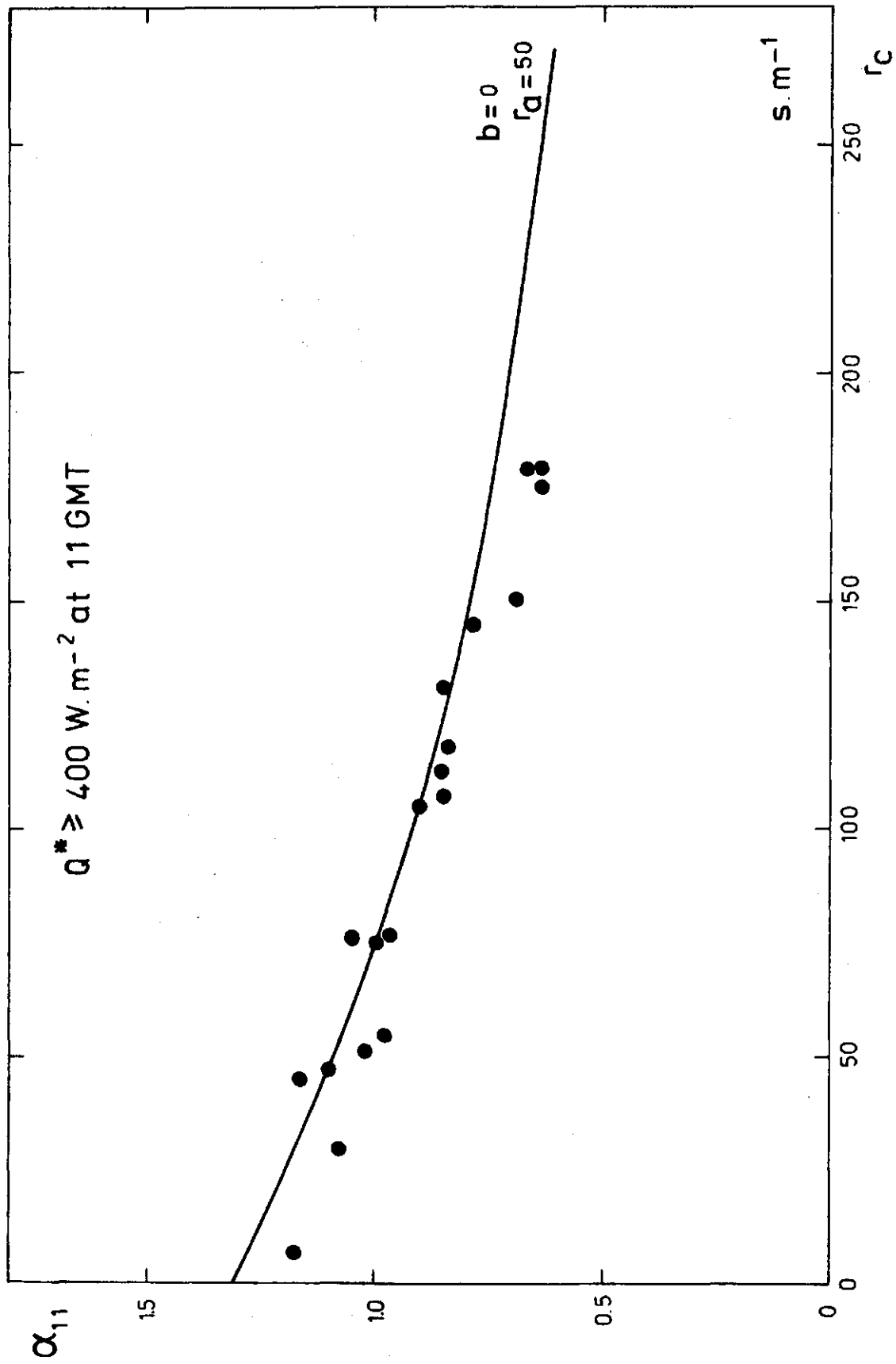


Fig. 8. Comparison between measured and computed values of α_{11} ; observations at Cabauw in 1977, $b = 0, r_a = 50 \text{ s.m}^{-1}$.

responding value of r_c are plotted as observed for grass at Cabauw in the summer of 1977. For more information on these observations see De Bruin and Holtslag (1982). The data depicted in Fig. 8 refer to hours around 11 GMT during which the averaged net radiation was at least 400 W.m^{-2} . Then it is likely that the conditions were convective. In Fig. 8 also the curve is drawn representing the relation between α_{11} and r_c as calculated with our model taking $b = 0$ and $r_a = 50 \text{ s.m}^{-1}$, using the initial data observed at 31 May 1978, which are typical for a convective day in the Netherlands.

From Fig. 8 we may conclude that the results of our model are encouraging; it predicts the dependence of α on r_c for convective days rather realistically.

6. Discussion and conclusions

In this study a coupled model for the surface fluxes of sensible heat and water vapor and the atmospheric boundary layer is presented. With this model we calculated the daytime variation of the Priestley-Taylor parameter α . The model can be regarded as an extension of the one by Perrier (1980). Perrier pointed out that in the Penman-Monteith equation the air temperature and humidity are not independent variables, but that they are related to the surface fluxes. He constructed a simple model in which he accounted for this interrelation. However, his description of the atmospheric boundary layer is very crude. He assumed that it is closed at the top, while its height h is constant. A consequence of these assumptions is that the air temperature and humidity can reach unrealistically high values, which can lead to wrong estimates of the surface fluxes.

The present model uses a more complete description of the boundary layer. For this we applied the boundary layer model of Driedonks (1981, 1982) derived for clear days with sufficient net radiation. In this description h is a function of the heat input at the surface. Also the fluxes of heat and moisture at the top of the boundary layer are taken into account in our model; a simple parameterization is

used. The fluxes at $z = h$ are assumed to be proportional to the surface fluxes.

With our model we found the following:

- (i) α depends mainly on the surface resistance for water vapor r_c . It varies between about 1.2 at $r_c = 0$ to $\alpha = 0.6$ at $r_c = 250 \text{ s.m}^{-1}$. In the range $30 < r_c < 120 \text{ s.m}^{-1}$, which is a typical range found at Cabauw, α varies between about 0.8 and 1.2 and is on the average about 1. This is in good agreement with observations (see Fig. 7).
- (ii) The parameter b describing the entrainment of dry air at the top of the surface layer is not very important, except for small values of r_c .
- (iii) Only when $r_c > 120 \text{ s.m}^{-1}$ the aerodynamic resistance r_a (and thus the wind speed) has significant influence on α . For $r_c < 120$ α is almost independent of the wind speed.

Our model illustrates the dependence of the surface fluxes on the various parameters involved. For this we made some simplifications by which our equations become more transparent. In principle, the model can also be used for forecasting purposes. Then some of our simplifications must be replaced by more sophisticated descriptions. For instance our parameterization of the entrainment of dry air at the top of the boundary layer can be replaced by a more complete one (Driedonks, 1981; Reiff et al., 1982). However, it is still necessary to specify the surface wetness characterized by r_c . This quantity can be very variable, in space but also in time, while its value is very uncertain. This opens the question whether it is worthwhile to adopt this type of model for weather forecast purposes. For these it is perhaps much more convenient to characterize the surface wetness directly with the Priestley-Taylor parameter α as proposed by De Bruin and Holtslag (1982) and others. The results of our study support this approach because we found with our model that α is mainly determined by r_c ; it is only slightly dependent on other factors.

Appendix

The calculation scheme

The main lines of our calculation scheme are described in the following.

A time step of half an hour is used. It is assumed that within this interval h , K^\dagger , Q^* , τ and $(\delta q)_e$ are constant. Then (33) can be solved exactly. The calculations start with the determination of a new value of θ_m (eq. 17), τ (eq. 34) and $(\delta q)_e$ (eq. 35). For the latter we need $Q^* - G$, which according to (27) equals $0.9 Q^*$. Net radiation is calculated with (30) from K^\dagger (which is given), the new θ_m values and θ_s from the previous time step. The error made by this is small, because θ_s is part of a small correction term).

Then δq is computed from (33). After this a better estimate of Q^* is obtained from (30) and (32). The next steps are the evaluation of H and λE from (21) and (22), of the Priestley-Taylor parameter α and of the heat-input integral I [eqs. (1) and (18)]. From the latter h for the next time step can be determined with (16) and the calculations can be repeated.

- V. The Priestley-Taylor evaporation model applied to a large, shallow lake in the Netherlands. †

Abstract

The applicability of the model of Priestley and Taylor (1972) for evaporation of saturated surfaces is examined for the former Lake Flevo (The Netherlands). This lake had an area of about 460 km² and an average depth of 3 m. Daily values of evaporation in the period July-September 1967, determined with the energy-budget method, are compared with the corresponding estimated values obtained by the Priestley-Taylor model. The agreement appears to be satisfactory. The diurnal variation of the parameter α of the Priestley-Taylor model is found to be pronounced. From standard meteorological observations at Oostvaardersdiep, a station at the perimeter of the lake, and an energy-budget model of Keijman (1974) an indirect extension of the available time series is obtained. In this way energy-budget data for the period April-October 1967 became available. Analysis of this data set leads to the preliminary conclusion that α has a seasonal variation. This is due to the fact that there is a linear relation between the daily latent heat flux LE and the *equilibrium* latent heat flux LE_{EQ} with a non-zero intercept.

† Published in J. Appl. Meteor., 1979, 18, 893-903
J.Q. Keijman as co-author.

List of symbols

c_1	constant	(-)
c_2	constant	($W.m^{-2}$)
c_p	specific heat of air at constant pressure	($J.kg^{-1}.s^{-1}$)
$f(u)$	function of wind speed	($W.m^{-2}$)
q_2	specific humidity at 2 m	(-)
q_s	saturation specific humidity	(-)
s	slope of saturation specific humidity - temperature curve	(K^{-1})
u	wind speed	($m.s^{-1}$)
E	evaporation	($kg.m^{-2}.s^{-1}$)
G	surface heat flux (density)	($W.m^{-2}$)
H	sensible heat flux (density)	($W.m^{-2}$)
K^{\dagger}	global radiation	($W.m^{-2}$)
L	latent heat of vaporization	($J.kg^{-1}$)
Q	net radiation	($W.m^{-2}$)
T_2	air temperature at 2 m	(K)
T_o	sub-surface temperature	(K)
T_s	surface skin temperature	(K)
α	Priestley-Taylor parameter	(-)
β	the Bowen ratio	(-)
$\gamma = c_p/L$		(K^{-1})

1. Introduction

Priestley and Taylor (1972) found that evaporation from saturated surfaces is empirically related to the total energy available for the latent and sensible heat fluxes according to the relation

$$LE = \alpha \frac{s}{s+\gamma} (Q^{\star} - G), \quad (1)$$

where E is the evaporation, L the latent heat of vaporization, α the so-called Priestley-Taylor parameter, s the slope of the saturation specific humidity-temperature curve, Q^{\star} the net radiation, G the surface heat flux, $\gamma = c_p/L$ and c_p is the specific heat of air at constant pressure. The term $s/(s+\gamma)(Q^{\star} - G)$ is often denoted as the equilibrium latent heat flux LE_{EQ} .

In fact the Priestley-Taylor model implies that LE is proportional to the first term of Penman's combination equation Penman (1948):

$$LE = \frac{s}{s+\gamma} (Q^{\star} - G) + \frac{\gamma}{s+\gamma} f(u) \{q_s(T_s) - q_z\}, \quad (2)$$

where $f(u)$ is a function of the wind speed u , q_z is the specific humidity and $q_s(T_s)$ the saturation specific humidity at T_s , both at 2 m.

From this it follows that the first and second terms are proportional to each other (Ferguson and Den Hartog, 1975) which implies that LE is also linearly related to the second term of Penman's equation (De Bruin, 1978).

For saturated land surfaces the soil heat flux G is small compared to Q^{\star} when 24-hour values are considered. Thus, for this case, the Priestley-Taylor model can be read as

$$LE = \alpha \frac{s}{s+\gamma} Q^{\star} \quad (3)$$

It is interesting to note that about twenty years ago Makkink (1957) proposed an empirical relation for saturated grass surfaces very similar to (3), namely

$$LE = c_1 \frac{s}{s+\gamma} K^{\downarrow} + c_2, \quad (4)$$

where K^{\downarrow} is the daily global radiation and c_1 and c_2 are constants (c_1 is approximately 1, c_2 is small, about -8 Wm^{-2}). From a practical point of view (4) is to be preferred to (3), because K^{\downarrow} is much easier to evaluate than Q^{\downarrow} . On the other hand it is to be expected that the value of c_1 depends on crop factors such as albedo and roughness.

In advection-free conditions an average value of $\alpha = 1.26$ was obtained both for water surfaces and saturated land surfaces. Several authors have confirmed this value: Ferguson and Den Hartog (1975), Stewart and Rouse (1976 and 1977), Davies and Allen (1973) and Mukammal and Neumann (1977). Some of these authors found the same value for small, shallow lakes, e.g. Stewart and Rouse (1976 and 1977). This is a somewhat surprising result, because the influence of advection on the energy-budget of small lakes is not negligible. This suggests that there is no need to be unduly strict about the range of applicability of the Priestley-Taylor model. However, this does not hold for very small water surfaces, such as an evaporation pan. In that case advection influences the value of the parameter α considerably (Mukammal and Neumann, 1977).

Tsann-Wann Yu (1977) studied the diurnal variation of α using data of the Wangara experiment (Clarke et al., 1971). His findings, however, apply to an unsaturated surface and will not be considered here.

Combining Eq. (1) with the energy-budget equation

$$LE + H = Q^{\downarrow} - G, \quad (5)$$

(where H is the sensible heat flux), we obtain a relation between α and the Bowen ratio $\beta = H/LE$:

$$\alpha = \left[\frac{s}{s+\gamma} (1+\beta) \right]^{-1} \quad \text{or} \quad (6a)$$

$$\beta = \frac{1}{\alpha} \frac{\gamma}{s} + \frac{1-\alpha}{\alpha}. \quad (6b)$$

Hicks and Hess (1977) analysed several sets of open water data and found that the empirical relation

$$\beta = 0.63 \frac{\gamma}{s} - 0.15 \quad (7)$$

gives a better fit to the data than Eq. (6b) with $\alpha = 1.26$. Eq. (7) leads to

$$LE = \frac{s}{0.85s + 0.63\gamma} (Q^* - G). \quad (8)$$

It is the purpose of this paper to test Eqs. (1), (6a), (6b) and (8). We will use the data collected in the summer and autumn of 1967 during the Flevo-project. We will also investigate a possible diurnal and seasonal variation of the parameter α .

2. Experimental

In the framework of a reclamation programme of a part of Lake IJssel (The Netherlands) in 1966/1967 a dike was built in Southern Flevoland. This dike enclosed together with the old coastline a water area of 467.6 km². In this way a temporary lake, called Lake Flevo, was created. Figure 1 shows a map of the area under consideration. In the summer and autumn of 1967 detailed micro-meteorological and hydrological data were collected at this lake.

At the main station, at the centre of the lake, net radiation, wind speed at 2, 4 and 8 m, dry and wet bulb temperature at 2 and 4 m,

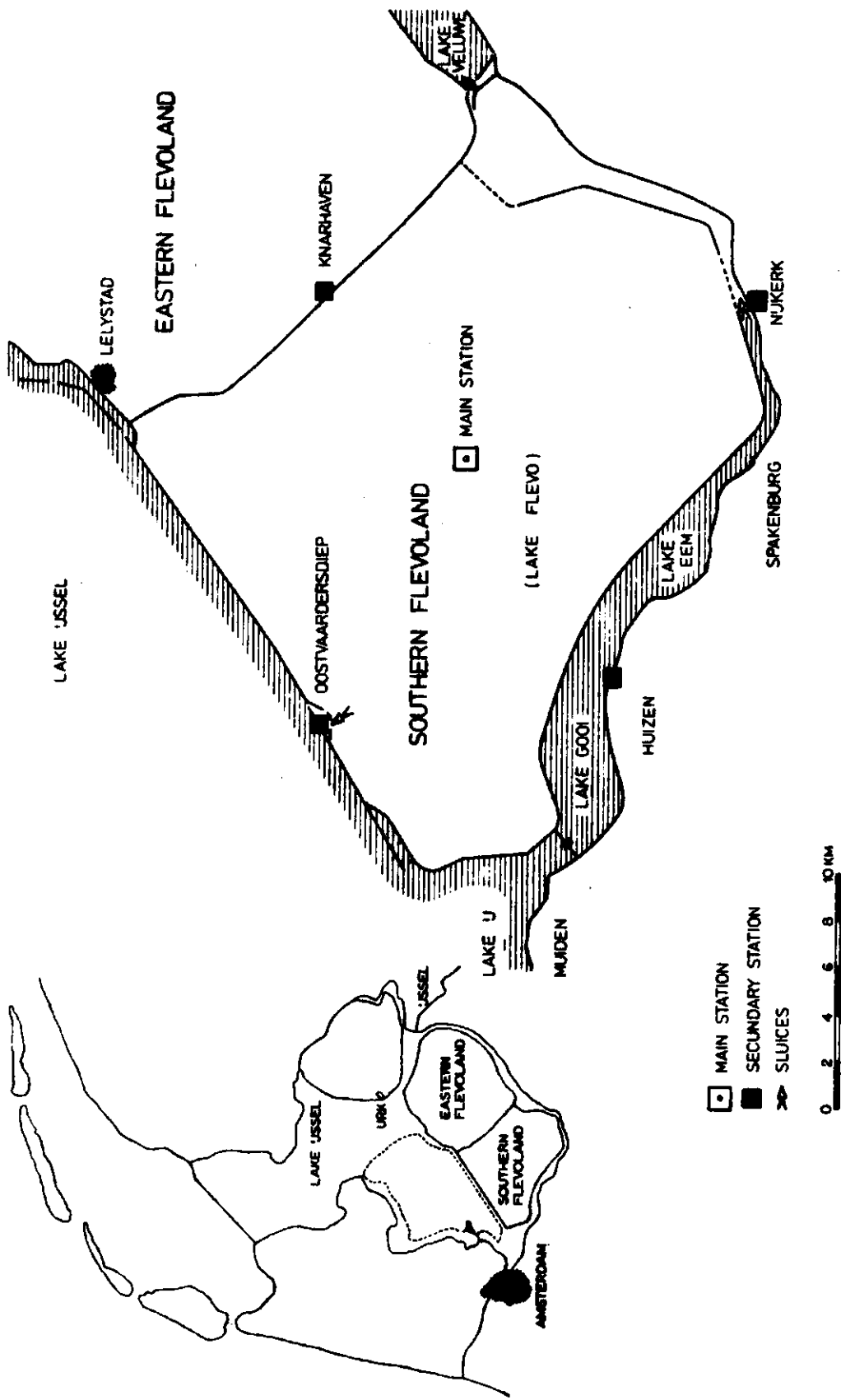


Fig. 1. Map of the Lake Flevo area.

water temperature at several depths, including the water surface, and the heat flux from the water body into the underlying soil were measured continuously. At several places (see Figure 1) precipitation and water-level changes were determined. At four secondary stations along the perimeter of the lake, standard meteorological data were collected, namely air temperature and humidity at screen height, wind speed at 3 m and the duration of sunshine. Extensive measurements of turbulent fluctuations of wind and temperature were made (Wieringa, 1973), but these fall outside the scope of this study.

With the data collected at the centre of the lake it was possible to determine the evaporation using different methods, while the available data set allowed also calculations of evaporation with the water-budget method. Comparing the evaporation determined with the water-budget method and the evaporation determined with the energy-budget method gives for the average value and the standard error of the ratio of these quantities 0.97 ± 0.04 . This comparison is based on seven water-budget periods with an average length of 4.6 days (Keijman and Koopmans, 1973). Therefore, in this study the energy-budget measurements of E are considered the true values of the evaporation. This is a generally accepted procedure (Stewart and Rose, 1977), which implies that E is determined with:

$$LE = \frac{Q^* - G}{1 + \beta_{\text{obs}}} \quad (9)$$

where β_{obs} , the observed value of the Bowen ratio, is calculated from the usual formula:

$$\beta_{\text{obs}} = \gamma \frac{T_0 - T_2}{q_s(T_0) - q_2} \quad (10)$$

in which T_0 is the surface temperature, T_2 the air temperature at 2 m,

$q_s(T_o)$ the saturated specific humidity at T_o , and q_2 the specific humidity at 2 m. For a given time interval β_{obs} is calculated from the time average values of T_o , T_2 and q_2 . The surface skin temperature of a waterbody, which we will denote by T_s , is generally lower than the subsurface temperature, denoted above by T_o . Because the fluxes of sensible and latent heat depend on T_s rather than on T_o , one may wonder what the effect would be of using T_s instead of T_o . Estimating $(T_o - T_s)$ with the model of Hasse (1971), we find a value of approximately $+0.5^\circ\text{C}$. This leads to a correction of $+3\%$ in $(1+\beta)^{-1}$, LE and α . This small correction has been neglected in our calculations.

3. Results

a. Daily values

In Figure 2 the mean daily values of LE measured with the energy-budget method are plotted against LE_{EQ} . Linear regression calculations forcing the regression line through the origin yield a value of $\alpha = 1.25 \pm 0.01$. The corresponding correlation coefficient is 0.991. Defining the error of estimate by the root mean square of the differences between measured and calculated values, this error is found to be 7.0 Wm^{-2} . The regression line with non-zero intercept is $LE = 1.17(+0.02)LE_{EQ} + 7.0(+1.4) (\text{Wm}^{-2})$. The corresponding error of estimate is 6.0 Wm^{-2} . This is only slightly smaller than the error of estimate of the zero-intercept line. We therefore conclude that the Priestley-Taylor model yields very good results for daily evaporation values at Lake Flevo. As energy-budget measurements of LE are only available for July through September, this test holds only for summertime and early autumn.

Figure 3 shows the results of the model of Hicks and Hess, which is a modification of the Priestley-Taylor concept. The slope of the regression line through the origin is 0.98, the correlation coefficient 0.992 and the error of estimate 6.7 Wm^{-2} . The differences between the

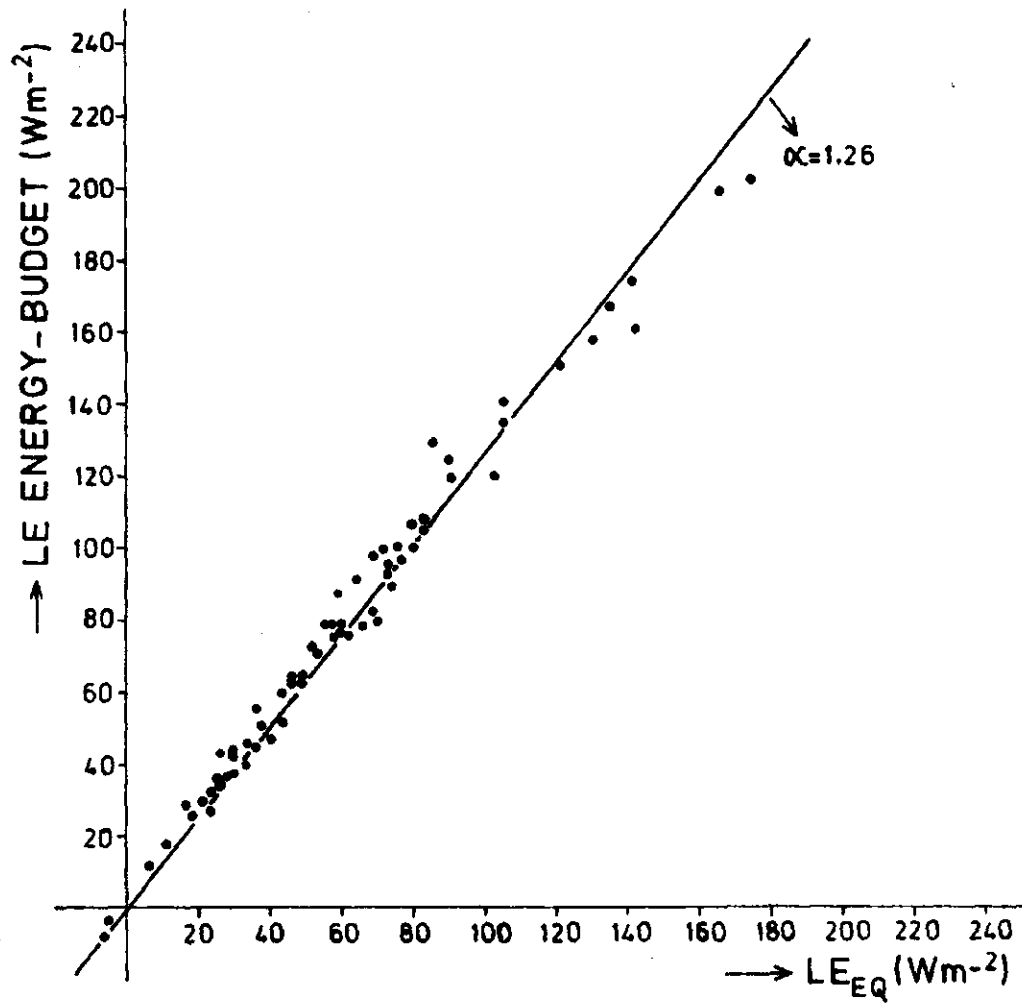


Fig. 2. Test of the Priestley-Taylor model. Comparison of daily average measurements of LE and LE_{EQ} .

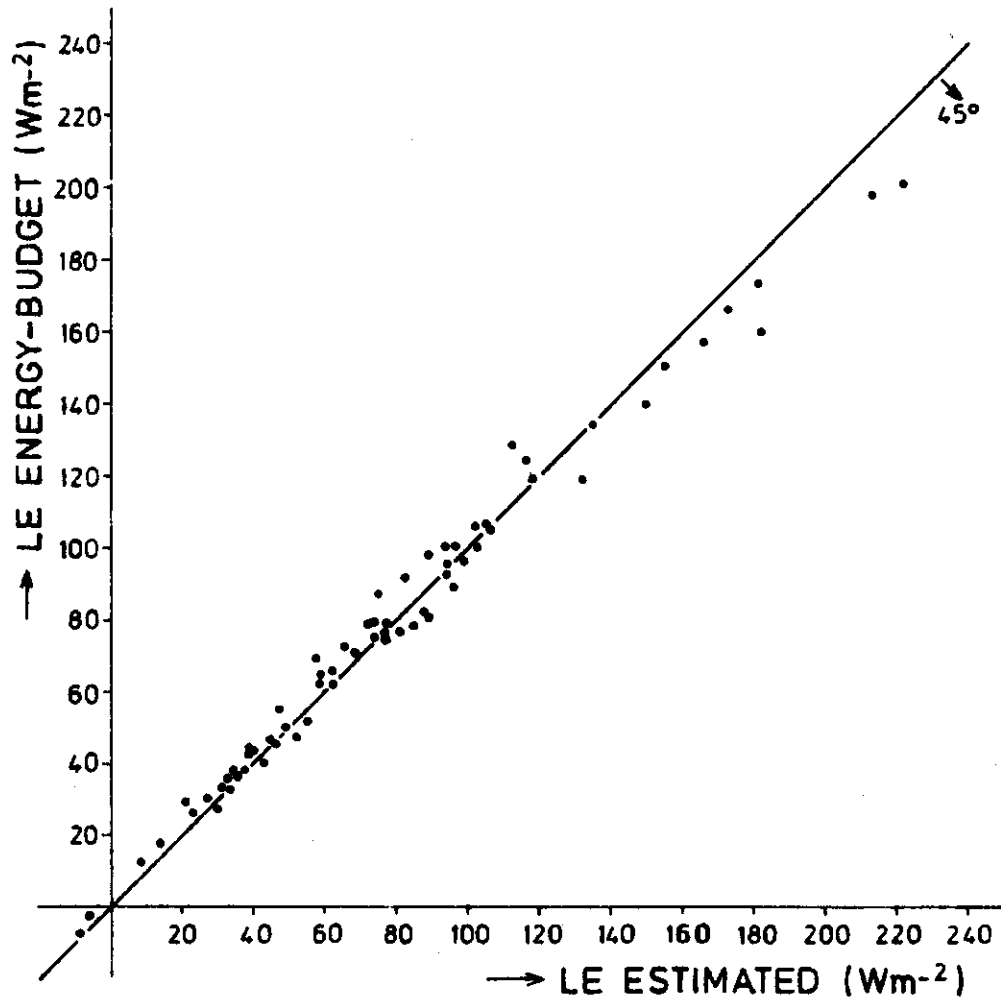


Fig. 3. Test of the model of Hicks and Hess for daily values.

two models are small. This is not very surprising. During the test period the mean daily water and air temperature fell in the range 15-20°C. In this range the differences between the two models are small.

It should be noted that the observed high correlation between LE and LE_{EQ} is partly due to the fact that both quantities contain $(Q^* - G)$. This is because we have considered the energy-budget measurements of LE the true latent heat flux. As mentioned before, this is justified by the fact that these energy-budget measurements compare satisfactorily with the water-balance data. However, the choice of the energy-budget method as a reference implies that scatter due to measuring errors in $(Q^* - G)$ is not incorporated in the applied statistical analysis. Therefore our results (Figures 2 and 3) show less scatter than they would have shown if LE and LE_{EQ} had no common factor. This also reflects on the computed standard deviation of α . However, because the energy-budget method compares well with the water-balance, the root mean square value of α itself, as evaluated by our approach, will not be effected significantly by measuring errors in $(Q^* - G)$. Therefore, our conclusion that the Priestley-Taylor model yields good results at $\alpha \approx 1.26$ is not changed by the fact that LE and LE_{EQ} both contain $(Q^* - G)$.

b. The diurnal variation of α

The diurnal variation of α has been studied with 3-hour averages of T_0 , T_2 and q_2 . We computed β_{obs} with the aid of Eq. (7) and then α with Eq. (6). Average values of these quantities for July and August 1967 are shown in Figure 4. There is a certain day-to-day scatter, which is small however, so these average values are representative for any given day in the months under consideration. From Figure 4 it is seen that in both months the parameter α has a pronounced diurnal variation with a minimum early in the day and a maximum in the late afternoon. The minima are 1.15 and 1.16 for July and August respectively and the maxima 1.42 and 1.41. The daily average value of α for both months is 1.29. This is in good agreement with the regression calcu-

lation of the preceding paragraph, based on mean daily values. As the temperature function $(s+\gamma)/s$ is nearly constant during the day, the variation of α is due to the variation of β_{obs} . It can be seen from Figure 4 that the variation of β_{obs} is, in its turn, chiefly due to the variation in $T_0 - T_2$ because $q_0 - q_2$ is nearly constant.

The diurnal variation of the air temperature T_2 is much larger than the variation of the surface water temperature T_0 . It is noted that the air temperature never exceeds the surface water temperature. This results in a Bowen ratio which is always positive with a minimum in the late afternoon. This variation of β_{obs} leads to the variation of α already mentioned above.

c. The seasonal variation of α

The Priestley-Taylor model has only been tested in summertime and early autumn. This holds also for the test given in section 3. So it is certainly possible that α varies in the course of the year. Unfortunately, no direct measurements of LE and LE_{EQ} are available for the other seasons. In order to get an impression of a possible seasonal variation of α we followed an indirect way. We used an energy-budget model with standard meteorological observations as input. These data were collected at Oostvaardersdiep in April-October 1967. As is seen from Figure 1 Oostvaardersdiep was completely surrounded by water and thus it can be considered representative for Lake Flevo. No data were available for a complete year.

From the daily average values of air temperature, air humidity, wind speed and duration of sunshine of this station the terms of the energy-budget equation (5) were calculated with a model developed by one of us (Keijman, 1974). This model has a solid physical basis, but contains one important simplification. It is assumed that the water body has no thermal stratification. However, in summertime, when a thermal stratification is most likely to occur, the model yields good results for Lake Flevo (Keijman, 1974). This can be explained by the fact that Lake Flevo has a depth of only a few meters. Therefore it can easily be stirred by the wind. For further information on the model the reader is referred to Keijman (1974).

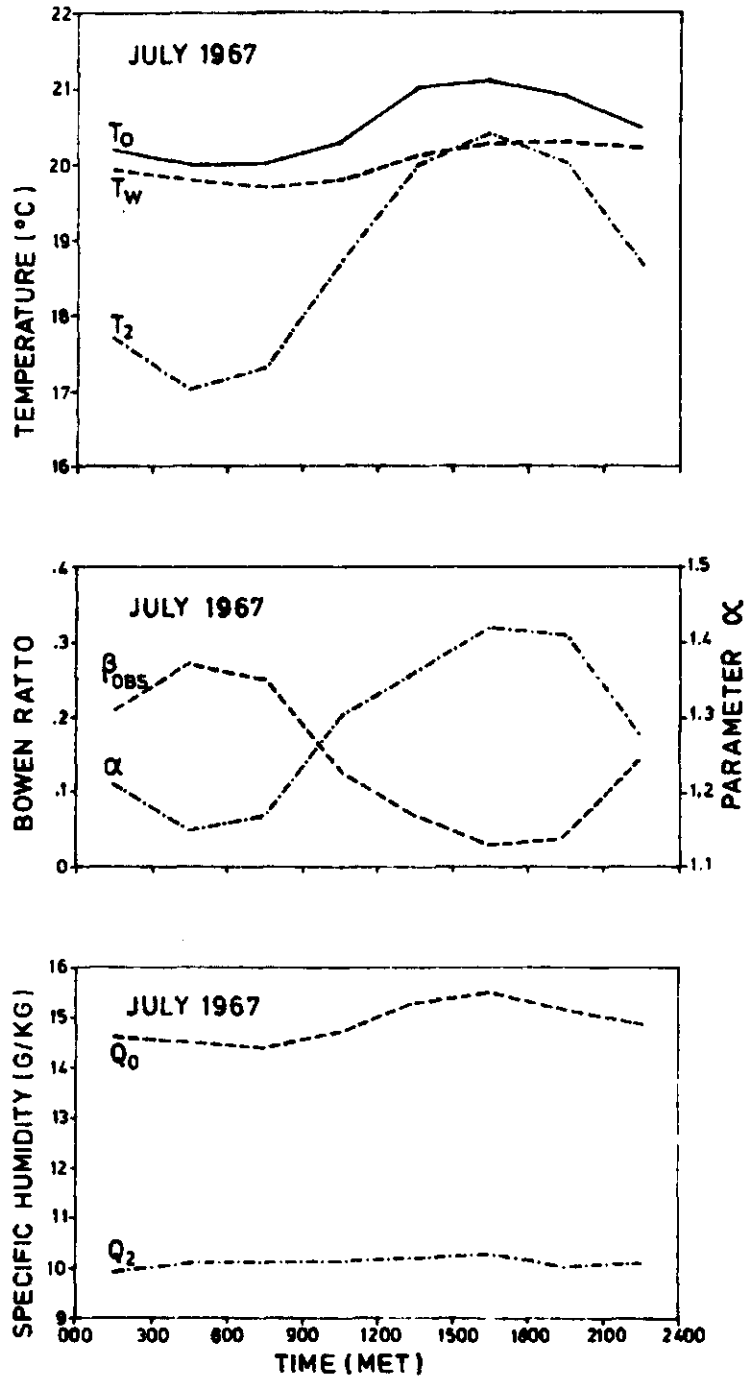


Fig. 4a. Diurnal variation of parameter α , the Bowen ratio B_{obs} , surface water temperature T_o , T_w , depth-averaged water temperature, air temperature T_2 and specific humidity q_2 over Lake Flevo in July 1967.

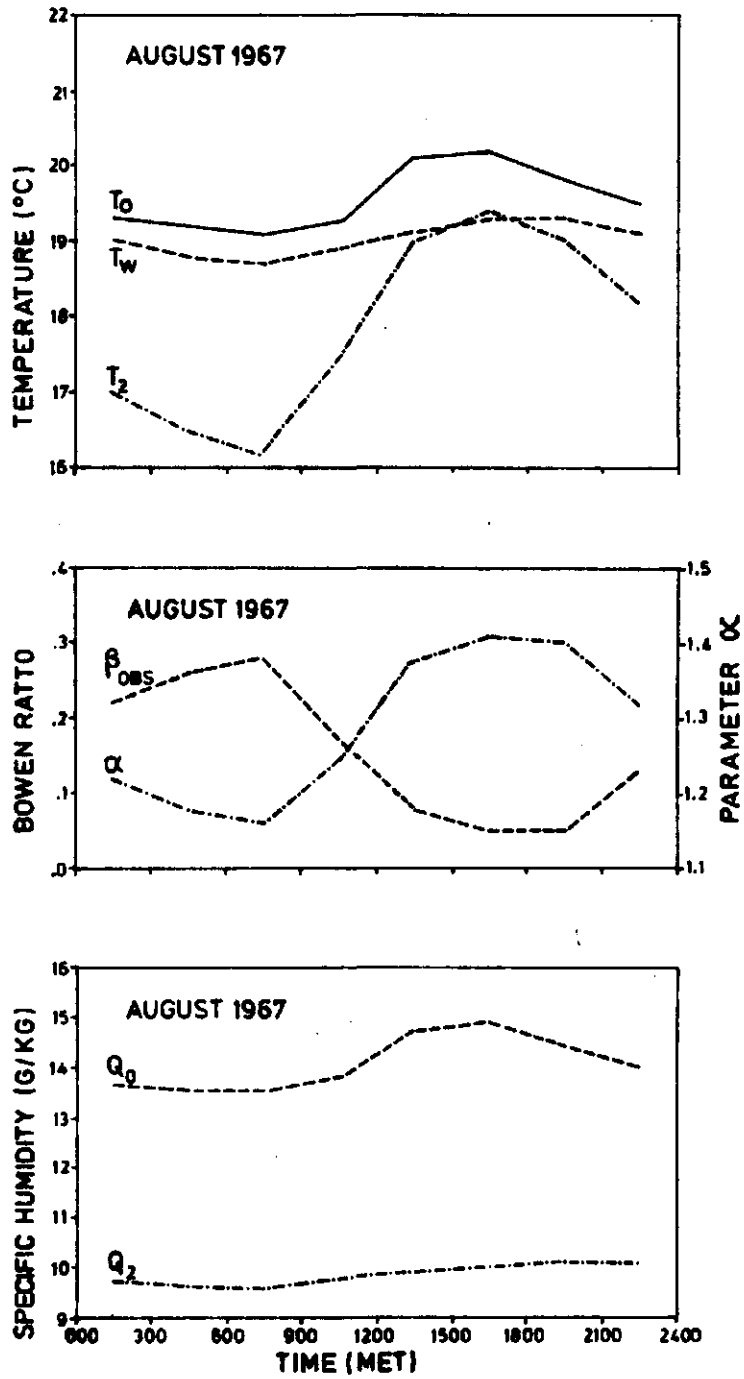


Fig. 4b. As in Fig. 4a except for August 1967.

For each month we applied linear regression techniques to the daily values of LE and LE_{EQ} . This yields the coefficients a and b of the regression lines $LE = a LE_{EQ} + b$, the correlation coefficients r and the least square estimates of α , the latter obtained by forcing the regression lines through the origin. The values of a, b, α and r are listed in Table 1. Furthermore α is plotted per month in Figure 5. It is seen from Table 1 that the correlation coefficients are at least 0.98. Thus, like the Priestley-Taylor model, the energy-budget model predicts a good linear relation between LE and LE_{EQ} .

Table 1. The coefficients a and b of the regression equation $LE = a LE_{EQ} + b$, where both LE and LE_{EQ} are calculated per day with the model of Keijman; the corresponding correlation coefficient r and the least square estimate of the Priestley-Taylor parameter α .

	a	b(Wm^{-2})	r	α
April	1.32	7.7	0.98	1.50
May	1.07	17.6	0.98	1.28
June	1.15	7.7	0.99	1.25
July	1.08	11.9	0.99	1.21
August	1.09	9.5	0.99	1.20
September	1.18	4.5	0.99	1.25
October	1.24	17.4	0.98	1.49

Figure 5 shows a rather pronounced seasonal variation of α . In May through September its value differs only slightly from 1.26, but in April and October α is about 1.50. This is due to the fact that the intercept b is positive for all months (see Table 1). In summertime the daily values of LE are large compared to b, which means that then the deviation of the Priestley-Taylor model will be small. This is no longer the case in spring and autumn, due to the smaller values of LE. The result is that, if one stays with the Priestley-Taylor model and estimates α from a regression line forced through the origin, an α is found with a seasonal variation as given in Figure 5.

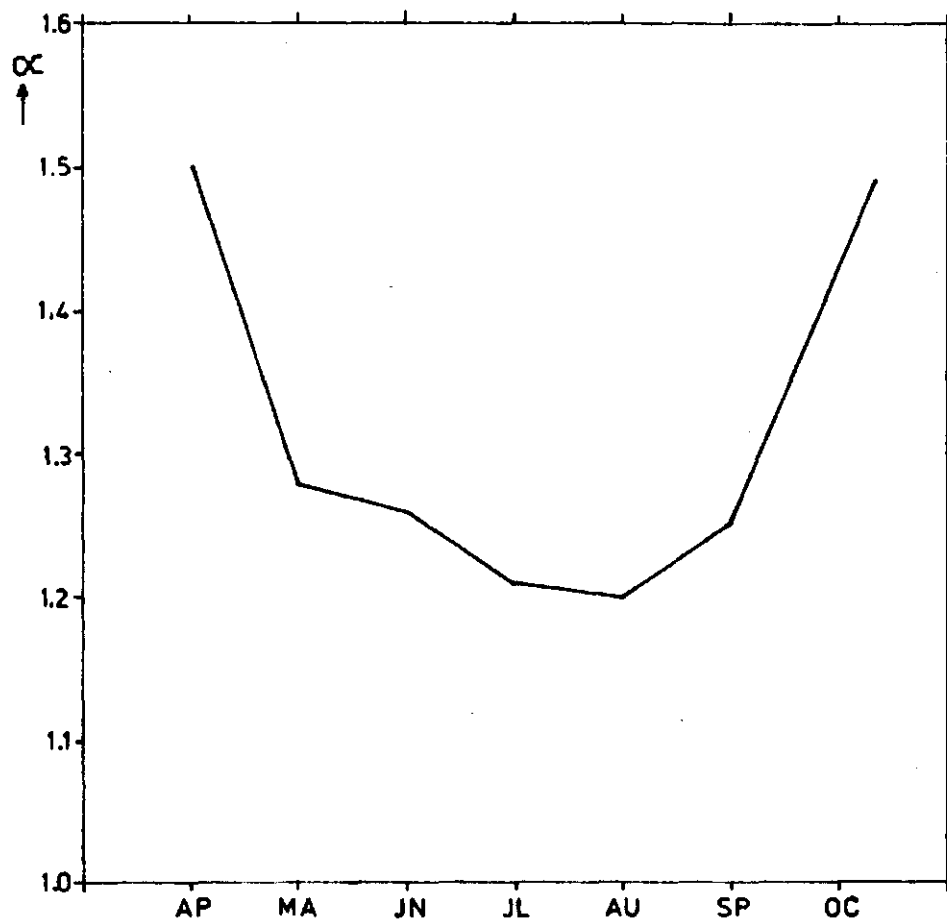


Fig. 5. The seasonal variation of α as predicted by the model of Keijman.

Summarizing we can say that the energy-balance model used in this study predicts a linear relation between LE and LE_{PQ} , just like the Priestley-Taylor concept, but with a positive intercept. This positive intercept causes a seasonal variation of the Priestley-Taylor parameter.

4. Discussion

Our results can be summarized as follows:

1. In summertime, over 24-hour periods the Priestley-Taylor model yields quite satisfactory results at $\alpha = 1.26$.
2. There is a seasonal variation of α due to the fact that the regression line between daily values of LE and LE_{PQ} has a non-zero intercept.
3. The parameter α shows a diurnal variation.

The first result substantiates the findings of Priestley and Taylor (1972) and Stewart and Rouse (1977). Their results, however, are related to much smaller lakes ($\approx 0.1 - 35 \text{ km}^2$). We are tempted to conclude therefore that in summertime the Priestley-Taylor model, with $\alpha = 1.26$, is applicable to all lakes regardless their size. Strictly speaking, this conclusion is contrary to the original concept proposed by Priestley and Taylor, because they restricted themselves to advection-free conditions. Small water bodies are strongly influenced by advection while even large water bodies like Lake Flevo are to a certain extent affected by it. If there exists a general mechanism which at the moment is not understood and which leads to the Priestley-Taylor model at $\alpha = 1.26$ for advection-free conditions, then from our first and third results we may conclude that over 24-hour periods the advective influences are smoothed out (in summer), and that the observed diurnal variation of α is due to advection. The latter conclusion implies that a diurnal variation of α will depend on the advective influences and on how the water body reacts on these influences. So it is to be expected that the diurnal variation of α will depend on the size and depth of the lake and on the specific climatological conditions of the region in which the lake is situated.

What are the conditions for finding a diurnal variation of α of the type observed at Lake Flevo? The diurnal variation of the air temperature over the surrounding land must be large compared to the variation of the water temperature and there must be sufficient advection of heat from

land to lake. The diurnal variation of the water temperature will be small if the water depth is at least a few meters and there is sufficient mixing to prevent a thermal stratification. The diurnal variation of the air temperature over land depends on many factors of climate, soil and vegetation, but is generally much larger than a few degrees. As for many lakes these conditions will be met, we conclude that the parameter α will often have a variation similar to that at Lake Flevo.

Our second result implies that a linear relation of the type $LE = a LE_{EQ} + b$ better fits the data than the original Priestley-Taylor concept. We did not have enough data to calculate reliable values of the parameters a and b per month, but a is somewhat less than 1.26 and b is of the order of 10 Wm^{-2} . In summer, when LE is much larger than b , the difference between the one-parameter and the two-parameter model is not significant.

- VI. Temperature and energy balance of a water reservoir determined from standard weather data of a land station.[†]

Abstract

A model for the determination of the temperature and energy-budget of a well-mixed water reservoir from standard meteorological data observed at a nearby land station is investigated. The main features are discussed. A verification of the model is given consisting of a comparison over several years between the measured and calculated temperature of two adjacent water reservoirs. The results are satisfactory.

[†] To appear in J. of Hydrology.

List of symbols

c_w	specific heat of water	($\approx 4200 \text{ J.kg}^{-1}.\text{K}^{-1}$)
e_a	water vapour pressure at screen height	(mb)
e_s	saturation water vapour pressure	(mb)
$f(u)$	wind function	($\text{kg.m}^{-2}.\text{mb}^{-1}$)
h	water depth	(m)
p	relative duration of bright sunshine	(-)
s	de_s/dT at $T = T_n$	(mb.K^{-1})
t	time or day-number	(s or d)
Δt	time interval	(s or d)
u	wind speed	(m.s^{-1})
A_k	amplitude of the k^{th} Fourier component of T_w	(K)
E	evaporation	($\text{kg.m}^{-2}.\text{s}^{-1}$)
G	change per unit time and area of heat stored in the water	(W.m^{-2})
H	flux density of sensible heat	(W.m^{-2})
K^\dagger	incoming shortwave radiation	(W.m^{-2})
L^\dagger	incoming longwave radiation	(W.m^{-2})
L_v	latent heat of vaporization	(J.kg^{-1})
Q^x	net radiation	(W.m^{-2})
Q_n^x	net radiation when $T_w = T_n$	(W.m^{-2})
T_a	air temperature	(K)
T_e	equilibrium temperature	(K)
T_n	wet-bulb temperature	(K)
T_w	water temperature	(K)
T_k	amplitude of the k^{th} Fourier component of T_e	(K)
α	albedo of the water surface	(-)
α_k	change of phase-angle of the k^{th} Fourier component of T_w	(rad)
γ	psychrometric constant	($\approx 0.66 \text{ mb.K}^{-1}$)
ϵ	emissivity of the water surface	(-)
ϕ_k	phase-angle of the k^{th} Fourier component of T_e	(rad)
ρ_w	density of water	($\approx 1000 \text{ kg.m}^{-3}$)
σ	constant of Stefan-Boltzman	($5.67 \cdot 10^{-8} \text{ W.m}^{-2}.\text{K}^{-4}$)
τ	time constant	(s)

1. Introduction

Modelling of the energy-budget and temperature cycle of lakes and water reservoirs is of practical interest. For instance, man-made thermal pollution can only be determined if the natural and artificial influences on water temperature can be separated.

Furthermore the evaporative losses of water reservoirs and lakes are of practical importance. In this paper a model is considered which yields, among other things, the temperature and evaporation of water bodies as a function of weather. It is developed by Edinger et al. (1968) and applied to well-mixed lakes by Keijman (1974). The latter tested the model for Netherlands conditions in summertime. In this study a verification is presented concerning the entire annual cycle for two water reservoirs with different depth. Strictly speaking the model requires weather data collected over water. Often, however, only observations at a nearby land station are available. It will be shown that this difficulty can be removed by using an adapted empirical wind function.

2. Experimental data

In this study use is made for testing purposes of the measured water temperatures of two adjacent water reservoirs. Their location is shown in Fig. 1. The reservoirs are:

- a). *De Grote Rug* with an area of about 0.5 km^2 and an average depth of 5 m, and
- b). *Petrus Plaat*, with an area of about 1 km^2 and a depth of 15 m.

The water temperature of *De Grote Rug* is measured once a week with a mercury-in-glass thermometer. The time of observation is generally 10.00 hr local time.

The water temperature measurement of the *Petrusplaat* is measured continuously. Weekly values averaged over depth and time were available for this study. In order to prevent thermal stratification the water of the *Petrusplaat* is mixed artificially.

In both reservoirs the horizontal advection of heat can be neglected because the amounts of water occasionally let in and out are small compared to the total water content of the reservoirs.



Fig. 1. Map of the Netherlands in which the location of the meteorological station and the water reservoirs are indicated.

The relevant weather data, notably mean air temperature and humidity, mean wind speed at 10 m and relative sunshine duration, were obtained from the main meteorological station at De Bilt (see Fig. 1) situated at 45 km N.N.E. from the reservoirs. Since its distance to the coast is about the same as those of the reservoirs and 10-day mean values are used, this station can be considered representative.

3. The model

From the energy-balance equation, the bulk-aerodynamic formulae for sensible and latent heat flux, the assumption that the water is isothermal and neglecting the heat flux to the underlying soil it can be shown that under horizontal homogeneous conditions the water temperature T_w can be described by (Edinger et al., 1968)

$$\rho_w c_w h \frac{\partial T_w}{\partial t} = (1-\alpha) K^\dagger + L^\dagger - \epsilon \sigma T_w^4 - L_v f(u) (s+\gamma) (T_w - T_n) \quad (1)$$

where ρ_w and c_w are the density and specific heat of water, h the water depth, t the time, α the albedo, K^\dagger and L^\dagger the incoming short- and long-wave radiation respectively, ϵ the emissivity in the longwave region, σ the Stefan-Boltzmann constant, L_v the latent heat of vaporization, $f(u)$ a function of wind speed u , s the slope of the temperature-saturation water vapour curve at T_n the wet-bulb temperature at height z and γ the psychrometric constant. By approximating T_w^4 by $4T_n^3(T_w - T_n) + T_n^4$ and taking $\epsilon = 1$ Keijman (1974) simplified (1) and obtained:

$$\frac{\partial T_w}{\partial t} + \frac{T_w}{\tau} = \frac{T_e}{\tau}, \quad (2)$$

in which the *equilibrium temperature* T_e is defined by

$$T_e = T_n + \frac{Q_n^x}{4\sigma T_n^3 + L_v f(u) (s+\gamma)} \quad (3)$$

and the *time constant* τ is given by

$$\tau = \frac{\rho_w c_w h}{4 \sigma T_n^3 + L_V f(u) (s+\gamma)} \quad (4)$$

Q_n^* is the net radiation if the surface temperature equals T_n . The equilibrium temperature T_e represents the atmospheric forcing. From Eq. (2) it is seen that T_w tries to reach T_e . The time scale on which this occurs is τ which is proportional to the water depth. For more detailed information on the physical background of the model the reader is referred to Edinger et al. (1968), Keijman (1974) and Fraedrich et al. (1977).

The quantities T_e and τ can be evaluated from standard weather data (see later): then Eq. (2) can be solved. Since the time constant τ is much greater than 1 day ($\tau \approx 10$ d for $h = 5$ m and $\tau \approx 30$ d for $h = 15$ m), T_n will react mainly on variations of T_e with a time scale of several days, whereas the response to frequencies of 1 d^{-1} or more is expected to be small.

Mathematically this can be seen from a decomposition of $T_e(t)$ in a Fourier series over 1 d.

$$T_e(t) = \bar{T}_e + \sum_{k=1} T_k \sin \left(\frac{2\pi kt}{\Delta t} + \phi_k \right), \quad (5)$$

where $\Delta t = 1$ d, \bar{T}_e the mean of T_e over Δt , T_k the amplitude and ϕ_k the phase-angle of the k^{th} Fourier component. Then, provided τ is constant the following solution of Eq. (2) is obtained:

$$T_w(t) = C e^{-t/\tau} + \bar{T}_e + \sum_k A_k \sin \left(\frac{2\pi kt}{\Delta t} + \phi_k - \alpha_k \right), \quad (6)$$

$$\text{with } A_k = \frac{T_k}{\sqrt{1 + \epsilon_k^2}} \quad (7)$$

$$\alpha_k = \arctan \epsilon_k, \quad (8)$$

$$\epsilon_k = \frac{2\pi}{\Delta t} k \tau, \quad (9)$$

C is an integration constant.

In our case τ is 10 days or more, so $\epsilon_k \geq 60 k$. This implies that $A_k < T_k/60 k$.

We found that in summertime a typical value of T_k is $20/k$ K for $k = 1, 2, 3$, while the higher order values can be neglected. This shows that the amplitudes A_k are negligibly small, except possibly the first component. Since we are only interested in the annual cycle of T_w and not in the diurnal changes we can choose an initial time t_0 in such a way that the first Fourier component of T_w in Eq. (6) vanishes. Since $\alpha \approx \frac{\pi}{2}$ and T_e reaches its maximum round about noon (Edinger et al., 1968) an appropriate choice of t_0 is 00.00 hr local time. Then we can neglect the last term in Eq. (5) and the solution of T_w at $t = t_0 + \Delta t$ is given by

$$T_w(t_0 + \Delta t) = \bar{T}_e + [T_w(t_0) - \bar{T}_e] e^{-\Delta t/\tau} \quad (10)$$

This is the same solution Keijman (1974) obtained by assuming that T_e is constant at \bar{T}_e .

From the above it follows (Eq. (9)) that this solution applies only for $\tau \gg 1$ d. In the case of very shallow lakes the solution given by (10) does not hold, because τ becomes too small.

When \bar{T}_e and τ do not change significantly over a period of, say, N days, the solution for T_w at $t_0 + N\Delta t$ reads

$$T_w(t_0 + N\Delta t) = \bar{T}_e [1 - \exp(-\Delta t/\tau)] \sum_{j=1}^N \exp[-(j-1)\Delta t/\tau] + T_w(t_0) \exp[-N\Delta t/\tau] \quad (11)$$

Since

$$\sum_{j=1}^N \exp[-(j-1)\Delta t/\tau] = \frac{1 - \exp(-N\Delta t/\tau)}{1 - \exp(-\Delta t/\tau)}, \quad (12)$$

this leads to

$$T_w(t_0 + N\Delta t) = \bar{T}_e + [T_w(t_0) - \bar{T}_e] \exp(-N\Delta t/\tau). \quad (13)$$

In this study Eq. (13) will be applied for $N = 10$.

4. Important features of the model

After having determined T_w as a function of time, we can evaluate the flux densities of sensible heat H and water vapour E from the well-known (Dalton-type) bulk formulae. Furthermore the net radiation Q^x (see later) and the change per unit time and area of the heat stored in the water G can be computed. To illustrate the main features of the model, the calculated mean values of H , LE , Q^x and G are shown in Figs. 2 and 3. These calculations are carried out over 1971 through 1976 using weather data of De Bilt (10-day averages). Figs. 2 and 3 are related to small inland water reservoirs with a depth of 5 and 15 m respectively (such as *De Grote Rug* and *Petrusplaat*). It is seen that in both case the net radiation is almost in phase with the noon-solar elevation, while it is only slightly dependent on water depth. The influence of the water depth on the other terms of the energy balance, in particular the heat

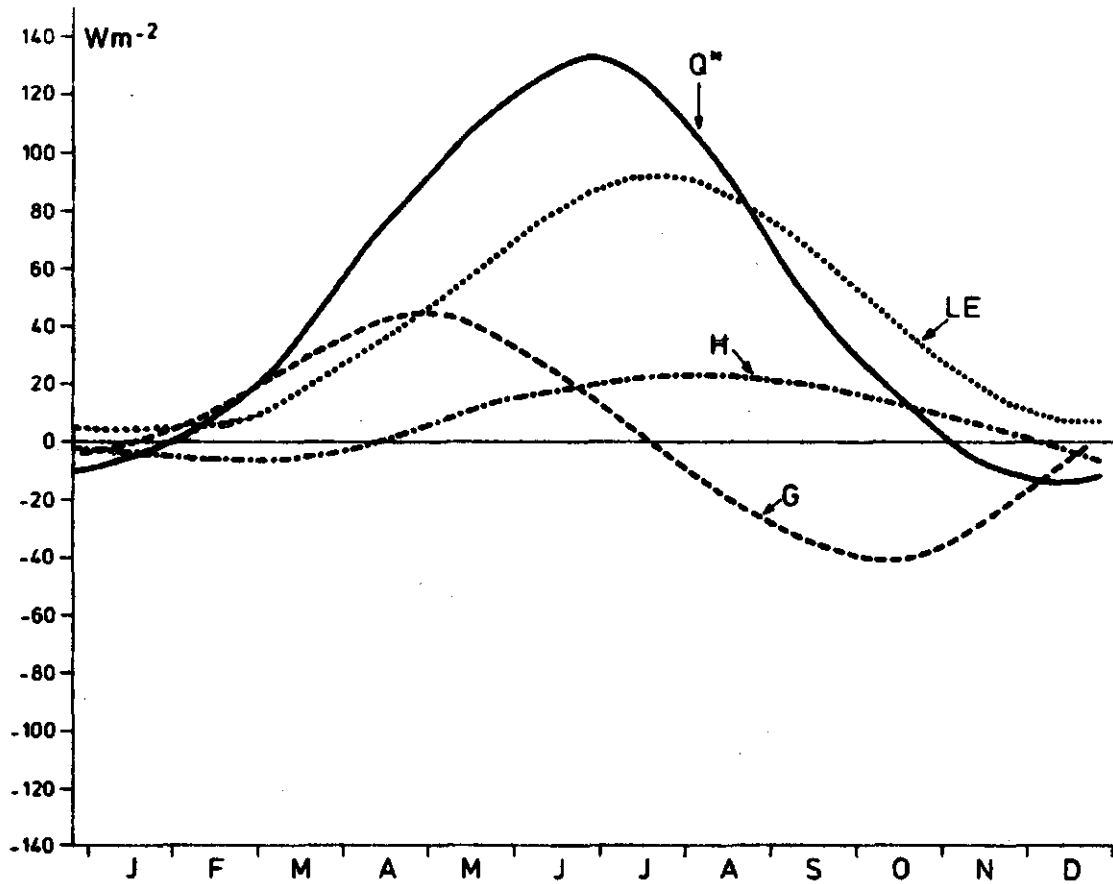


Fig. 2. The mean annual cycle of net radiation Q^* , sensible and latent heat flux H and LE , and the heat storage term G as evaluated by the model. Water depth = 5 m.

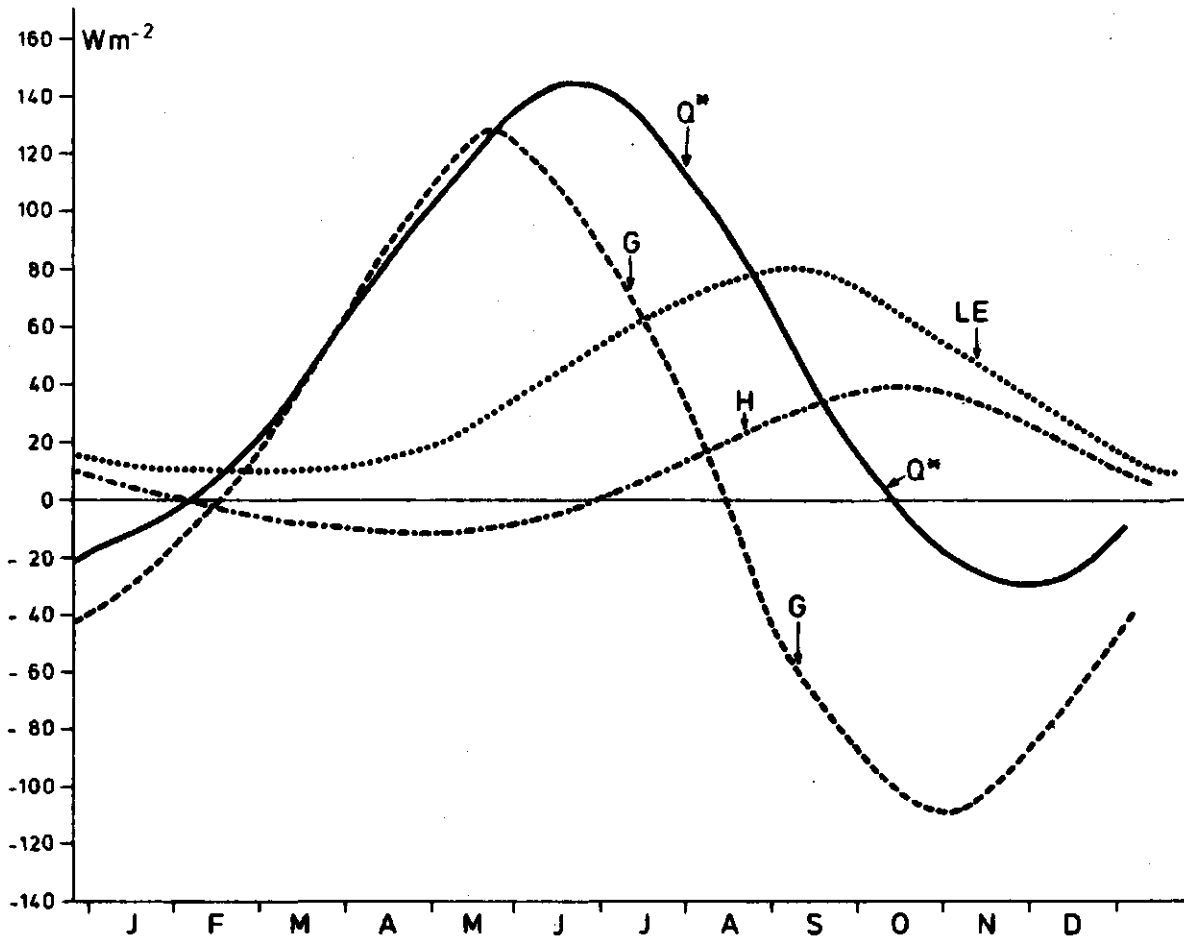


Fig. 3. As Fig. 2 with a waterdepth = 15 m.

storage term G , is more pronounced. This is due to the fact that in Spring and early Summer solar energy is stored in the water. For well-mixed bodies of water the amount of stored energy is proportional to the water depth. The mean of G over several years is zero; therefore the heat stored in Spring and early Summer will be released later in the year. This released energy will be used for evaporation and sensible heat transferred to the atmosphere. This explains qualitatively why there is a phase shift between evaporation and net radiation, and why this phase shift increases with water depth.

To illustrate the behaviour of the water temperature in Fig. 4 the mean annual cycle of T_w is drawn together with that of the equilibrium temperature T_e . The indices 5 and 15 refer to the water depth. It is seen that T_e is slightly retarded with respect to the noon solar elevation, while in turn T_w^5 and T_w^{15} are retarded with respect to T_e . Furthermore the sine curves of T_w^5 and T_w^{15} are damped. These features follows directly from Eq. (2) when the mean annual variation of T_e is assumed to be a single sine (see e.g. Edinger et al., 1968). In this way it can easily be shown that the phase shift of T_w equals $\frac{365}{2\pi} \arctan\left(\frac{2\pi\tau}{365}\right) \approx \tau$ days when $\tau \ll 365$, so that it is proportional to the water depth.

From the assumption that the mean annual cycle of T_e is described by a single sine it further follows that the mean of the heat storage term $G (= \rho_w c_w h \partial T_w / \partial t)$ can be written as

$$G = \rho_w c_w h \frac{2\pi}{365} A_1 \cos\left(\frac{2\pi}{365} t + \phi_1 - \alpha_1\right) \quad (14)$$

The amplitude of the T_e curve is about 10 K (see Fig. 4), while it reaches its maximum at about 15 July. With (7)-(9) this leads to

$$G = \frac{8.4 h}{\sqrt{1 + \left(\frac{2\pi\tau}{365}\right)^2}} \sin\left[\frac{2\pi}{365} (t - 14 - \tau)\right], \quad (15)$$

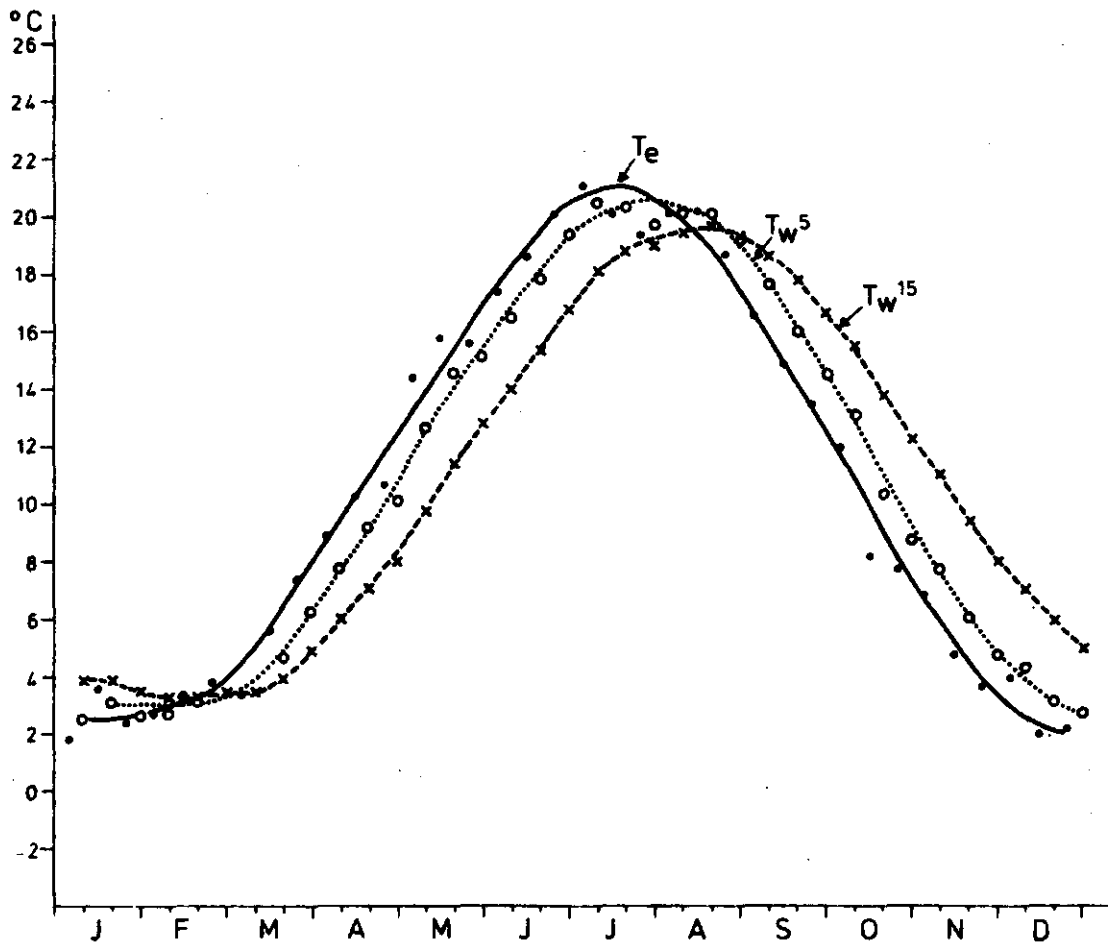


Fig. 4. The mean annual cycle of the equilibrium temperature T_e and the water temperature T_w^5 and T_w^{15} (water depth 5 and 15 m respectively) as evaluated by the model.

In (14) and (15) t is the day-number (at 1 January $t = 1$, etc) and τ is expressed in days. As before $\arctan\left(\frac{2\pi\tau}{365}\right)$ is approximated by $\frac{2\pi\tau}{365}$, which is permitted for $\tau \leq 30$ d.

The G-curves shown in Figs. 2 and 3 are rather well described by (15). With expressions (14) or (15) a simple estimate of G is obtained which can be used for practical calculations of lake evaporation with the Penman formula. However, it should be noted that (15) refers to an average over several years. In a particular period the deviations from (15) can be large.

5. Net radiation and wind function

To estimate net radiation Q^{net} , which is no variable observed on a routine base, and the related quantity Q_n^{net} (see eq. (3)) the following semi-empirical expression is used in this study:

$$Q^{\text{net}} = K_0^{\downarrow} (1-\alpha) (0,2 + 0,48 p) - \sigma T_a^4 (0,47 - 0,067 \sqrt{e_a}) \\ \times (0,2 + 0,8 p) + 4 \sigma T_a^3 (T_w - T_a), \quad (16)$$

where K_0^{\downarrow} is the incoming shortwave radiation across a horizontal plane at the outer limit of the atmosphere, p the relative duration of bright sunshine, T_a the air temperature (K) and e_a the vapour pressure (mb). This relation is a modification of the expression used by Kramer (1957) for evaporation calculations in the Netherlands. The modification consists of the addition of the last term of (16). This has been done because the outgoing longwave radiation is described by σT_w^4 instead of σT_a^4 . The quantity Q_n^{net} is obtained by replacing T_w by T_n in (16). The albedo α is taken at 0.06.

The wind function $f(u)$ is related to the turbulent exchange coefficients for transfer of water vapour and sensible heat at the air-water interface. It depends, besides winds speed, upon a number of factors

such as stability, measuring height of the relevant meteorological elements and surface roughness. In principle it is possible to deduce an expression for $f(u)$ from the similarity-theory of Monin and Obukhov (see e.g. Hicks, 1975). However, application of such an approach meets some problems caused by the following:

- a). In most practical applications a time interval of 24 hr or longer is used (also in this study), but when stability effects are taken into account a time step of, say, 1 hr must be applied.
- b). The assumption of horizontal homogeneity is often not realistic, notably in our case where small inland lakes are considered. This reflects on the "effective" exchange coefficients and thus on $f(u)$.
- c). Mostly, the meteorological observations are taken at a nearby land station. This is also done in this study. Since a land and a water surface have a significantly different aerodynamic roughness this has consequences for $f(u)$.

For these reasons it is better to rely on empirically derived wind functions rather than on theoretical ones. In this study we adopted the function proposed by Sweers (1976), based on the study of McMillan (1973) on a Welsh cooling pond of 5 km²:

$$L_v f(u) = 4.4 + 1.82 u_{10}, \quad (\text{W.m}^{-2}.\text{mbar}^{-1}) \quad (17)$$

where u_{10} is the wind speed measured at 10 m at a nearby land station. Sweers obtained this function from an analysis of the hydrological literature. The usual procedure to determine $f(u)$ is measuring independently the evaporation, the water temperature, the vapour pressure and wind speed at a particular height z above the water. Mostly averages over 1 day or longer (e.g. 1 month) are taken. Then $f(u)$ is found by plotting $E/(e_s(T_w) - e_a)$ against u , assuming that Dalton's formula for evaporation holds:

$$E = f(u) (e_s(T_w) - e_a), \quad (18)$$

where $e_s(T_w)$ is the saturation vapour pressure at T_w . In this way wind functions are determined for the case that the vapour pressure and wind speed are observed at a nearby land station. This applies also for Eq. (17). It is noted that application of eq. (17) requires that air temperature and humidity are observed at 10 m. But since we are taking averages over 1 day or longer the use of temperature and humidity data collected at standard height (about 2 m) does not introduce large errors.

6. Verification of the model

In this study measured and calculated water temperatures are compared over several years. This has been done for *De Grote Rug* and *Petrusplaat* which differ significantly in depth.

Since we mainly pay our attention to the annual variation of T_w a time step of 10 days was chosen. Hence eq. (13) has been applied in this study for $N = 10$. An experiment over one year in which time steps of 1 and 10 days were used reveals that there is no significant loss of information when a 10-day time step is chosen. The choice of this time step^{*} has the additional advantage that the estimation procedures for net radiation and $f(u)$ are more accurate for longer periods. In Figs. 5 and 6 the comparisons are shown. It is seen that the course of T_w is simulated well by the model. However, there are occasional deviations of 1°C or more. Some of these are presumably caused by things like measuring errors in T_w , temporary non-representativeness of the weather input data, unknown changes of the water level etc., but others are certainly due to imperfections of the model. First of all, the semi-empirical expressions Q_n^* and $f(u)$ are not perfect. Furthermore during calm and sunny periods

^{*} In fact, the time intervals used were not exactly 10 days, but the first and second 10 days of a month and the remaining period. Thus, the latter has a length varying between 8 and 11 days. This time interval is common in meteorological practice.

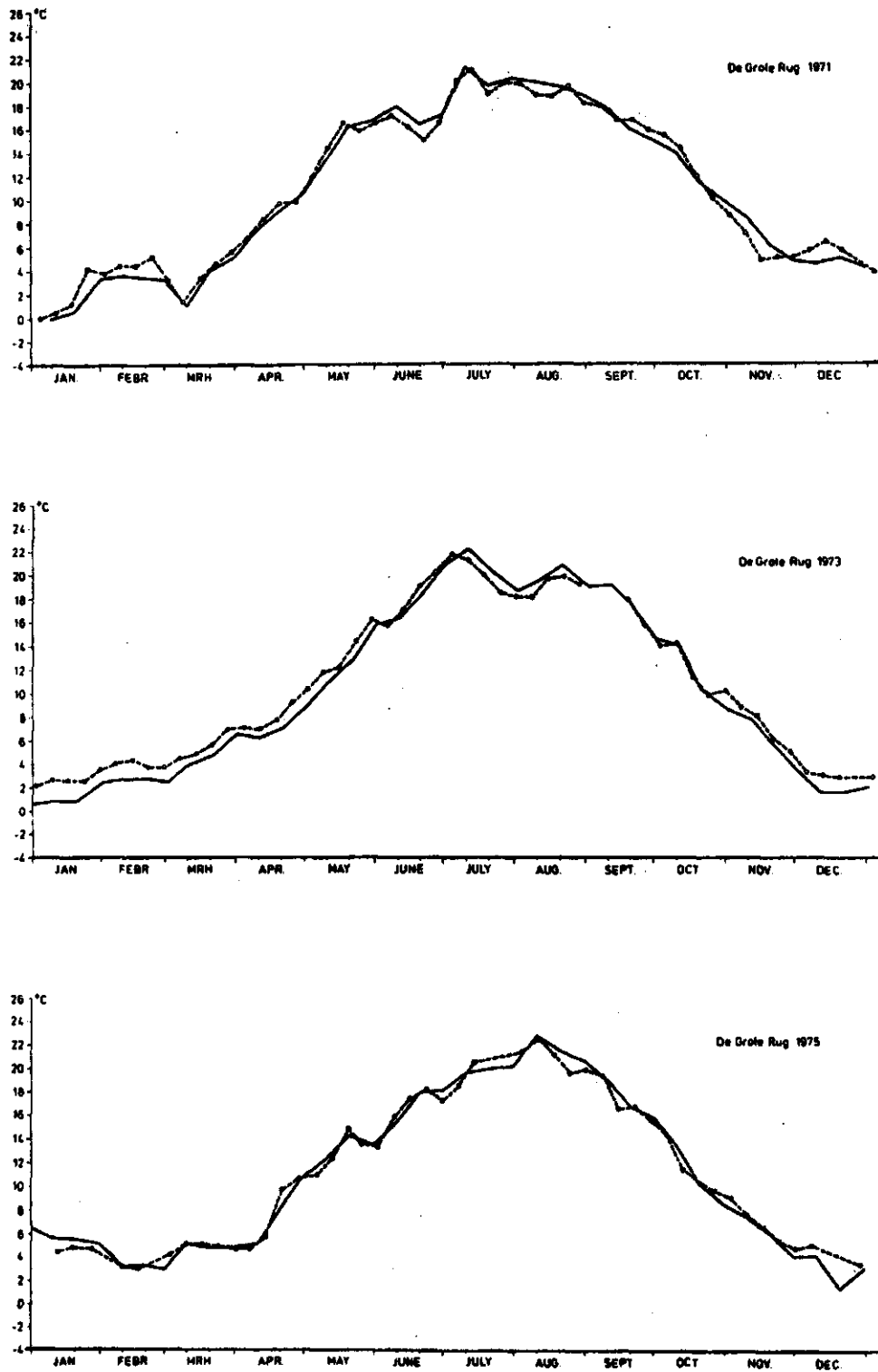


Fig. 5a. A comparison between the measured and computed water temperature of De Grote Rug [observed (●---●), computed (●—●)]; 1971-1973.

VI.17

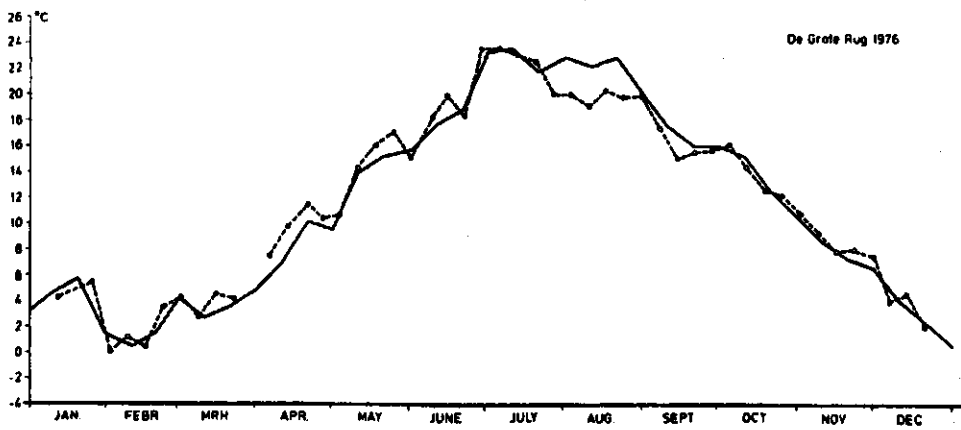
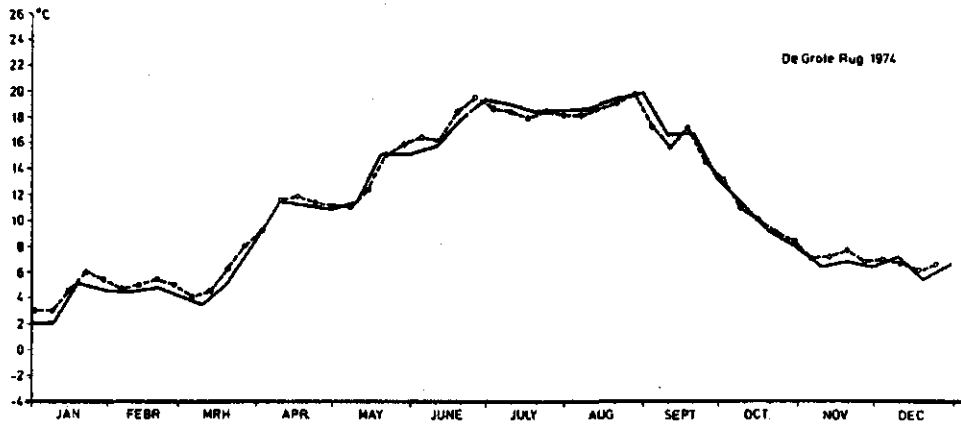
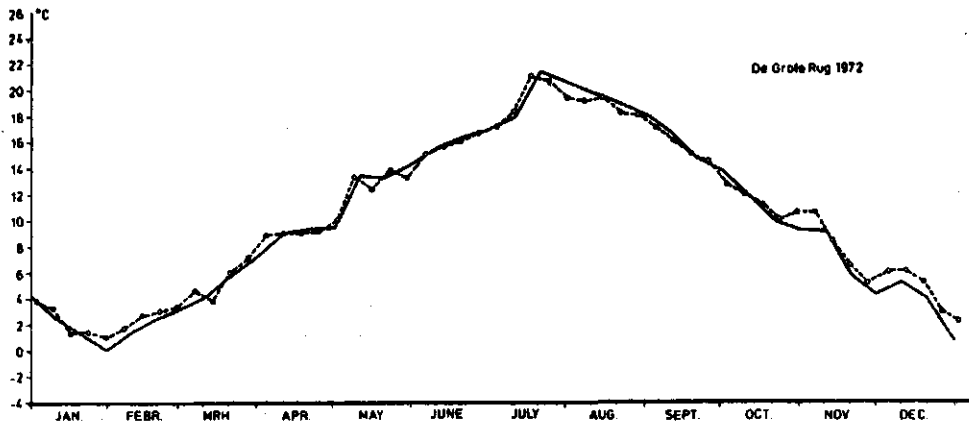


Fig. 5b. As 5a except for 1974-1976.

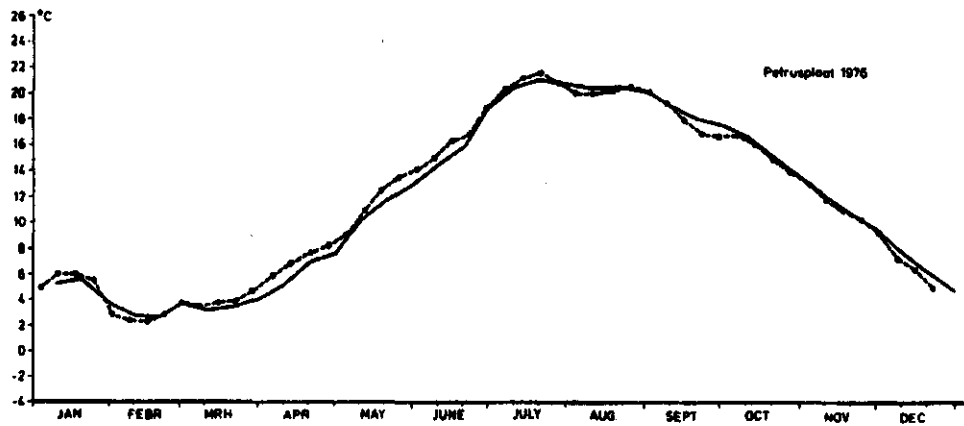
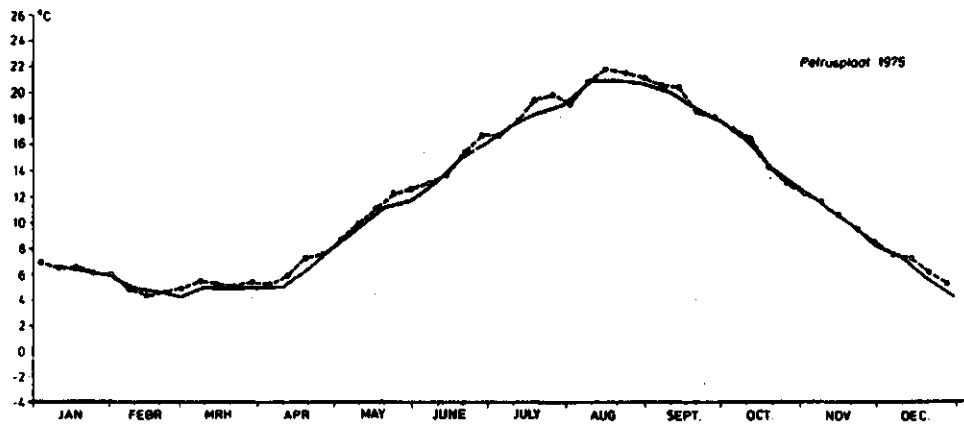
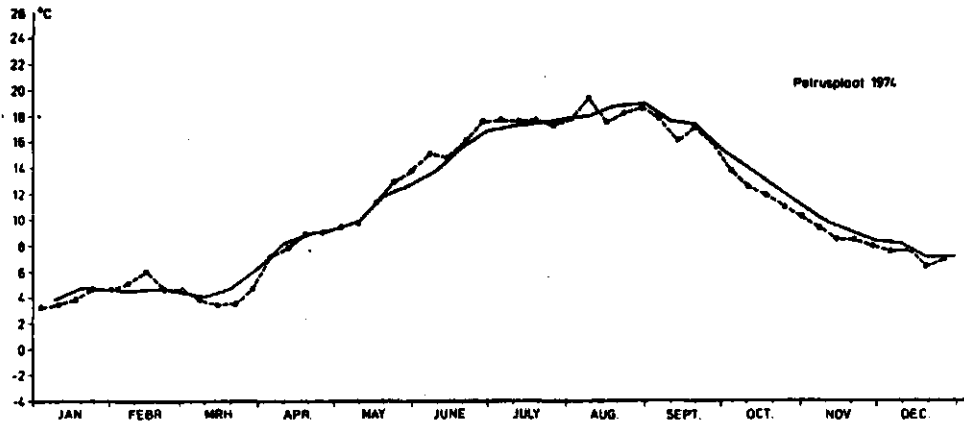


Fig. 6. As Fig. 5, but for Petrusplaat.

the essential assumption of an isothermal stratification in the water is not met. A pronounced variation of the temperature of the top water layer of, say, 1 m then occurs (see e.g. Sweers, 1979). This makes that, in that case, point measurements of T_w highly depend on the time of observation. This reflects on the water temperature data of *De Grote Rug* in 1976 when there was an extremely hot spring and summer. This possibly explains the relatively large scatter shown in Fig. 2 for that year. Because summers like in 1976 are very rare in the Netherlands, it may be concluded that the model, including the semi-empirical expressions (16) and (17) for Q^* and $f(u)$, yields good results for the entire annual cycle under Netherlands climatological conditions.

7. Conclusions

The results of this study reveals that the simple model resulting in Eq. (10) describes the annual course of the temperature of a well-mixed water reservoir or lake satisfactorily, when the empirical expressions (16) and (17) for net radiation and the wind function $f(u)$ are applied. The attractiveness of the model is that (a) it has a clearly physical basis and (b) it needs only standard meteorological observations.

Because, bodies of water with a depth up to, say, 10 m very often are mixed naturally by wind the model is of great practical importance.

Applications of the model lie in the field of e.g.:

- thermal pollution problems (determination of natural water temperatures; trend studies using time series of the natural water temperature computed from climatological data; evaluation of frequency distributions of natural water temperature);
- water budget studies (determination of evaporation);
- planning purposes (estimation of the temperature of cooling ponds to be planned).

VII. References

- Brutsaert, W. and H. Stricker, 1979: An advection-aridity approach to estimate actual regional evapotranspiration. Wat. Resources. Res., 15, 443-450.
- Businger, J.A., 1973: Turbulent transfer in the atmospheric surface layer. Workshop on micrometeorology. Haugen, D.A., Ed., AMS, Boston, Mass., 67-98.
- Businger, J.A., Wyngaard, J.C., Izumi, Y., and E.F. Bradley, 1971: Flux-profile relationships in the atmospheric surface layer. J. Atmos. Sci., 28, 181-189.
- Burrige, D.M. and A.J. Gadd, 1977: The meteorological office operational 10-level numerical weather prediction model. Scientific Paper 34, Met. Off., London.
- Clarke, R.H., Dyer, A.J., Brook, R.R., Reid, D.G. and A.J. Troup, 1971: The Wangara experiment: Boundary layer data. CSIRO Tech. Pap. No. 19. Melbourne, Australia, pp. 340.
- Crawford, T.V., 1965: Moisture transfer in free and forced convection. Quart. J. R. Met. Soc., 91, 18-27.
- Davies, J.A. and D.C. Allen, 1973: Equilibrium, potential and actual evaporation from cropped surfaces in southern Ontario. J. Appl. Meteor., 12, 649-657.
- De Bruin, H.A.R., 1978: A simple model for shallow lake evaporation. J. Appl. Meteor., 17, 1132-1134.
- De Bruin, H.A.R., 1981: The determination of (reference crop) evapotranspiration from routine weather data. Com. Hydr. Res. TNO Proc. and Information No. 28, pp. 25-36.

VII.2

- De Bruin, H.A.R. and A.A.M. Holtslag, 1982: A simple parameterization of the surface fluxes of sensible and latent heat during daytime compared with the Penman-Monteith concept. Submitted to J. Appl. Meteor. (Chapter III of this thesis).
- De Bruin, H.A.R. and J.Q. Keijman, 1979: The Priestley-Taylor evaporation model applied to a large shallow lake in the Netherlands. J. Appl. Meteor., 18, pp. 898-903 (Chapter V of this thesis).
- De Bruin, H.A.R. and H. Stricker, 1982: A comparison of different models for actual and potential evapotranspiration. In preparation.
- De Bruin, H.A.R. and W. Kohsiek, 1979: Toepassingen van de Penman formule. (With English summary). KNMI Scientific Report 79-3.
- Driedonks, A.G.M., 1981: Dynamics of the well-mixed atmospheric boundary layer. KNMI Scientific Report WR 81-2.
- Driedonks, A.G.M., 1982: Sensitivity analysis of the equations for a convective mixed-layer. Boundary Layer Meteorol., 22, 183-191.
- Dyer, A.J., 1974: A Review of flux-profile relationships. Boundary Layer Meteorol., 7, 363-372.
- Dyer, A.J. and B.B. Hicks, 1970: Flux-gradient relationships in the constant flux layer. Quart. J. R. Met. Soc., 98, 206-212.
- Edinger, J.E., Duttweiler, D.W. and J.C. Geyer, 1968: The response of water temperature to meteorological conditions. Wat. Res. Res., 14, 1137-1143.
- Ferguson, H.L. and G. den Hartog, 1975: Meteorological studies of evaporation at Perch Lake, Ontario. Hydrological studies on a small basin on the Canadian Shield: Evaporation studies. P.J. Barry, Ed. AECL Chalk River Nuclear Laboratories, pp. 417-448.

VII.3

- Fraedrich, K., Erath, B.G. and G. Weber, 1977: A simple model for estimating the evaporation from a shallow water reservoir. Tellus, 29, 428-434.
- Funk, J.P., 1959: Improved polythene-shielded net radiometer. J. Sci. Inst., 36, 267-270.
- Grant, D.R., 1975: Comparison of evaporation measurements using different methods. Quart. J. R. Met. Soc., 101, pp. 543-550.
- Hasse, L., 1971: The sea surface temperature deviation and the heat flow at the sea-air interface. Boundary-Layer Meteorol., 1, pp. 368-379.
- Hicks, B.B., 1975: A procedure for the formulation of bulk transfer coefficients over water. Boundary-Layer Meteorol., 8, 515-524.
- Hicks, B.B., 1981: An examination of turbulence statistics in the surface boundary layer. Boundary-Layer Meteorol., 21, 382-402.
- Holtslag, A.A.M., De Bruin, H.A.R. and A.P. van Ulden, 1980: Estimation of the sensible heat flux from standard meteorological data for stability calculations during daytime. Proc. of the 11th Int. Techn. Meet. on Air Poll. Model and its Appl., Amsterdam, 21-25 Nov., Plenum, New York.
- Itier, B., 1980: Une méthode simplifiée pour la mesure du flux du chaleur sensible. J. Rech. Atmos., 14, 17-34.
- Itier, B., 1981: Une méthode simple pour la mesure de l'évapotranspiration réelle à l'échelle de la parcelle. Agronomie. (Accepted for publication).
- Kaimal, J.C. and J.A. Businger, 1970: Case study of a convective plume and dust devel. J. Appl. Meteorol., 9, 612-620.

VII.4

- Keijman, J.Q., 1974: The estimation of the energy balance of a lake from simple weather data. Boundary-Layer Meteor., 7, 399-407.
- Keijman, J.Q. and R.W.R. Koopmans, 1973: A comparison of several methods of estimating the evaporation of Lake Flevo. Hydrology of Lakes, Proc. Helsinki. Symp., IAHS Publ. No. 109, pp. 225-232.
- Kramer, C., 1957: Berekening van de gemiddelde grootte van de verdamping voor verschillende delen van Nederland volgens de methode van Penman. (in Dutch with English summary). KNMI Meded. en Verh., 70, pp. 85.
- Louis, J., 1979: A parametric model of vertical eddy fluxes in the atmosphere. Boundary-Layer Meteorol., 17, 187-202.
- Lumley, J.L. and H.A. Panofsky, 1964: The structure of atmospheric turbulence, Wiley Interscience, New York, pp. 239.
- MacMillan, W., 1973: Cooling from open water surfaces. Final report, Part 1: Lake Trawsfynydd cooling investigation. Scientific Services Department, CE GB, Manchester.
- Makkink, G.F., 1957: Testing the Penman-formula by means of lysimeters. J. Int. Wat. Eng. London, 11, 277-288.
- McNaughton, K.C., 1976: Evaporation and advection I: Evaporation from extensive homogeneous surfaces. Quart. J. R. Met. Soc., 102, 181-191.
- Monin, A.S. and A.M. Obukhov, 1954: Basic laws in turbulent mixing in the ground layer of the atmosphere. Akad. Nauk. SSSR, Geofiz. Inst. Trudy, 151, 163-187.
- Monin, A.S. and A.M. Yaglom, 1971: Statistical Fluid Mechanics, Vol. 1, MIT Press, Cambridge Mass, pp. 769.
- Monteith, J.L., 1965: Evaporation and environment. Symp. Soc. Exp. Biol., XIX pp. 205-234.

VII.5

Monteith, J.L., 1981: Evaporation and surface temperature. Quart. J. R. Met. Soc., 107, 1-27.

Monteith, J.L. and G. Szeicz, 1961: The radiation balance of bare soil and vegetation. Quart. J. R. Met. Soc., 87, 159-170.

Mukammal, E.I., and H.H. Neumann, 1977: Application of the Priestley-Taylor evaporation model to assess the influence of soil moisture on the evaporation from a large weighing lysimeter and Class A pan. Boundary-Layer Meteor., 12, 243-256.

Nielsen, L.B., Prahm, L.P., Berkowicz, R., and K. Conradsen, 1981: Net incoming radiation estimated from hourly global radiation and/or cloud observations. J. of Climatology, 1, 255-272.

Obukhov, A.M., (1946) 1971: Turbulence in an atmosphere with a non-uniform temperature. Boundary-Layer Meteor., 2, 7-29. (First published in Trud. Inst. Teor. Geof. AN SSSR, No. 1, 1946).

Paulson, C.A., 1970: The mathematical representation of wind speed and temperature profiles in the unstable atmospheric surface layer. J. Appl. Meteor., 9, 857-861.

Perman, H.L., 1948: Natural evaporation from open water, bare soil and grass. Proc. R. Soc., A, 193, 120-145.

Perrier, A., 1980: Etude micro-climatique des relations entre les propriétés de surface et les caractéristique de l'air: application aux échanges régionaux. "Météorologie et Environnement", ETVRY (France), Octobre.

Prandtl, L., 1932: Meteorologische Anwendungen der Strömungslehre. Beitr. Phys. fr. Atmosph., 19, 188-202.

Priestley, C.H.B. and R.J. Taylor, 1972: On the assessment of surface heat flux and evaporation using large-scale parameters. Mon. Weather. Rev., 106, 81-92.

- Reiff, J., Blaauboer, D., De Bruin, H.A.R. and A.P. van Ulden, 1982:
A boundary layer/trajectory model for short range weather forecasting.
In preparation.
- Reitsma, T., 1978: Wind-profile measurements above a maize crop. Ph. D.
dissertation. Agricul. Univ. Wageningen, Pudoc. pp. 103.
- Rijtema, P.E., 1965: An analysis of actual evapotranspiration. Agric. Res.
Rep., 659, 1-107.
- Riou, Ch., 1982: Une expression analytique du flux de chaleur sensible en
conditions suradiabatiques a partir de mesures du vent et de la
temperature a deux niveaux. Accepted for publication by J. de Rech.
Atmos., 16, no. 1.
- Saugier, B. and E.A. Ripley, 1978: Evaluation of the aerodynamic method of
determining fluxes over natural grassland. Quart. J. R. Met. Soc., 104,
257-270.
- Schmidt, W., 1915: Strahlung und Verdunstung an freien Wasserflächen; ein
Beitrag zum Wärmehaushalt des Weltmeers und zum Wasserhaushalt der Erde.
Annalen der Hydrographie und Maritime Meteorologie, 111-124.
- Sellers, W.D., 1965: Physical Climatology. The Univ. of Chicago Press. pp. 272.
- Shuttleworth, W.J. and I. Calden, 1979: Has the Priestley-Taylor equation
any relevance to forest evapotranspiration? J. Appl. Meteor., 18, pp. 639-
646.
- Slob. W.H., 1978: The accuracy of aspiration thermometers. KNMI, Scientific
Rep. 78-1.
- Soer, G.J.R., 1977: The Tegra model - a mathematical model for the simulation
of the daily behaviour of crop surface temperature and actual evapo-
transpiration. ICW nota 1014.

VII.7

- Stewart, R.B., and W.R. Rouse, 1976: A simple method for determining the evaporation from shallow lakes and ponds. Wat. Res. Res., 12, 623-628.
- Stewart, R.B. and W.R. Rouse, 1977: Substantiation of the Priestley and Taylor parameter $\alpha = 1.26$ for potential evaporation in high latitudes. J. Appl. Meteor., 16, 649-650.
- Stricker, H. and W. Brutsaert, 1978: Actual evapotranspiration over a summer period in the "Hupsel Catchment". J. of Hydrol., 39, 139-157.
- Sweers, H.E., 1976: A nomogram to estimate the heat-exchange coefficient at the air-water interface as a function of wind speed and temperature, a critical survey of some literature. J. of Hydrol., 30, 375-401.
- Sweers, H.E., 1979: De natuurlijke watertemperatuur. Wat is dat? (In Dutch). H₂O, 12, pp. 2-5.
- Swinbank, W.C., 1963: Long-wave radiation from clear skies. Quart. J. R. Met. Soc., 89, 339-348.
- Tennekes, H., 1973: A model for the dynamics of the inversion above a convective boundary layer. J. Atmos. Sci., 30, 558-567.
- Tillman, J.E., 1972: The indirect determination of stability, heat and momentum fluxes in the atmospheric boundary layer from simple scalar variables during dry unstable conditions. J. Appl. Meteor., 11, 783-792.
- Thom, A.S. and H.R. Oliver, 1977: On Penman's equation for estimating regional evaporation. Quart. J. R. Met. Soc., 103, 345-358.
- Tsann-Wang Yu, 1977: Parameterization of surface evaporation rate for use in numerical modelling. J. Appl. Meteor., 16, 393-400.
- Van Ulden, A.P. and A.A.M. Holtslag, 1982: A scheme for estimating the surface fluxes of heat and momentum from routine weather data. In preparation.

- Wieringa, J., 1973: Applications of turbulence measurements over Lake Flevo. D. Sc. dissertation, Univ. of Utrecht, the Netherlands, 96 pp.
- Wieringa, J., 1980: A reevaluation of the Kansas mast influence on measurements of stress and cup anemometer overspeeding. Boundary-Layer Meteorol., 18, 411-430.
- Wieringa, J., 1981: Estimation of mesoscale and local-scale roughness for atmospheric transport modeling. 11th Internat. Techn. Meeting of NATO CCMS, Amsterdam, Nov. 1980. "Air Pollution Modeling and its Application", Plenum, New York, USA, pp. 279-295.
- Wyngaard, J.C., Coté, O.R. and Y. Izumi, 1971: Local free convection, similarity and budgets of shear stress and heat flux. J. Atmos. Sci., 28, 1171-1182.
- Yaglom, A.M., 1977: Comments on wind and temperature flux-profile relationships. Boundary-Layer Meteorol., 11, 89-102.

Curriculum vitae

De schrijver van dit proefschrift werd in 1943 geboren te 's Gravenhage. In Amsterdam bezocht hij de lagere school en de HBS (de "3e vijf", het latere van der Waals lyceum). Het diploma HBS-B werd in 1963 behaald. In dat zelfde jaar begon de auteur zijn studie in de natuurkunde aan de Gemeentelijke Universiteit van Amsterdam. Het kandidaatsexamen werd in 1966 met goed gevolg afgelegd. De bijvakken waren wiskunde en sterrenkunde. Kort daarop trad hij als kandidaat-assistent in dienst bij het van der Waals laboratorium. Daar verrichtte hij zijn praktisch werk voor zijn doctoraalstudie in de experimentele natuurkunde. In 1969 werd het doctoraaldiploma behaald met als bijvakken wiskunde en mechanica. Tevens werd een onderwijsbevoegdheid verkregen voor natuurkunde en sterrenkunde. In 1970 werd dit pakket uitgebreid met een bevoegdheid voor wiskunde. Op 1 januari 1970 trad de auteur in dienst bij het KNMI, waar hij de eerste jaren werkzaam was bij de afdeling Klimatologie en Landbouwmeteorologie. Op het ogenblik werkt hij bij de onderafdeling Fysische Meteorologie en is hij lid van de werkgroep Grenslaagmeteorologie. Sinds 1978 is hij tevens 'lecturer in meteorology' aan het International Institute for Hydraulic and Environmental Engineering te Delft voor studenten uit voornamelijk ontwikkelingslanden.